

การพัฒนาตำรับยาเม็ดโบโรโมคริปทีนมีไซเลทแบบไมโครอิมัลชันชนิดเกิดด้วยตัวเอง

นางสาวสิริกุล ทองรังษะภู

จุฬาลงกรณ์มหาวิทยาลัย
CHULALONGKORN UNIVERSITY

บทคัดย่อและแฟ้มข้อมูลฉบับเต็มของวิทยานิพนธ์ตั้งแต่ปีการศึกษา 2554 ที่ให้บริการในคลังปัญญาจุฬาฯ (CUIR)
เป็นแฟ้มข้อมูลของนิสิตเจ้าของวิทยานิพนธ์ ที่ส่งผ่านทางบัณฑิตวิทยาลัย

The abstract and full text of theses from the academic year 2011 in Chulalongkorn University Intellectual Repository (CUIR)
are the thesis authors' files submitted through the University Graduate School.

วิทยานิพนธ์นี้เป็นส่วนหนึ่งของการศึกษาตามหลักสูตรปริญญาเภสัชศาสตรดุษฎีบัณฑิต

สาขาวิชาเภสัชกรรม ภาควิชาวิทยาการเภสัชกรรมและเภสัชอุตสาหกรรม

คณะเภสัชศาสตร์ จุฬาลงกรณ์มหาวิทยาลัย

ปีการศึกษา 2557

ลิขสิทธิ์ของจุฬาลงกรณ์มหาวิทยาลัย

DEVELOPMENT OF BROMOCRIPTINE MESYLATE SELF-
MICROEMULSIFYING SYSTEM TABLET

Miss Sirigul Thongrangsalit



A Dissertation Submitted in Partial Fulfillment of the Requirements
for the Degree of Doctor of Philosophy Program in Pharmaceutics
Department of Pharmaceutics and Industrial Pharmacy
Faculty of Pharmaceutical Sciences
Chulalongkorn University
Academic Year 2014
Copyright of Chulalongkorn University

Thesis Title	DEVELOPMENT OF BROMOCRIPTINE MESYLATE SELF-MICROEMULSIFYING SYSTEM TABLET
By	Miss Sirigul Thongrangsalit
Field of Study	Pharmaceutics
Thesis Advisor	Professor Garnpimol Ritthidej, Ph.D.
Thesis Co-Advisor	Associate Professor Vimolmas Lipipun, Ph.D.

Accepted by the Faculty of Pharmaceutical Sciences, Chulalongkorn
University in Partial Fulfillment of the Requirements for the Doctoral Degree

.....Dean of the Faculty of Pharmaceutical Sciences
(Assistant Professor Rungpetch Sakulbumrungsil, Ph.D.)

THESIS COMMITTEE

.....Chairman
(Associate Professor Parkpoom Tengamnuay, Ph.D.)

.....Thesis Advisor
(Professor Garnpimol Ritthidej, Ph.D.)

.....Thesis Co-Advisor
(Associate Professor Vimolmas Lipipun, Ph.D.)

.....Examiner
(Assistant Professor Nontima Vardhanabhuti, Ph.D.)

.....Examiner
(Phanphen Wattanaarsakit, Ph.D.)

.....Examiner
(Associate Professor Pompen Werawatganone, Ph.D.)

.....External Examiner
(Associate Professor Thawatchai Phaechamud, Ph.D.)

สิริกุล ทองรังสฤษฎ์ : การพัฒนาตำรับยาเม็ดโบรโมคริปทีนมีไซเลทแบบไมโครอิมัลชันชนิดเกิดด้วยตัวเอง (DEVELOPMENT OF BROMOCRIPTINE MESYLATE SELF-MICROEMULSIFYING SYSTEM TABLET) อ.ที่ปรึกษาวิทยานิพนธ์หลัก: ศ. ภญ. ดร. กาญจน์พิมล ฤทธิเดช, อ.ที่ปรึกษาวิทยานิพนธ์ร่วม: รศ. ภญ. ดร.วิมลมาศ ลิปิพันธ์, 200 หน้า.

การละลายน้ำต่ำและการถูกเมแทบอลิซึมที่ตับสูงของยาโบรโมคริปทีนมีไซเลทที่ใช้สำหรับรักษาโรคพาร์กินสัน เป็นสาเหตุให้อัตราสารเข้าระบบชีวภาพของยามีค่าน้อย ดังนั้นยาเม็ดแบบไมโครอิมัลชันชนิดเกิดด้วยตัวเองที่ประกอบไปด้วยกรดไขมันสายยาวในวัฏภาคน้ำมันจึงถูกพัฒนาขึ้นเพื่อเพิ่มการละลาย, กระตุ้นการสังเคราะห์ลิโปโปรตีนซึ่งส่งเสริมการลำเลียงยาทางน้ำเหลือง หลีกเลียงการเมแทบอลิซึมที่ตับ และส่งยาไปสู่สมองที่เป็นเป้าหมาย น้ำมันธรรมชาติที่ประกอบไปด้วยกรดไขมันที่มีความบริสุทธิ์สูงถูกคัดเลือกมาใช้ และผลของสารลดแรงตึงผิวที่ไม่มีประจุและสารลดแรงตึงผิวร่วม ต่อความสามารถในการเกิดไมโครอิมัลชันชนิดเกิดด้วยตัวเองได้ถูกประเมิน ของเหลวไมโครอิมัลชันถูกเตรียม, ถูกดูดซับโดยตัวพาที่เป็นของแข็งประกอบด้วยแอร์ซิล200, แอร์เฟิล300 และนูซิลลิน ยูเอส2 ในอัตราส่วนที่เหมาะสม ได้เป็นผงไมโครอิมัลชันชนิดเกิดด้วยตัวเองและถูกตอกอัดเป็นเม็ดต่อไป การศึกษานอกกายโดยวิธีการเพาะเลี้ยงเซลล์ถูกทดสอบในเซลล์คาโค-2 และเซลล์เพาะเลี้ยงร่วมของเซลล์เอนโดทีเลียล (bEnd.3) และแอสโตรไซท์ (CTX TNA2) ผลการทดลองพบว่าการซึมผ่านของยาจากยาเม็ดที่จำหน่ายในท้องตลาดผ่านเซลล์คาโค-2 มากกว่ายาเม็ดไมโครอิมัลชันชนิดเกิดด้วยตัวเองอย่างมีนัยสำคัญ แต่อย่างไรก็ตามการดูดซึมยาที่สูงกว่าจะพบได้จากยาเม็ดไมโครอิมัลชันชนิดเกิดด้วยตัวเอง ($p < 0.05$) นอกจากนั้นตำรับไมโครอิมัลชันชนิดเกิดด้วยตัวเองที่บรรจุสารเรืองแสงยังให้ค่าการดูดซึมสารเรืองแสงของเซลล์เพาะเลี้ยงมากกว่าตำรับที่บรรจุสารเรืองแสงในน้ำมันหรือสารลดแรงตึงผิว ยาเม็ดไมโครอิมัลชันชนิดเกิดด้วยตัวเองให้ค่าการสังเคราะห์ลิโปโปรตีนที่แสดงเป็นปริมาณอะโพลีโพรตีน บี ที่พบในโคไลไมครอนที่ถูกหลั่งออกมา และค่าการดูดซึมยาในเซลล์เพาะเลี้ยงร่วมของเซลล์เอนโดทีเลียล (bEnd.3) และแอสโตรไซท์ (CTX TNA2) สูงที่สุด เมื่อเปรียบเทียบกับยาเม็ดที่จำหน่ายในท้องตลาด ($p < 0.05$) ดังนั้นตำรับยาเม็ดไมโครอิมัลชันชนิดเกิดด้วยตัวเองน่าจะมีศักยภาพในการนำส่งยาโบรโมคริปทีนมีไซเลทไปที่สมองผ่านการลำเลียงทางน้ำเหลืองโดยเพิ่มการสังเคราะห์ลิโปโปรตีน

ภาควิชา	วิทยาการเภสัชกรรมและเภสัช	ลายมือชื่อนิสิต
	อุตสาหกรรม	ลายมือชื่อ อ.ที่ปรึกษาหลัก
สาขาวิชา	เภสัชกรรม	ลายมือชื่อ อ.ที่ปรึกษาร่วม

5376963633 : MAJOR PHARMACEUTICS

KEYWORDS: BROMOCRIPTINE MESYLATE/SELF-MICROEMULSIFYING/LIPOPROTEIN SYNTHESIS/LYMPHATIC TRANSPORT/BRAIN

SIRIGUL THONGRANGSALIT: DEVELOPMENT OF BROMOCRIPTINE MESYLATE SELF-MICROEMULSIFYING SYSTEM TABLET. ADVISOR: PROF. GARNPIMOL RITTHIDEJ, Ph.D., CO-ADVISOR: ASSOC. PROF. VIMOLMAS LIPIPUN, Ph.D., 200 pp.

The poor water solubility and high hepatic metabolism cause low oral bioavailability of bromocriptine mesylate (BM) used for Parkinson's treatment. Therefore, self-microemulsion (SME) tablets were developed to improve solubility, stimulate lipoprotein synthesis which promote lymphatic transport, avoid hepatic metabolism and target drug to brain. Natural oils composed of high purity of long chain fatty acids were selected and the effect of nonionic surfactants and co-surfactants on the SME formation ability was investigated. The SME liquid was prepared, adsorbed by solid carriers, Aerosil[®] 200, Aeroperl[®] 300 or NeusilinUS2[®] at suitable ratios, yielding SME powders and then compressed as tablet. The *in vitro* cell culture studies were investigated in Caco-2 cells and co-culture of endothelial cells (bEnd.3) and astrocytes (CTX TNA2). The results indicated that the marketed tablet gave a significantly higher drug permeated through Caco-2 cells than those obtained from SME tablet, however, the higher drug uptake was found when SME formulations were given ($p < 0.05$). In addition, the fluorescein loaded SME tablet showed the higher cellular uptake than fluorescein loaded in oil or surfactant. The highest lipoprotein synthesis expressing as content of apolipoprotein B found in secreted chylomicron and drug uptake in co-culture of bEnd.3 and CTX TNA2 were obtained from drug loaded SME tablet compared to marketed tablet ($p < 0.05$). Therefore, the SME tablet might potentially deliver BM to the brain via lymphatic transport by increasing the lipoproteins synthesis.

Department: Pharmaceutics and Student's Signature

 Industrial Pharmacy Advisor's Signature

Field of Study: Pharmaceutics Co-Advisor's Signature

Academic Year: 2014

ACKNOWLEDGEMENTS

I would like to express my deep thankfulness to Professor Garnpimol C. Ritthidej, my thesis advisor, for her great advice, precious guidance, and encouragement throughout my research. Her endurance, kindness and understanding are also profoundly appreciated. I also wish to express my gratefulness to Associate Professor Vimolmas Lipipun, my thesis co-advisor, for her valuable assistance, construction and support.

I also wish to acknowledge H.M. the King Bhumibhol Adulyadej's 72nd Birthday Anniversary Scholarship from the graduate school, Chulalongkorn University for granting the financial support, tuition fees, monthly allowance and materials expense, for Ph.D. program.

Additionally, I would like to thank all members of thesis committees, Associate Professor Parkpoom Tengamnuay, Assistant Professor Nontima Vardhanabhuti, Dr. Phanphen Wattanaarsakit, Associate Professor Pornpen Werawatganone and Associate Professor Thawatchai Phaechamud for their valuable time and suggestions.

In addition, I would like to give thanks to my friends, colleagues and staffs for their encouragement and great support.

Finally, I would like to express my gratitude to my beloved mother and father for their care, mental support, cheerfulness and understanding.

CONTENTS

	Page
THAI ABSTRACT	iv
ENGLISH ABSTRACT	v
ACKNOWLEDGEMENTS	vi
CONTENTS	vii
LIST OF TABLES	viii
LIST OF FIGURES	xiii
LIST OF ABBREVIATIONS	xvii
CHAPTER I INTRODUCTION.....	1
CHAPTER II REVIEW LITERATURE	4
CHAPTER III MATERIALS AND METHODS	37
CHAPTER IV RESULTS AND DISCUSSION	63
CHAPTER V CONCLUSIONS.....	120
REFERENCES	125
APPENDIX A Self-microemulsion liquid.....	139
APPENDIX B Self-microemulsion powder and tablet.....	158
APPENDIX C <i>In vitro</i> cell culture studies.....	176
VITA.....	200

LIST OF TABLES

	Page
Table II-1 Different characteristics between emulsion and microemulsion (ME).....	11
Table II-2 Advantages of microemulsions system.	14
Table II-3 Percent fatty acid content and required HLB of selected oils (65).....	18
Table II-4 The physical properties and compositions of selected solid carriers (87)...	28
Table III-1 The compositions contained in both single surfactant and surfactant mixture systems with/without cosurfactant.....	41
Table III-2 Independent variables and there factor levels.....	50
Table III-3 Optimization method parameters for central composite design and response results.....	50
Table IV-1 The compositions contained in both single surfactant and surfactant mixture systems with/without cosurfactant and the ME/SME formation ability.....	64
Table IV-2 Particle size, size distribution and zeta potential of preconcentrate ME after being diluted with 250 ml of purified water.....	80
Table IV-3 Drug solubility in long chain triglyceride oils, surfactants and selected SME system.....	81
Table IV-4 Particle size, size distribution and zeta potential of drug loaded preconcentrate ME after being diluted with 250 ml of purified water.	82
Table IV-5 The relationship between the flow property and compressibility index (%) (107).....	83
Table IV-6 Compressibility index and corresponding flow properties of solid SMEDDS.....	85
Table IV-7 Hardness, friability and disintegration time of optimized SME tablet.....	92
Table IV-8 Composition of ingredients in SME tablet.	94

Table IV-9 Particle size and size distribution of SME tablet after dilution with 250 ml of purified water or 0.1N HCL.	97
Table IV-10 Physical characteristics and drug content of SME tablet.	98
Table IV-11 Similarity and difference factors of SME tablet compared to marketed tablet.	100
Table IV-12 Drug content calculated as %Labeled amount of SME tablets.	101
Table IV-13 Percent recovery of drug found in SME tablet at 50%, 100% and 150% concentrations of actual drug loaded in the SME tablet.	105
Table IV-14 Percent drug content in mobile phase at 100% concentrations of actual drug loaded in the SME tablet.	106
Table IV-15 Apparent permeability coefficients (P_{app}) and percent TEER of Caco-2 cells at the end of studies.	110
Table IV-16 Content of apolipoprotein B (apo B) detected in Caco-2 cells and secreted lipoprotein and percent TEER at the end of study.	113
Table IV-17 Drug content in chylomicron and VLDL.	115
Table IV-18 TEER values ($\text{ohm}\times\text{cm}^2$) of bEND3 cells monoculture and bEND3 cocultured with CTX TNA2 cells.	116
Table A-1 Pseudoternary phase diagram of ME systems.	139
Table A-2 Statistical testing: Effect of amount of castor oil (10, 15, 20 and 25% w/w) on particle size.	151
Table A-3 Solubility of drug (mg/ml) in various oils, surfactants and selected SME system at 25 ± 0.1 °C for 48 hours.	153
Table A-4 Statistical testing: Effect of solvents on drug solubility.	154
Table A-5 Statistical testing: Effect drug loading on of particle size.	157
Table B-1 Stability index of SME powders.	158
Table B-2 Basic flow energy (BFE) of SME powders.	159

Table B-3 Linear regression analysis: Effect of Polyvinylpyrrolidone K90, Kollidon [®] CL and Magnesium stearate on disintegration time.....	160
Table B-4 Linear regression analysis: Effect of Polyvinylpyrrolidone K90, Kollidon [®] CL and Magnesium stearate on hardness.	162
Table B-5 Statistical testing: Effect of solid carriers on particle size of SME tablets after reconstitution.....	163
Table B-6 Statistical testing: Effect of dilution mediums (0.1N HCL and purified water) on particle size of Aerosil [®] 200 SME tablets after reconstitution.....	165
Table B-7 Statistical testing: Effect of dilution mediums (0.1N HCL and purified water) on particle size of Aeroperl [®] 300 SME tablets after reconstitution.....	166
Table B-8 Statistical testing: Effect of dilution mediums (0.1N HCL and purified water) on particle size of Neusilin US2 [®] 300 SME tablets after reconstitution.	167
Table B-9 Diameter, thickness and hardness of SME tablets.....	168
Table B-10 Percent drug dissolved from SME tablets at 5, 10, 20 and 30 minutes...	169
Table B-11 Stability of drug-loaded Aeroperl [®] 300 SME tablet after storage at 40±2°C/75±5%RH, 25±2°C/60±5%RH and 5°C±3°C for 3 months.	171
Table B-12 Drug concentrations and responding area obtained from HPLC chromatograms.	172
Table B-13 Percent recovery at 50%, 100% and 150% concentrations of actual drug loaded in the SME tablet.	173
Table B-14 Percent recovery at 100% concentrations of actual drug loaded in the SME tablet in different 3 days.....	174
Table B-15 Calculation of LOD and Quantitation Limit LOQ.	175
Table C-1 Toxicity results in Caco-2 cells.....	176
Table C-2 Permeation of drug through Caco-2 cells at 2, 4 and 6 hours.....	177

Table C-3 Statistical testing: Effect of formulations on drug permeated through Caco-2 cells at 2 hours.....	179
Table C-4 Statistical testing: Effect of formulations on drug permeated through Caco-2 cells at 4 hours.....	181
Table C-5 Statistical testing: Effect of formulations on drug permeated through Caco-2 cells at 6 hours.....	183
Table C-6 Statistical testing: Effect of formulations on P_{app} values.....	185
Table C-7 Drug uptake in Caco-2 cells at 6 hours.....	186
Table C-8 Statistical testing: Effect of formulations on drug uptake in Caco-2 cells at 6 hours.....	186
Table C-9 TEER values of Caco-2 cells before and after permeation and uptake studies.....	188
Table C-10 ApolipoproteinB content in Chylomicron (chy), VLDL and Caco-2 cells.	188
Table C-11 Statistical testing: Effect of formulations on apolipoprotein B content found in Caco-2 cells.....	189
Table C-12 Statistical testing: Effect of formulations on apolipoprotein B content found in Chylomicron.....	190
Table C-13 Statistical testing: Effect of formulations on apolipoprotein B content found in VLDL.....	192
Table C-14 TEER values of Caco-2 cells before and after ApolipoproteinB analysis.	193
Table C-15 Statistical testing: Effect of formulations on drug content found in chylomicron.....	193
Table C-16 Statistical testing: Effect of formulations on drug content found in VLDL.....	195
Table C-17 TEER values ($\text{ohm} \times \text{cm}^2$) of bEND3 cells monoculture and bEND3 cocultured with CTX TNA2 cells.....	197

Table C-18 Toxicity results in bEND3 cells and CTX TNA2 cells.	197
Table C-19 Drug uptake in bEND3 cocultured with CTX TNA2 cells.	198
Table C-20 Statistical testing: Effect of formulations on drug uptake in bEND3 cocultured with CTX TNA2 cell.	198



LIST OF FIGURES

	Page
Figure II-1 Prospective population-based incidence studies of Parkinson's disease (28).....	4
Figure II-2 DA biosynthesis in a nigrostriatal nerve terminal (30).....	6
Figure II-3 Medication used in the initial therapy of early Parkinson's disease in the U.S. (12).....	7
Figure II-4 Chemical structure of bromocriptine mesylate (36).....	8
Figure II-5 Formation of three types ME at different ratios of oil, surfactant and water represented in the ternary phase diagram (40).....	12
Figure II-6 Intraluminal process of SMEDDS a) Dispersion in stomach and delivery to small intestine and b) Digestion of lipid droplets by bile salts and biliary lipids (44, 68) after oral administration.....	20
Figure II-7 Absorption process of lipid-based delivery system across enterocytes (24).....	21
Figure II-8 Intracellular process in enterocyte of long chain fatty acid transported via portal blood and lymphatic system (25).....	22
Figure II-9 Lipoprotein assemble within enterocyte and drug transportation to lymphatic system (69).....	23
Figure II-10 Plasma drug concentration versus time profiles after oral administration of a)SMEDDS formulation, b)Oil-free formulation to rat pretreated with saline (■) or cyclohexamide (◆) (22).....	24
Figure II-11 The relationship between percent of drug absorbed into intestinal lymphatic and percent of drug associated with chylomicron in the <i>ex vivo</i> model (69).....	26
Figure II-12 Structure of blood brain barrier (BBB) (88, 90).....	30

Figure II-13 Drug transport pathway across BBB a) Receptor-mediated transcytosis, b) Absorptive-mediated transcytosis, c) Carrier-mediated transport (91).	31
Figure II-14 Fluorescence uptake by incubation of bEnd3 cells with autofluorescence nanoparticles.....	33
Figure II-15 Expression of tight junction proteins in bEnd3 cells.....	35
Figure II-16 Transendothelial electrical resistance (TEER) of primary porcine brain endothelial cell (PBEC) monoculture (●), PBEC co-cultured with primary rat astrocytes (■), PBEC co-cultured with rat astrocyte cell line, CTX TNA (▲) (104).....	36
Figure III-1 Flowability measurement using FT4 Powder Rheometer.	48
Figure IV-1 Phase diagram of a)corn oil/Tween [®] 80+Span [®] 80 at ratio 1:1.89, b)sunflower oil/Tween [®] 80+Span [®] 80 at ratio 1:2.97, c)olive oil/Tween [®] 80+Span [®] 80 at ratio 1:2.97 and d)castor oil/Tween [®] 80 +Span [®] 80 at ratio 1:0.103.	70
Figure IV-2 Phase diagram of long chain triglyceride oils including a) corn oil, b) sunflower, c) olive oil and d) castor oil in the Tween [®] 80 and Span [®] 20 mixtures system at ratio 1:1.....	72
Figure IV-3 Phase diagram of long chain triglyceride oils including a) olive oil and b) castor oil in the Tween [®] 80 and Cremophor [®] EL mixture system at ratio 1:1.....	73
Figure IV-4 Effect of cosurfactant on %Wmax in a) Castor oil/Tw80/cosurfactant system, b) Castoroil/Tw80+Sp80/cosurfactant system, c) Castor oil/Tw80+Sp20/cosurfactant system, d) Castor oil/Tw80+CreEL/cosurfactant system.	74
Figure IV-5 Effect of cosurfactant on %Omax in a) Castor oil/Tw80/cosurfactant system, b) Castoroil/Tw80+Sp80/ cosurfactant system, c) Castor oil/Tw80+Sp20/cosurfactant system, d) Castor oil/Tw80+CreEL/cosurfactant system.	76
Figure IV-6 The minimum S/W values of both single surfactant and surfactant mixture system without cosurfactant.....	78

Figure IV-7 The appearance of liquid after dilution with 250 ml of purified water at the weight ratio a) 2:8, b) 2.5:7.5 and c) 3:7 of castor oil to Tw80+CreEL (1:1) mixtures.....	79
Figure IV-8 TEM micrograph of the ME droplets after dilution with 250 ml of purified water of castor oil/Tween [®] 80/Cremophor [®] EL (1:1) system at 20%w/w castor oil at magnitude a)x100,000 and b)x200,000.	81
Figure IV-9 The compressibility index (%) results of SME powders containing Aerosil [®] 200, Aeroperl [®] 300 or Neusilin US2 [®] at various weight ratios of SME liquid to solid carrier.....	86
Figure IV-10 The stability index (SI) value of adsorbed Aerosil [®] 200, Aeroperl [®] 300 and Neusilin US2 [®] at various ratios of SME to carrier.....	88
Figure IV-11 The BFE value of adsorbed Aerosil [®] 200, Aeroperl [®] 300 and Neusilin US2 [®] at various ratios of SME to carrier.....	89
Figure IV-12 The morphology of a) Aerosil [®] 200, b) Aeroperl [®] 300, c) Neusilin US2 [®] , d) SME powder at 1.5:1 ratio of SME liquid to Aerosil [®] 200, e) SME powder at 2:1 ratio of SME liquid to Aeroperl [®] 300, f) SME powder at 2.5:1 ratio of SME liquid to Neusilin US2 [®]	89
Figure IV-13 DSC chromatogram of bromocriptine mesylate, physical mixer of drug and solid carriers (1:1) and drug loaded SME powders.....	91
Figure IV-14 Particle size of droplets from SME tablet after dilution with 250 ml of purified water compared to SME liquid.....	96
Figure IV-15 Dissolution profile of bromocriptine mesylate SME tablets prepared by Aerosil [®] 200, Aeroperl [®] 300 or Neusilin US2 [®] tablets compared to marketed tablet.....	100
Figure IV-16 Percent drug content in SME tablet after storage at 40±2°C/75±5%RH, 25±2°C/60±5%RH and 5°C±3°C for 3 months (n=3).....	102

Figure IV-17 HPLC chromatogram of a) BM, b) BM spiked placebo SME tablet, c) BM exposed to 0.1N HCL, d) BM exposed to 0.1N NaOH, e) BM exposed to 30% H ₂ O ₂ , f) BM exposed to heat (60°C) and g) BM exposed to UV light.....	104
Figure IV-18 Relationship between peak area and concentrations of BM.....	107
Figure IV-19 Percent cell viability of Caco-2 cells after treatment of test sample at various drug concentrations.	108
Figure IV-20 Permeation of drug through Caco-2 cells after treatment with test samples at 2, 4 and 6 hours, *p<0.05 significantly different from marketed tablet..	109
Figure IV-21 Drug content in Caco-2 cells after treatment with test samples for 6 hours, *p<0.05 significantly different from marketed tablet.	110
Figure IV-22 Fluorescein uptake of Caco-2 cells after 6 hours incubation with DAF loaded a) medium solution, b) castor oil tablet, c) Tween [®] 80 tablet, d) Cremophor [®] EL tablet and e) SME tablet.	112
Figure IV-23 Percent cell viability of bEnd.3 after incubation with test sample for 6 hours.	116
Figure IV-24 Percent cell viability of CTX TNA2 after incubation with test sample for 6 hours.....	117
Figure IV-25 Content of drug in bEnd.3 cocultured with CTX TNA2 cells after incubation with test samples for 6 hours, *p<0.05 significantly different from marketed tablet, **p<0.05 significantly different from drug loaded SME tablet.	118

LIST OF ABBREVIATIONS

PD	=	parkinson's disease
DA	=	dopamine
L-DOPA	=	levo-dopa
BC	=	bromocriptine
BM	=	bromocriptine mesylate
SME	=	self-microemulsion
ME	=	microemulsion
HLB	=	hydrophilic-lipophilic balance
o/w	=	oil in water
w/o	=	water in oil
EtOH	=	ethanol
PG	=	propylene glycol
Gly	=	glycerin
%O _{max}	=	maximum percentage of oil solubilized
%W _{max}	=	maximum percentage of water
S/W	=	ratio of surfactant to water
Chy	=	Chylomicron
VLDL	=	very low density lipoprotein
LDL	=	low density lipoprotein
Papp	=	apparent permeability coefficient
TEER	=	trans-epithelial electrical resistance
DMSO	=	dimethyl sulfoxide
apo B	=	apolipoprotein B
ELISA	=	enzyme-linked immunosorbent assay
HPLC	=	high performance liquid chromatography
SD	=	standard deviation
TEM	=	transmission electron microscope
SEM	=	scanning electron microscope

PBS	=	phosphate buffer saline
M	=	molar
g	=	gram
μg	=	microgram
μl	=	microliter
mg	=	milligram
mm	=	millimeter
BFE	=	basic flow energy
SI	=	stability index
DSC	=	differential scanning calorimetry
$^{\circ}\text{C}$	=	degree celsius
CO_2	=	carbon dioxide
UV	=	ultraviolet



CHAPTER I

INTRODUCTION

Parkinson's disease (PD) is one of the neurodegenerative disorders which most commonly found beside the Alzheimer's disease (1, 2). The incidence of PD obviously increased with age, especially over 60 years olds (3). The cause of PD is still unknown. Losing of dopamine (DA) in the striatum is the pathological hallmark of the condition (4, 5). To date, PD cannot be cured by any treatments yet but it was only slow down the progression of disease. Improving the restoration of the dopamine level in the CNS is the treatment approach for PD (6). Levodopa (L-Dopa), precursor of dopamine, still is the first line drug and most widely used for PD (4, 7), however, they also cause significant dyskinesias and motor fluctuations which limit their effectiveness for long-term usage (8-10). The continuing of neuron cells death when the disease progress resulting in lower response to L-Dopa because of losing ability to store and release DA (10). The uncertain DA released lead to pulsatile stimulation of DA receptor which cannot mimic the physiological condition that these receptors are activated continuously. Therefore, the treatment approach to reduce the motor complications was considered (11). DA agonists have found to be an alternative to L-Dopa for initial treatment due to less dyskinesia and motor fluctuation because of their longer half-life (12-15). Moreover, they directly attach to DA receptor at post-synaptic neuron, bypassing conversion step to change the L-Dopa to DA (12).

Bromocriptine mesylate (BM) is the dopamine agonist used in the treatment of Parkinson's disease, however, the low solubility, marked affinity to various tissues, rapid hepatic extraction and high hepatic metabolism of the absorbed fraction cause very low blood levels following oral doses (16). Many researchers (17-19) developed the BM formulations to avoid the hepatic metabolism, improve the bioavailability and effectiveness or reduce the motor complications. Self-microemulsifying drug delivery system (SMEDDS) is one of lipid-based systems that has been shown to improve the solubility of poorly-water soluble drugs, enhance the bioavailability of drugs administered orally (20, 21) and transport drug to systemic circulation via lymphatic pathway, bypass the liver (22). Microemulsions (ME) could spontaneously formed when they were diluted with an external aqueous medium or biological fluid under mild agitation or digestive motility after *in vivo* administration (21). Due to their spontaneous formation, not all ingredients can produce ME. Therefore, a reasonable selection of excipients is the most important for ME preparation. Moreover, the compositions of lipid in SMEDDS will determine the transport pathway. Generally, short and medium chain fatty acids ($C < 12$) enter to blood capillaries while long chain fatty acids ($C > 12$) are secreted into mesenteric lymph (23).

The apolipoprotein B-containing chylomicron and VLDL are primarily secreted lipoproteins from enterocyte cells which transport the drug to capillaries of mesenteric lymphatics. Finally, it is directly drained into blood circulation at the junctions of left jugular and left subclavian veins, bypass the liver (24). Therefore, this transport pathway could enhance the bioavailability for drugs which are extensively metabolized by the liver (25) such as BM.

Due to the parkinson's treatment of BM, the transportation of drug to the brain is required. The effect of lymphatic transport on oral bioavailability of rapamycin loaded SMEDDS was studied by Sun et al. (22). They reported that SMEDDS with suitable oil concentration could stimulate the lymphatic transport, enhancing oral bioavailability of rapamycin. Those secreted apolipoprotein B-containing lipoproteins may bind to LDL receptors which express on brain

endothelial cells leading to transcytosis to abluminal side of BBB, releasing and being taken up by neurons (26).

However, some disadvantages of self-microemulsions (SME) liquid such as low stability and portability and a few choice of dosage forms, solid SMEDDS has been introduced as alternative approaches. Solid SMEDDS are the solid dosage forms that possess the self-microemulsions properties. The advantages of SMEDDS such as improving solubility and bioavailability and solid dosage form such as high stability and better patient compliance were combined in solid SMEDDS. There are many techniques to transform the liquid SME to the solid SME. An adsorption technique is a simple method and provide the free-flowing powders and good content uniformity (27). In addition, such powders can be mixed with the other diluents and then compressed into tablet.

Therefore, the objectives of this study were to improve the drug solubility, increase lymphatic transport to avoid the hepatic metabolism and target the drug across endothelial cells via LDL receptors using SME tablet as delivery system. Natural oils composing of high purity of long chain fatty acid including castor oil (87% ricinoleic acid), olive oil (80% oleic acid), sunflower oil (68% linoleic acid) and corn oil (60% linoleic acid) were selected and the effect of nonionic surfactants and co-surfactants on the SME formation ability was also investigated. The SME properties such as transparency, size and size distribution and morphology of SME liquid and the solid state and physical properties of SME powders and SME tablets were characterized. The uptake and permeation of selected SME tablet were evaluated in Caco-2 cells. In addition, the apolipoprotein B and drug content in Caco-2 cells and secreted lipoproteins (chylomicron and VLDL) representing lymphatic transport were determined by ELISA and HPLC method, respectively. Co-culture of mouse brain endothelial cells (bEnd.3) and astrocytes (CTX TNA2) was used as *in vitro* BBB model to study the brain uptake and permeation.

CHAPTER II

REVIEW LITERATURE

Parkinson's disease

Parkinson's disease (PD) is one of the neurodegenerative disorders which most commonly found beside the Alzheimer's disease (1, 2). The incidence of PD obviously increased with age, especially over 60 years olds (3). The diagnosis of PD is primarily based on clinical examination which is characterized by a triad of motor symptoms including bradykinesia (slowness of movement), rigidity (an increase in muscle tone causing resistance to externally imposed joint movements) and resting tremor (4, 8) because the reliable diagnostic test or marker for PD are still not available (28, 29).

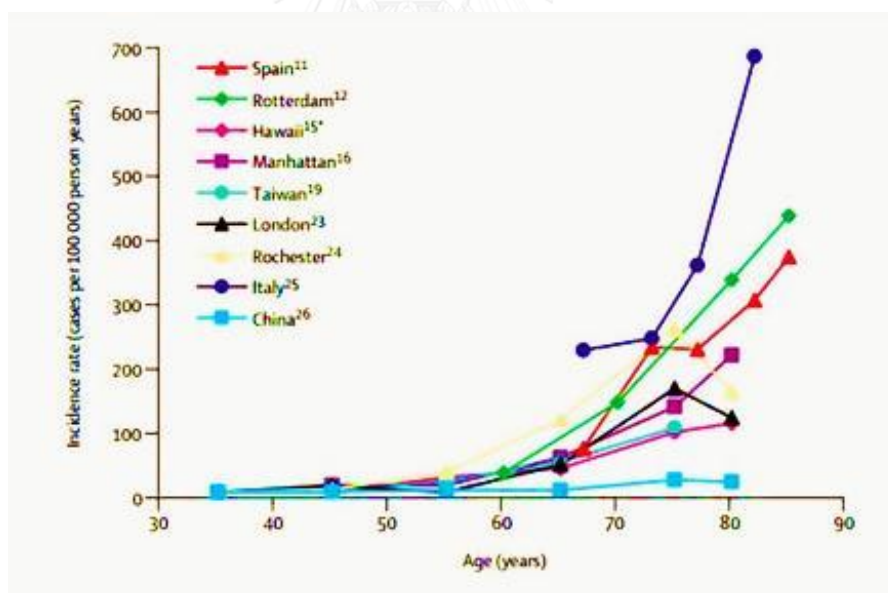


Figure II-1 Prospective population-based incidence studies of Parkinson's disease (28).

The cause of PD is still unknown but the environment and genetic factors were taken into account to identify the etiology of disease (5, 28). Losing of dopamine (DA) in the striatum resulting from the degeneration of the dopaminergic neurons in the pars compacta of the substantia nigra with the formation of α -synuclein positive staining cytoplasmic inclusion, known as Lewy bodies, is the pathological hallmark of the condition (4, 5). The failure of DA transmission from the substantia nigra to other brain centers such as the caudate nucleus and the putamen lead to deterioration of initiating and coordinating motor activity (1, 6). The pathogenetic mechanisms might cause from oxidative stress, mitochondrial dysfunction and inflammation resulting in cell death (1).

To date, PD cannot be cured by any treatments yet but it was only slow down the progression of disease. Improving the restoration of the dopamine level in the CNS is the treatment approach for PD (6). Since 1960s, Levodopa (L-Dopa), precursor of dopamine, still was the first line drug and most widely used for PD (4, 7). Its zwitterionic property lead them being transported across blood-brain barrier (BBB) more than DA which cannot cross the BBB due to its positive charge (6). As seen in Figure II-2, the decarboxylase enzyme (DDC) will change the L-Dopa to DA at both peripheral and CNS. The storage DA in vesicle at pre-synaptic neuron will be released into the synaptic cleft and attach with the DA receptor (DAR) at the post-synaptic neuron. The DA will be returned and stored into the pre-synaptic neuron by the DA transporter. However, the concentration of DA delivered to DA receptor might decrease by being metabolized via mitochondria monoamine oxidase type B (MAO-B) and catechol-O-methyltransferase (COMT) into the 3,4-dihydroxyphenylacetic acid (DOPAC) and 3-methoxytryamine (3-MT), respectively. Moreover, the reuptake of DA at presynaptic terminals also undergoes via transporter (10, 30). Any substances that can block these enzyme functions or inhibiting the reuptake will keep more DA level at post-synaptic neuron. Therefore, the carbidopa or benserazide (peripheral decarboxylase inhibitor), selegiline (MAO-B inhibitor) and entacapone (COMT inhibitor) were normally combined with L-Dopa to improve treatment efficiency (12).

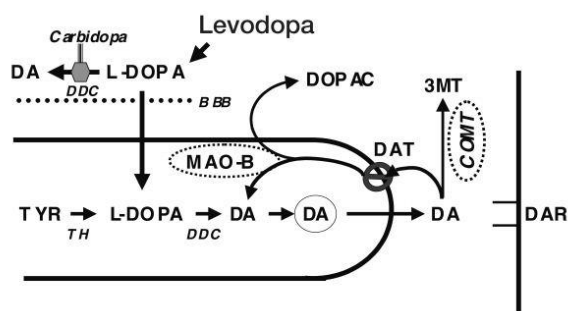


Figure II-2 DA biosynthesis in a nigrostriatal nerve terminal (30).

Although L-Dopa is still the most efficacious drug for PD treatment, they also caused significant dyskinesias and motor fluctuations which limit their effectiveness for long-term usage (8-10). The continuing of neuron cells death when the disease progress resulting in lower response to L-Dopa because of losing ability to store and release DA (10). The uncertain DA released lead to pulsatile stimulation of DA receptor which cannot mimic the physiological condition that these receptors are activated continuously. Therefore, the treatment approach to reduce the motor complications was considered (11). DA agonists have found to be an alternative to L-Dopa for initial treatment due to less dyskinesia and motor fluctuation because of their longer half-life (12-15). Moreover, they directly attach to DA receptor at post-synaptic neuron, bypassing conversion step to change the L-Dopa to DA (12).

Bromocriptine Mesylate

Bromocriptine (BC) is the first DA agonist which is indicated for PD treatment (31). It is D_2 receptors agonist and mild D_1 and 5-hydroxytryptamine (5-HT) antagonist (13, 31, 32). Since 1978, BC is still used in early stage as monotherapy to delay therapy with L-Dopa or adjunct therapy to prolong L-Dopa treatment and reduce the motor complications (12, 15, 33, 34).

Generic Name	Mechanism(s)	Initial Dose	Maintenance Dose
Amantadine	Multiple	100 mg b.i.d.	100 mg b.i.d.-t.i.d.
Benztropine	Anticholinergic	0.5 mg q.h.s.	1 mg b.i.d.-t.i.d.
Bromocriptine	Dopamine agonist	1.25 mg q.d.-b.i.d.	5–10 mg b.i.d.-t.i.d.
Carbidopa/levodopa	Converted to dopamine	25 mg/100 mg b.i.d.	Variable
Pergolide	Dopamine agonist	0.05 mg q.d.-b.i.d.	0.75–1 mg t.i.d.
Pramipexole	Dopamine agonist	0.125 mg t.i.d.	1.5 mg t.i.d.
Ropinirole	Dopamine agonist	0.25 mg t.i.d.	2–8 mg t.i.d.
Selegiline	MAO-B Inhibitor	5 mg q.d.-b.i.d.	5 mg b.i.d.
Trihexyphenidyl	Anticholinergic	1–2 mg q.d.	2 mg b.i.d.-t.i.d.

Figure II-3 Medication used in the initial therapy of early Parkinson's disease in the U.S. (12).

Moreover, Takashima et al. revealed that BC could protect dopaminergic neuron from L-Dopa toxicity which might relate to the generation of free radical such as hydrogen peroxide and quinones by oxidation reactions from dopamine metabolism. The toxicity represented as percent survival compared to control of dopaminergic neurons from rat embryonic ventral mesencephalon decreased after treating with L-Dopa. Supplementation with BC after L-Dopa treatment resulted in significant increase of neurons survival. However, the protective effect of BC was decreased when D_2 antagonist, sulpiride, was also supplemented. These data suggested that the neuroprotective effect of BC depend on its activation of D_2 agonist. The stimulation of dopamine autoreceptors of BC at axon terminal could reduce its dopaminergic excitability and inhibits DA synthesis and release, avoiding free radical generation from DA metabolism (35).

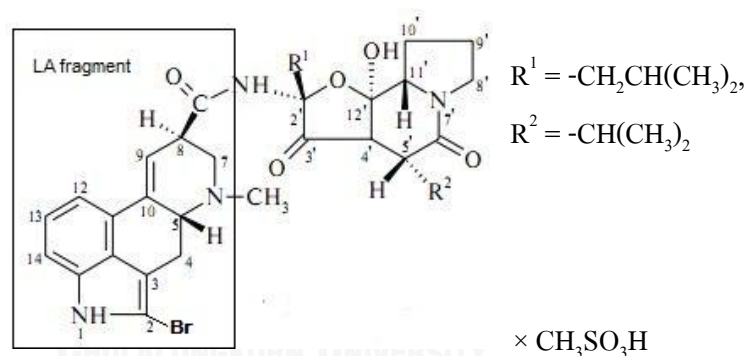


Figure II-4 Chemical structure of bromocriptine mesylate (36).

BC is 2-bromo- α -ergocryptine which is peptide ergot alkaloids containing the lysergic acid (LA) fragment and tripeptide group (Figure II-4) (36). The bromination of α -ergocryptine in C-2 position with N-bromosuccinimide in dioxane solution provides its potent dopaminergic agonist, preferably D_2 receptors. The form of BC in marketed formulation was bromocriptine mesylate (BM), 2-bromo- α -ergocryptine methanesulphonate. The molecular weight of the free base is 654.61 while their mesylate salt is 750.71 (16).

BM is poorly soluble in water (< 0.1% at 25°C) but freely soluble in methyl alcohol (> 70% at 25°C). The solubility in simulated gastric and intestinal fluids at 37 ± 2 °C is less than 0.1% (16). BM is well absorbed and peak plasma levels are reached within 1-3 hours after oral administration. The absorption half-life is between 0.2 – 0.5 hours. Ninety six percentages of drug bind to serum albumin. The high hepatic extraction rate and extensive metabolism leading to more than 90 percent of the absorbed drug metabolized by the liver via cytochrome P450 (CYP3A). Only about 7% of unchanged drug reach the systemic circulation. Almost all parent drug and their metabolites are excreted from feces via the liver while only 6% was eliminated by the kidney in urine.

Many studies (17-19) developed the BM formulation to avoid the hepatic metabolism, improve the bioavailability and effectiveness or reduce the motor complications. Degim et al. (17) incorporated BM into the gel formulation which was delivered via transdermal route. The advantages of transdermal over oral delivery are avoiding hepatic first pass effect and possible to terminate the drug administration suddenly in problematic cases. BM loaded gel formulations were applied to rabbit's skin compared to oral administration of commercial BM tablet. The comparable AUC values were found between the gel formulations containing either chitosan or Gantrez-SP215 and tablet formulation.

Lipid nanoparticles were also developed. Esposito et al. (18, 19) used the solid lipid nanoparticles (SLN), monoolein aqueous dispersions (MADs) and nanostructured lipid carriers (NLCs) as delivery systems to transport BM to the brain through blood brain barrier (BBB). The lipophilic nature of these systems was suitable to incorporate the lipophilic drug like BM into the formulation. In addition, their nano-size might ameliorate the brain transport through BBB which allowed the penetration of small and/or lipophilic molecules. The sustained release of drug from the solid matrix particles of such lipids would be expected to provide stable plasma levels and prolong drug half-life resulting in reducing motor complications. The experimental results showed that the slower drug release was found in the BM

encapsulated SLN than free BM. The drug efficiency for treating akinesia of all formulations was evaluated in hemiparkinsonian rats. Both free drug and drug loaded lipid formulations could reduce akinesia in 30 minutes after intraperitoneal administration but the longer effect was found in SLN and NLC compared to control (saline and empty SLN/NLC/MAD). The prolong DA receptor stimulation of SLN and NLC formulations might be related to their ability to sustain drug release and keep the drug level constant in plasma. Therefore, the authors suggested that the nanostructured lipid carrier encapsulation might be an innovative drug delivery system for BM by increasing patient's compliance to therapy and reducing side effects.

Microemulsions

Microemulsions (ME) are one of the colloidal and lipid-based drug delivery systems which was defined as a single optically isotropic and thermodynamically stable liquid solution composing oil, water, surfactant (occasionally combine with a cosurfactant) (37-39). Due to their thermodynamically stable, it means that they can form spontaneously which no energy required for preparation and no phase separation between oil and water (39). In addition, their small droplet size (10-100 nm) which have the diameter less than one-fourth of the visible light's wavelength cause no light refraction leading to transparency to the eyes while emulsion with larger droplet size between 100–100,000 nm appear turbid or milky (37). The different characteristics of emulsion and ME are shown in Table II-1.

Table II-1 Different characteristics between emulsion and microemulsion (ME) (37, 40).

Characteristics	Emulsion	Microemulsion
Size of droplet	100 – 100,000 nm	10 – 100 nm
Microstructure	Droplet	Droplet or bicontinuous
Number of phase	Two	One
Appearance	Turbid to milky	Transparent to translucent
Proportion of dispersed phase	30% – 60%	23% - 40%
Formation	High energy input required	Spontaneous
Stability	Thermodynamically unstable	Thermodynamically stable
Concentration of surfactant	2% - 3% by weight	More than 6% by weight

ME are likely formed into three types including oil in water (o/w), bicontinuous and water in oil (w/o) microemulsion depending on the compositions (41). The o/w ME are usually formed when the water volume fraction is higher than oil volume fraction, whereas w/o ME are produced when the water volume fraction is low. The similar amount of oil and water in the system will promote bicontinuous phase (Figure II-5) (40).

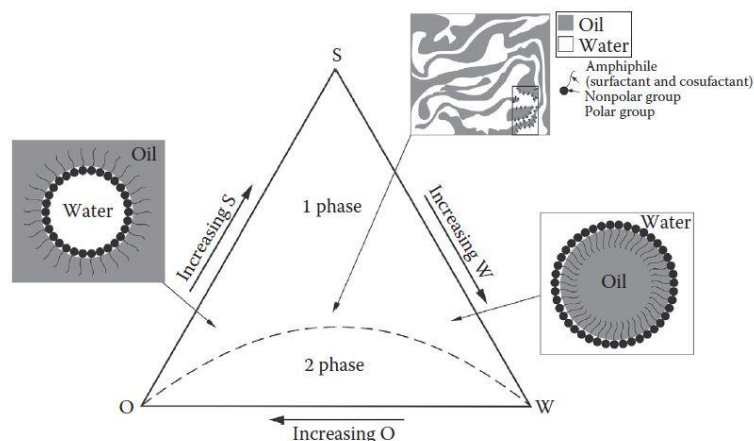


Figure II-5 Formation of three types ME at different ratios of oil, surfactant and water represented in the ternary phase diagram (40).

The capability to solubilize both soluble and poorly-soluble drugs of ME is useful for drug delivery system (39). In case of poorly-water soluble drugs which the dissolution is the rate limiting step for oral administration, they can be the solubilized form in the ME formulation when delivered into the gastro-intestinal (GI) tract, increasing drug absorption and bioavailability (38). These potential mechanisms were reported to enhance bioavailability including

1) Increasing in drug solubility

Poorly water soluble drugs can dissolve in oil phase and being in solubilized form until absorption (42). Moreover, the secretion of bile salts and biliary lipids are stimulated by the presence of lipids leading to the formation of intestinal mixed micelles, increasing solubilizing capacity of GI tract (43). In addition, such micelles could transport the drug through unstirred water layer which is a physical barrier for hydrophobic drugs before absorption (24).

2) Stimulation of lymphatic transport

Long chain fatty acid containing in the formulations may stimulate intestinal lymphatic transport, avoiding hepatic metabolism (44).

3) Changing barrier function of intestinal cells

Surfactants may disturb both biochemical barrier such as efflux transporters and physical barriers of intestinal cells, improving mucosal permeability (43).

In addition, the ME structure, partitioning of drug between oil and water phases, site or part of absorption, metabolism of ME, effect of ME on gastric emptying also result in improving the absorption. The other advantages of ME are shown in Table II-2.

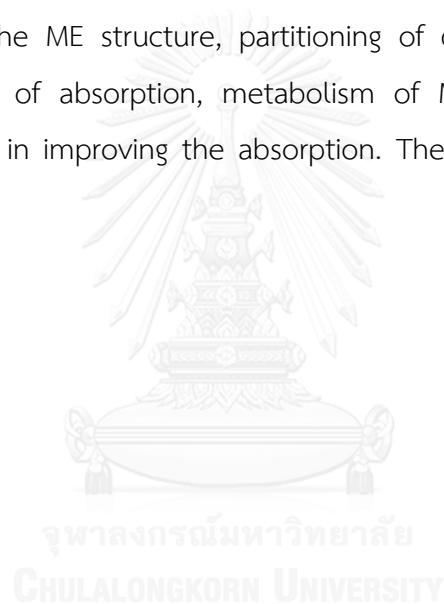


Table II-2 Advantages of microemulsions system.

General advantages
<ul style="list-style-type: none"> ● Easy to prepare ● Clear or transparent ● Stable ● Ability to be filtered ● Vehicle for drugs of different hydrophobicity in the same system ● Low viscosity leading to no pain on injection
Specific advantages
<p>1) Water in oil (w/o)</p> <ul style="list-style-type: none"> ● Protection of water soluble drugs ● Increasing bioavailability ● Sustained release of water soluble drug <p>2) Oil in water (o/w)</p> <ul style="list-style-type: none"> ● Increasing solubility of lipophilic drugs ● Increasing bioavailability ● Sustained release of oil soluble drug <p>3) Bicontinuous</p> <ul style="list-style-type: none"> ● Concentrated formulation of both oil and water soluble drugs

Self-microemulsion drug delivery systems (SMEDDS)

Self-microemulsion drug delivery systems (SMEDDS), microemulsion preconcentrates, are isotropic mixtures of oils, surfactants and/or cosurfactants. The difference between SMEDDS and ME is that no water contains in the SMEDDS but the ME could be spontaneously formed when they were diluted with an external

aqueous medium or biological fluid under mild agitation or digestive motility after *in vivo* administration (21).

The objectives of SMEDDS preparation are improving the solubility, absorption and bioavailability of poorly water soluble drugs as well as ME systems (21). Kang et al. (45) developed SMEDDS of simvastatin and evaluated the oral bioavailability in beagle dogs compared to conventional tablet (Zocor[®] tablet). The area under the curve (AUC) of SMEDDS was about 1.5 times greater than Zocor[®] tablet and the relative bioavailability of SMEDDS to Zocor[®] tablet was 158.9%. In addition, the effect of droplets size (33 and 150 nm) of SMEDDS formulation on the oral bioavailability was also observed. It was found that SMEDDS with smaller droplets size (158.9%) gave higher relative bioavailability than SMEDDS with larger droplets size (142.85%). They explained that a larger surface area obtained from small droplets size promoted the higher drug absorption. However, increasing in droplets size to 150 nm of SMEDDS still provided higher bioavailability than conventional tablet. The enhancing oral bioavailability of silymarin by SMEDDS was also studied by Wu et al. (46). Silymarin solution, suspension and SMEDDS were given to rabbits by gavage administration. After 2 hours administration, blood samples were collected and analysis. The SMEDDS showed greater relative bioavailability which was 1.88 and 48.82 folds of solution and suspension, respectively. They assumed that the lymphatic transport stimulated by long chain fatty acid might contribute to increase the bioavailability of SMEDDS because Peyer's patch was rich at the middle and distal parts of intestine which were absorption sites of silymarin. The increasing in absorption and bioavailability by SMEDDS was also reported in many studies (20, 47-52).

Due to their spontaneous formation, not all ingredients can produce ME. The effect of oils, surfactants or cosurfactants on the ME formation was investigated by many researchers (53-59). Until now, the certain factors that can generate ME are still debated. Therefore, a reasonable selection of excipients is the most important for ME preparation. There are many factors that should be considered. Therefore, a

reasonable selection of excipients is the most important for ME preparation. There are many factors that should be considered.

1. Selection of the excipients to prepare the SME formulations

Not all excipients could produce ME, therefore, the ME formation depends on the components contained in the system. Oils and surfactants and/or cosurfactants were selected corresponding to many consideration factors. The excipient's toxicity is the most important issue for pharmaceutically acceptable ME preparation (40). The second requirement is the capability of excipients to produce ME (60).

1.1) Oils

Many types of oils were selected to be used in pharmaceuticals. Most oils which were successfully used to prepare ME or SME are semi-synthetic such as fatty acid esters, mono-, di-, and triglycerides, polyethylene glycol derivatives of glyceride and fatty acids or polyglyceryl fatty acid esters rather than the natural or vegetable oils which contain mixing of fatty acids of varying chain lengths and degrees of unsaturation. The uncertain fatty acid distribution due to their natural origin, low purity, poor solubilizing ability and more difficult to microemulsify limit their usage (38, 40). However, using vegetable oils to produce ME are still receiving broader interest due to their low toxicological concern (61) and economical reason. Many researchers are paying attention to produce the biocompatible pharmaceutical ME based on excipients with food grade, generally recognized as safe status or orally safe. Using biocompatible excipients such as vegetable oils is the next challenge for ME development (21). Moreover, the advantage of long chain triglyceride oils over the others is the transportation of drug to lymphatic system, bypass hepatic first pass metabolism which is suitable for drug with extensively metabolized by the liver (23-25). The bioavailability of those drugs was improved when they were transported into the systemic system via lymphatic pathway (22, 62).

1.2) Surfactants

The ME are formed when an ultra-low interfacial tension ($< 10^{-3}$ mN/m) is reached. The quantity of surfactant molecules at oil/water interface must be enough to stabilize the created large surface area. Normally, the high concentration of surfactant (10-40%) is needed to produce ME (60). Therefore, the toxicity of surfactant used must be concerned. Non-ionic surfactants are more acceptable than ionic-surfactants for oral use due to their lower toxicity (63). In addition, they can resist to pH and electrolyte concentration because they are uncharged (41). Mostly lipid-based delivery systems used only non-ionic surfactants (64). Such non-ionic surfactants include polyoxyethylene sorbitan *n*-acyl ester, polyoxyethylene *n*-alkyl ethers, sucrose ester, polyglycerol fatty acid ester, polyoxyethylene castor oil and sorbitan ester (40, 41). However, not all of non-ionic surfactants have favorable safety profile. The single chain surfactants are more toxic than bulky surfactants such as polyoxyethylene sorbitan ester (Tween[®]) and polyethoxylated vegetable oils (Cremophor[®]), and ethers are more toxic than esters (64).

Besides the safety, the hydrophilic-lipophilic balance (HLB) of surfactants is also being the selection criteria. The lipophilic and hydrophilic properties of surfactants are classified according to their HLB value. Surfactants with low HLB values (<9) are considered to be lipophilic while those with high HLB values (>11) are considered to be hydrophilic (38, 65). The surfactants with high HLB were required to produce o/w emulsion or SME (66). Moreover, the HLB of surfactants should be matched with the required HLB of oils when the o/w emulsions were prepared (65). Such matching HLB gave the lowest interfacial tension between oil and water phases (56). The smallest size of emulsion droplets were also obtained when the HLB of surfactants and dispersed phase are matched (58). The desirable HLB are provided by blending of lipophilic and hydrophilic surfactants.

Table II-3 Percent fatty acid content and required HLB of selected oils (65).

Oils	Melting point	Myristic	Palmitic	Palmitoleic	Margarinic	Stearic	Oleic	Ricinoleic	Linoleic	Linolenic	Eicosanoic	Behenic	Required HLB
Caster oil	-12	-	2	-	-	1	7	87	3	-	-	-	14
Corn oil	-10	0.1	11	0.2	0.1	2	25	-	60	1	0.4	0.1	8
Olive oil	-6	-	9	0.6	-	3	80	-	6	0.7	0.4	-	7
Sunflower oil	-18	0.1	7	0.1	0.1	5	19	-	68	0.8	0.4	0.1	7



However, the formation of o/w emulsion would not depend on only HLB value. The structure of surfactants also affected the efficiency of emulsion stabilization (58, 67). Gullapalli and Sheth (58) reported that the similarity of chain length of lipophilic part between the surfactant and dispersed oil phase could produce the stable o/w emulsions. In addition, the inequality in chain length between two surfactants used and presence of double bond could generate the smallest size of nanoemulsions (67).

1.3) Cosurfactants

Generally, the main objectives of cosurfactants for ME preparations are dissolving the drug, increasing solvent capacity and improving the dispersion capability of the system by facilitating water penetration into the formulation (38, 64). The rigid hydrocarbon region of interfacial film was fluidized by cosurfactants leading to more flexible film and less condensed, promoting ME formation. Medium hydrocarbon chain length (C3-C8) with a polar head group such as hydroxyl, amine, sulfoxide or *n*-oxides were usually used as cosurfactants because their amphiphilic nature, short hydrophobic chain and terminal hydroxyl group enable them to diffuse between the immiscible phase and interfacial film and interact with surfactant monolayers at the interface thereby affecting their packing (40). In addition, the shorter chain length (C2) such as ethyl alcohol could swell the head region more than the tail region, giving the positive curvature, tending to promote o/w system (37). Moreover, the usefulness of short chain alcohols for ME preparation was the decreasing in surfactant concentration (59).

Intraluminal processing of SMEDDS

The intraluminal lipid processing is the important event determining *in vivo* absorption of lipid-based formulations such as SMEDDS. After oral administration, the lipid emulsification initially takes place at the stomach by a combination of gastric agitation and gastric emptying yielding nano-size droplets (Figure II-6a). Some triglyceride (TG) is hydrolyzed to diglyceride (DG) and fatty acid (FA) by gastric lipase secreted by gastric mucosa. Thereafter, the dispersed droplets enter the small intestine and the secretion of bile salts (BS), phospholipid (PL) and cholesterol (Ch) from gall bladder and pancreatic fluids (pancreatic lipase/co-lipase) from pancreas are stimulated by the presence of lipids (68).

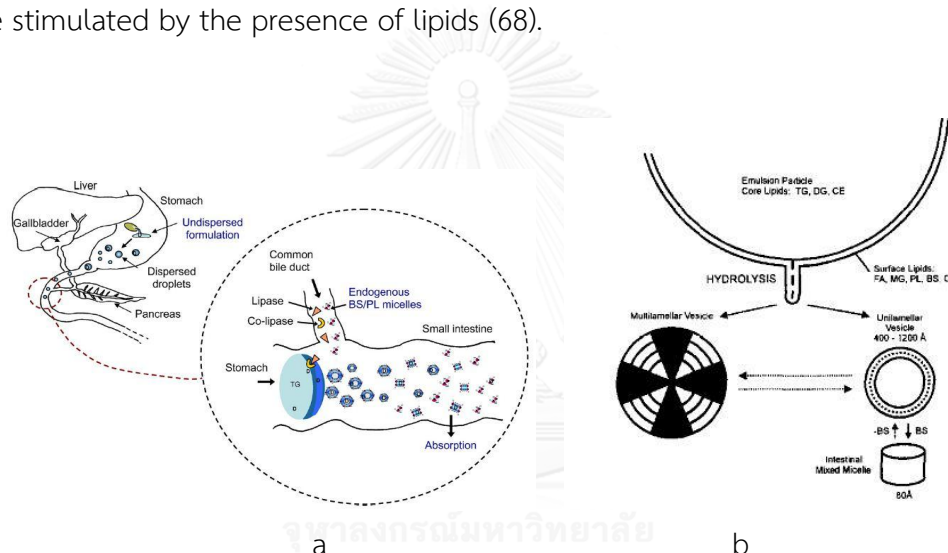


Figure II-6 Intraluminal process of SMEDDS a) Dispersion in stomach and delivery to small intestine and b) Digestion of lipid droplets by bile salts and biliary lipids (44, 68) after oral administration.

Bile salts, PL and Ch then adsorb at the surface of droplets, stabilising and reducing droplets size (Figure II-6b). The digestion processes continue by the action of pancreatic lipase/co-lipase complex. The hydrolysis of TG by pancreatic lipase produces 2-MG and two FA molecules. The activity of pancreatic lipase is inhibited

by binding of BS and PL at the oil/aqueous interface at physiological conditions. Such activity is restored by complexing with co-lipase at 1:1 lipase to co-lipase ratio. This complex allows binding of lipase at the surface of droplets. In addition, digestion products (FA and MG) also promote binding of lipase/co-lipase complex. As the lipolysis proceeds, digestion products will bud off from the droplets surface producing liquid crystalline structure which changes to multilamellar, unilamellar structure and finally intestinal mixed micelles when the sufficient BS concentrations are introduced (44). These mixed micelles could enhance up to 1000 folds luminal solubility of digestion products (23).

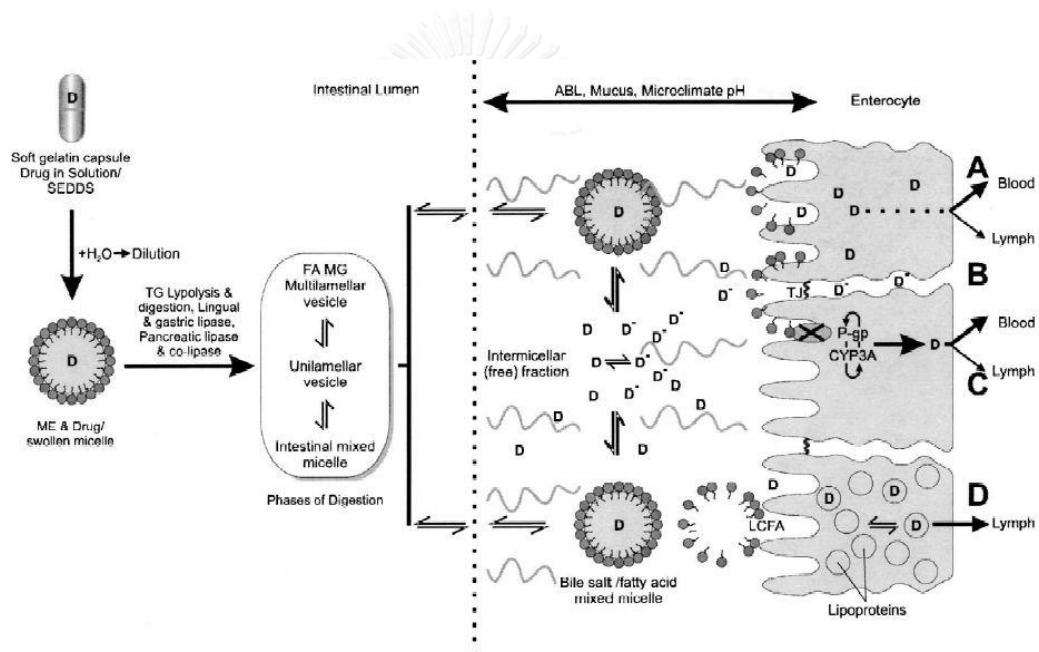


Figure II-7 Absorption process of lipid-based delivery system across enterocytes (24).

The intestinal mixed micelles deliver the drug solubilized fatty acid across unstirred water layer which is the absorption barrier of poorly water soluble drugs to the enterocyte cells, providing a concentration gradient for absorption (Figure II-7) (23). A microclimate acidic pH adjacent to enterocyte cells cause a dissociation of micelles and release the lipid for further absorption (24). The transport pathways of lipid across the enterocyte membrane occurs via both passive transport and specific membrane-bound carrier proteins such as fatty acid binding protein (FABP) (23).

Lymphatic transport systems

After lipid absorption into enterocytes, drug is then transported to systemic circulation through either portal blood or lymphatic pathway. Generally, short and medium chain fatty acids ($C < 12$) enter to blood capillaries while long chain fatty acids ($C > 12$) are secreted into mesenteric lymph (23).

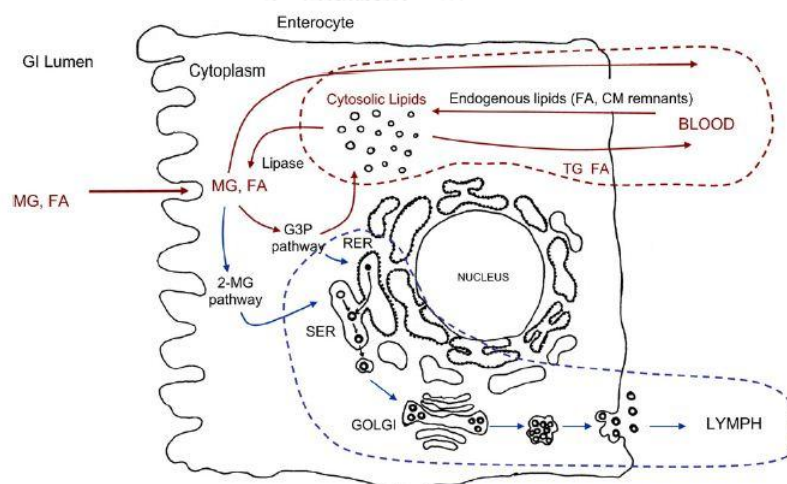


Figure II-8 Intracellular process in enterocyte of long chain fatty acid transported via portal blood and lymphatic system (25).

The intracellular process for lymphatic transport initially occurs at endoplasmic reticulum. Long chain fatty acids migrate from absorptive sites to endoplasmic reticulum (Figure II-8). Thereafter, fatty acids are re-esterified to triglyceride via 2-monoglyceride pathway or glycerol-3 phosphate pathway (25) and formed into TG-rich lipid droplets in smooth endoplasmic reticulum (SER) together with the synthesis of apolipoproteinB (apoB) in the rough endoplasmic reticulum (RER) and its association with phospholipid (PL) present in the ER membrane yielding apo B-PL complex (Figure II-9). The addition of neutral TG lipids to apo B-PL complex produces primordial lipoprotein (PLp) which is then released to the lumen of ER. The core expansion process continues by fusion of TG-rich lipid droplets formed in SER with primordial lipoprotein (PLp) formed in RER. The produced lipoproteins are then transferred to golgi apparatus, subsequently fuse with the basolateral membrane of enterocyte cells and released into lamina propria where they are absorbed by capillaries of mesenteric lymphatics (23). The types of secreted lipoproteins depend on amount of lipid loading. The very low density lipoprotein (VLDL) are more produced when low intestinal lipids are loaded (fasted state) while chylomicron production enhanced under high lipid loading conditions (23).

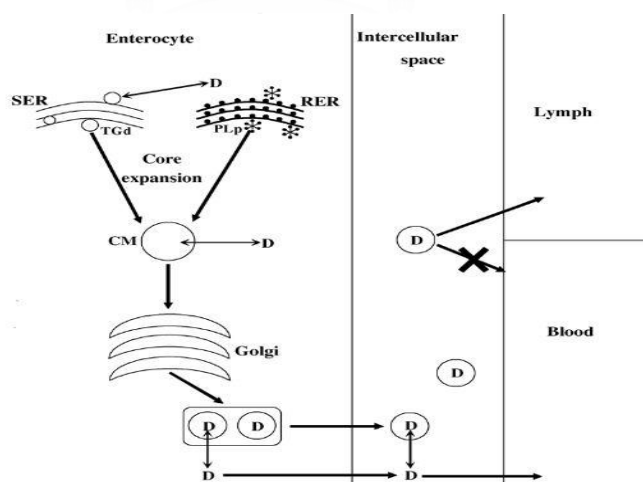


Figure II-9 Lipoprotein assemble within enterocyte and drug transportation to lymphatic system (69).

Following the secretion to capillaries of mesenteric lymph, the drug flows through lymph duct to the cisterni chyli and thoracic duct. Finally, it is directly drained into blood circulation at the junctions of left jugular and left subclavian veins, by pass the liver (24). Therefore, this transport pathway could enhance the bioavailability for drugs which are extensively metabolized by the liver (25).

The effect of lymphatic transport on oral bioavailability of rapamycin loaded SMEDDS was studied by Sun et al. (22). The chylomicron flow blocking approach using cycloheximide solution as chylomicron blocker was used to estimate the intestinal lymphatic transport. The chylomicron is mainly secreted lipoprotein to transport the drug via lymphatic pathway. It means that drug will be transported by only portal blood pathway if the chylomicron flow which is essential process for lymphatic transport is blocked. Therefore, the rats were pretreated with either cycloheximide solution or saline before drug administration. After that, drug loaded SMEDDS containing 25% oil or drug loaded oil-free formulation were given by gavage.

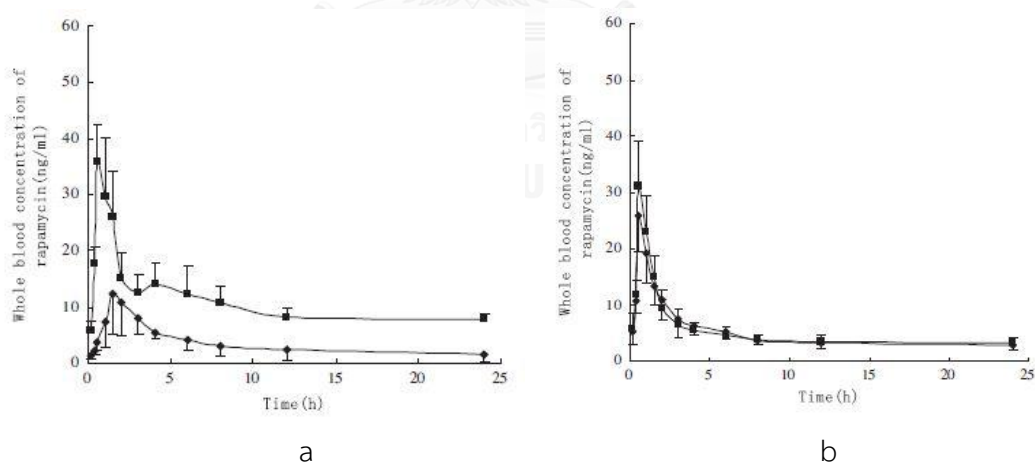


Figure II-10 Plasma drug concentration versus time profiles after oral administration of a) SMEDDS formulation, b) Oil-free formulation to rat pretreated with saline (■) or cycloheximide (◆) (22).

It was found that the plasma drug concentration after SMEDDS administration was significant higher in rats treated with saline than those treated with cycloheximide (Figure II-10a), whereas no difference between 2 groups was observed when the oil-free formulation was given (Figure II-10b). These results revealed that drug was transported via lymphatic pathway for SMEDDS because the oral bioavailability decreased when the lymphatic transport was inhibited. However, blocking of lymphatic pathway didn't affect the bioavailability of oil-free formulation leading to the same plasma concentration both in rats treated with saline and cycloheximide solution. The AUC of SMEDDS (258.0 ± 22.4) was significant higher than that of oil-free formulation (122.8 ± 29.4) ($p < 0.05$). This suggested that SMEDDS with suitable oil concentration could stimulate the lymphatic transport, enhancing oral bioavailability of poorly-water soluble drug such as rapamycin (22).

Caco-2 model for lymphatic transport study

Caco-2 cells are intestinal cell line derived from human colorectal carcinoma. They are usually used for screening and predicting the drug absorption and permeation before *in vivo* testing due to its easier and small quantities of drug required (70). In addition, not only intestinal permeation study, the lymphatic transport is also studied in Caco-2 cells because the lipid processing occurring *in vivo* exists in Caco-2 cells (24). The synthesis of ApoB followed by the production and secretion of lipoproteins such as chylomicron and VLDL which are essential for lymphatic transport has been identified and characterized in Caco-2 cells (71-74).

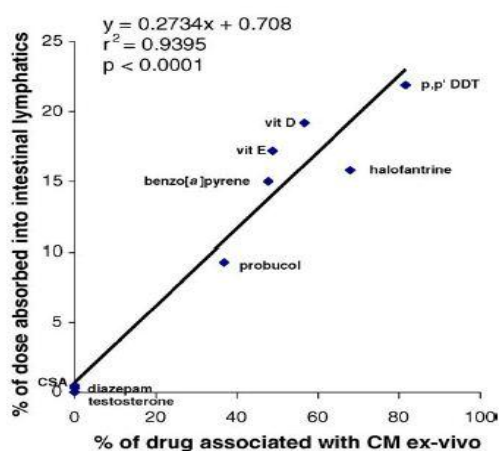


Figure II-11 The relationship between percent of drug absorbed into intestinal lymphatic and percent of drug associated with chylomicron in the *ex vivo* model (69).

The correlation between percent of drug incorporated into chylomicron and intestinal lymphatic bioavailability of lipophilic drug was also observed by Gershkovich and Hoffman (69). The lipophilic drugs which have shown to have significant absorbed and not absorbed into the lymphatic systems were incubated with isolated chylomicron to uptake the drug. The percent of drug uptake in chylomicron was then compared to the intestinal lymphatic bioavailability data from previous reports. It was found that drugs with higher uptake into chylomicron also showed the higher lymphatic bioavailability, whereas those drugs with no uptake in chylomicron showed the low lymphatic bioavailability. Moreover, a linear correlation ($r^2 = 0.94$, $p < 0.0001$) between percent drug uptake in chylomicron and intestinal lymphatic bioavailability was obtained (Figure II-11). This suggested that the study of lipophilic drug uptake in chylomicron can be used as screening model to predict the lymphatic bioavailability *in vivo*.

Solid self-microemulsion drug delivery systems (Solid SMEDDS)

Some disadvantages of SMEDDS liquid such as low stability and portability and a few choice of dosage forms, solid SMEDDS has been introduced as alternative approaches. Solid SMEDDS are the solid dosage forms that possess the self-microemulsions properties. The advantages of SMEDDS such as improving solubility and bioavailability and solid dosage form such as high stability and better patient compliance were combined in solid SMEDDS (27).

There are many techniques to transform liquid SMEDDS to solid SMEDDS including capsule filling, spray drying, adsorption to solid carriers, melt granulation, melt extrusion/extrusion spheronization (27). Therefore, various solid dosage forms were produced. The SMEDDS characteristics of spray dried powders (75, 76), adsorbed powders/granules (77, 78), hard gelatin capsules (79, 80), tablets (81), microcapsules (82), pellets (83) were prepared.

In this study, the adsorption technique was selected to prepare the SME powders because it is a simple method. The adsorption of SME liquid onto solid carriers is just mixing them together in mortar or blender. In addition, they can adsorb the high level (70% w/w) of liquid and provide the free-flowing powders and good content uniformity (27).

Hydrophilic fumed silica such as Aerosil[®] 200 was a basic porous carrier which was commonly used for liquid adsorption in many studies (77, 84, 85). However, their fuming characteristic probably makes them difficulty to operate. The granulated form of silicon dioxide such as Aeroperl[®] 300 might be used as an alternative choice. They consist of bead-like mesoporous granule and their higher tapped density causes them easier to handle and less dust. Besides pure silicon dioxide, magnesium aluminometasilicate, Neusilin US2[®], is also interesting in many studies due to their high liquid loading capacity and good flowability and tabletability (81, 84-86). Therefore, various pharmaceutically porous carriers including Aerosil[®] 200,

Aeroperl[®] 300 and Neusilin US2[®] with different characteristics were selected as solid carrier. Their properties before and after liquid adsorption were evaluated and compared. The physical properties of solid carriers are shown in Table II-4.

Table II-4 The physical properties and compositions of selected solid carriers (87).

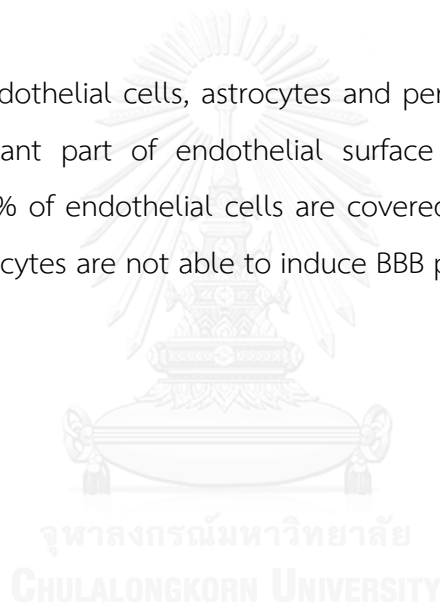
Solid carries	Characteristics	Compositions (%)	Mean particle Size (μm)
Aerosil [®] 200	Fine, white, amorphous powder	SiO ₂ ≥ 99.8	0.012 (primary particle size)
Aeroperl [®] 300	Fine, white, amorphous powder	SiO ₂ = 100	30
Neusilin US2 [®]	White powder, odorless and tasteless	Al ₂ O ₃ = 32.1 MgO = 12.5 SiO ₂ = 32.2	80

Solid SMEDDS could improve the oral bioavailability of poorly-water soluble drugs similar to liquid SMEDDS. Yi et al. (75) formulated the nimodipine into solid SMEDDS by spray-drying technique using dextran as solid carrier. The drug loaded solid SMEDDS and liquid SMEDDS were orally administered to rabbits compared to conventional tablet. The AUC values obtained from plasma concentration versus time profile of solid SMEDDS and liquid SMEDDS were not statistically different ($p > 0.05$) but significant greater than conventional tablet. These results were in line with Setthacheewakul et al. (83) who also observed the plasma concentration in rat after oral administration of curcumin loaded SMEDDS pellets, liquid SMEDDS and aqueous suspension. The results found that the AUC values obtained from SMEDDS pellets and liquid SMEDDS were about 10-13 times greater than those obtained from aqueous suspension.

Blood Brain Barrier (BBB)

Blood Brain Barrier (BBB) is the primary interface between the peripheral circulation and central nervous system (CNS) which consists of endothelial monolayer connected by tight junction (Figure II-12). Such tight junction acts as a barrier to restrict the drugs or toxic substances from blood to the brain. In addition, the low level of endocytosis and transcytosis characteristics of endothelial cells and large number of enzyme and efflux transporters located on the endothelial cells also increase the barrier functions (88). Due to the tight junction, the hydrophilic drug cannot enter to the brain via paracellular pathway (89).

Beside the endothelial cells, astrocytes and pericytes also promote the tight junction. The significant part of endothelial surface is covered by end feet of astrocytes and 22-32% of endothelial cells are covered by pericytes. The deficiency of astrocytes and pericytes are not able to induce BBB properties (88).



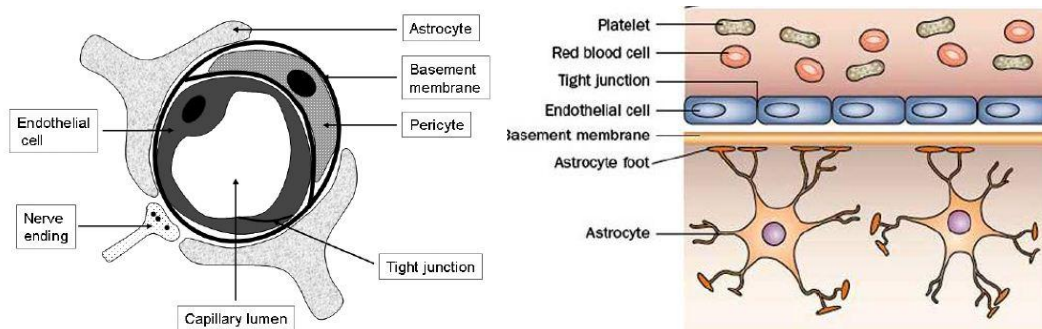


Figure II-12 Structure of blood brain barrier (BBB) (88, 90).

Brain transport

There are two major mechanisms involving transportation of drug across BBB including passive diffusion and endogenous carrier-mediated transport (Figure II-13).

1) Passive diffusion

The concentration gradient between blood and brain and physical properties of drugs will determine whether they can transport via this pathway. The poor BBB permeability of hydrophilic drugs which possess a molecular weight of > 400 Da, forming more than 8 hydrogen bonds with surrounding water, presence of quaternary ammonium group or more than 1 carboxy group were reported (90).

2) Endogenous carrier-mediated transport

Many drugs cannot transport by diffusion due to the limitation of their characteristics, however, the carriers or transporters specific to those drugs can deliver them across BBB.

2.1) Carrier-mediated transport

The pathway is responsible for delivery the nutrients such as sugar and amino acid, neurotransmitters and ions to the brain. Only small molecules are suitable for this mechanism due to its small and stereospecific pores (91).

2.2) Receptor-mediated transcytosis

The affinity of drugs or ligands to receptors is the primary requirement for receptor-mediated transcytosis. The activation of ligand-receptor complexes initiates the endocytosis from the blood side leading to formation transport vesicles followed by the exocytosis at the brain side of endothelial cells (90).

2.3) Absorptive-mediated transcytosis

The specific targeting is not necessary for this mechanism. This involves the charge interaction such as binding of polycationic molecules with negative charge on plasma membrane (91).

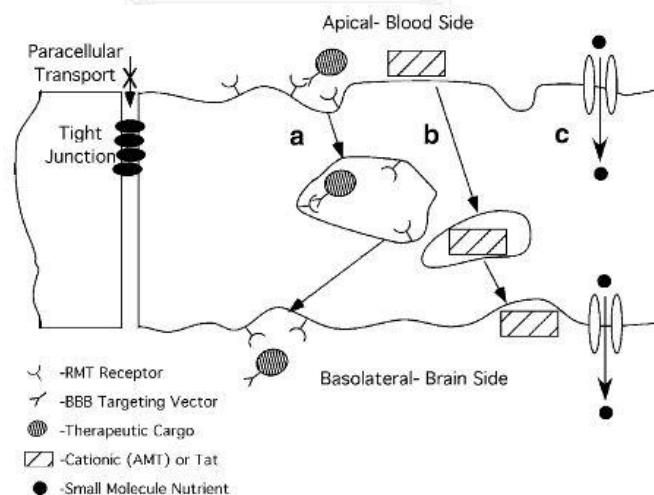


Figure II-13 Drug transport pathway across BBB a) Receptor-mediated transcytosis, b) Absorptive-mediated transcytosis, c) Carrier-mediated transport (91).

Role of apolipoprotein on brain transport

Low density lipoprotein (LDL) receptors are the cell-surface, expressing on brain endothelial cells. Their main function is removing apo B- and apo E-containing lipoproteins from plasma (92). The binding of apo B or apo E to LDL receptors lead to transcytosis to abluminal side of BBB, releasing and being taken up by neurons (26). Therefore, the specific of apolipoprotein to LDL receptors has been focused for targeting drug to the brain, overcoming BBB.

The surface-modified drugs by binding with apolipoprotein was approached to improve the brain transport. The LDL receptor-binding domain of the apo B was fused to targeted protein and given by i.p. injection to adult mice. The extent of delivered protein stained with immunofluorescence in CNS was determined. It was found that only fusing apo B LDL receptor-binding domain with proteins were observed in neurons and astrocytes as well as LDL receptor, whereas no staining of non-fusing proteins were found. These results revealed that LDL receptor-binding domain of the apo B promoted proteins uptake to CNS and LDL receptor was responsible for this uptake (26).

Apo E-modified nanoparticles were also prepared by attaching apo E3 to the surface of human serum albumin (HSA) nanoparticles. The fluorescence uptake by mouse brain endothelial cells (bEnd.3) of apo E-modified nanoparticles and PEGylated HSA nanoparticles were evaluated. (93). The intracellular uptake was significant higher when bEnd.3 cells were incubated with apo E-modified nanoparticles compared to PEGylated HSA nanoparticles and untreated cells. The difference in uptake was not observed between untreated cells and cells treated with PEGylated HSA nanoparticles. Moreover, the receptors involving the uptake were also determined. The bEnd.3 cells were incubated with either apo E-modified nanoparticles or PEGylated HSA nanoparticles together with LDL. As seen in Figure II-14, the percent uptake at 37 °C increased in case of apo E-modified nanoparticles (31.2% to 42.6% positive cells) whereas PEGylated HSA nanoparticles did not show

significant change in percent uptake (3.3% to 4.5% positive cells). At 4°C, no cellular uptake was observed in both nanoparticles formulations compared to untreated cells due to all active and energy consumptive transport processes are stopped at this incubation temperature. The observations suggested that LDL receptor involved the uptake of specific apo E-modified nanoparticles because the presence of LDL increased the binding capacity of apo E to receptors, enhancing the particles uptake. It is known that the presence of lipid such as phospholipids or lipoproteins lead to the high affinity of apo E to LDL receptors (93).

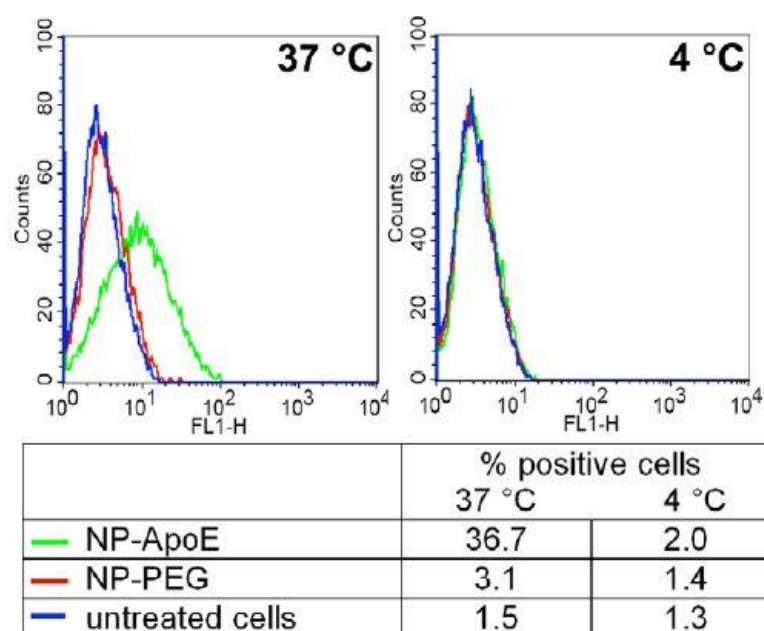


Figure II-14 Fluorescence uptake by incubation of bEnd3 cells with autofluorescence nanoparticles.

According to the improving brain transport of apolipoprotein, using polysorbate80 (Tween[®] 80) for targeting drug to brain has been interested because apolipoprotein could be absorbed on the surface of Tween[®] 80. The dalargin-loaded Poly (butyl Cyanoacrylate) (PBCA) nanoparticles and dalargin-loaded polysorbate 80-coated PBCA nanoparticles coated with or apo AII, B, CII, E or J were prepared by Kreuter at al. (94). The antinoinceptive response in mice was observed after i.v. injection. At 30 minutes after injection, only apo B- and apo E-coated nanoparticles showed a significant anti-analgesic effect better than uncoated nanoparticles. In addition, precoating nanoparticles with polysorbate80 before coating with apolipoprotein, all apo-coated nanoparticles gave the higher antinoinceptive response than nanoparticles without polysorbate 80-coating. This explained that coating apo B and apo E could enhance the transportation of dalargin-loaded nanoparticles across the brain. The polysorbate80 mainly acts as anchor to absorb plasma apo B and apo E on the surface after injection. The adsorption of apo B and apo E on nanoparticles mimics the endogenous lipoproteins leading to interact with LDL-receptor and then be taken up by endothelial cells via receptor-mediated endocytosis. The advantage of coating the drug or particles with polysorbate 80 for brain transport is also reported in many literatures (95-97).

In vitro cells line model of BBB

The advantages of cells line as a brain model over primary cultures are relatively low costs and no special skills required (88). The appropriate models should display a restrictive paracellular pathway, possess physiological realistic cell architecture such as morphology, distribution of organelles and transporters, the complexity of tight junction, display functional expression of transporter mechanisms and be easy to culture. Mouse brain endothelial cells bEnd.3 and bEnd.5 are the only immortalized cell lines commercially available from European Collection of Animal Cell Cultures (ECACC) or the American Tissue Culture Collection (ATCC) (98).

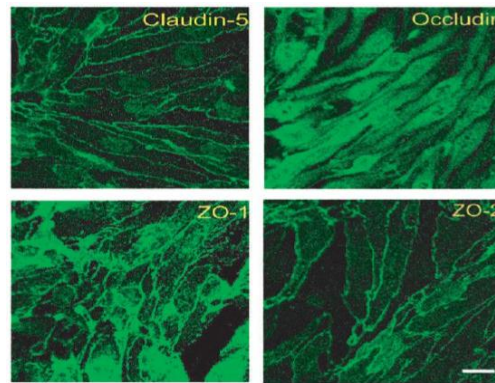


Figure II-15 Expression of tight junction proteins in bEnd3 cells.

The suitability of bEnd3 cells as BBB model was studied by Brown et al. (99). They found that mRNA for Claudin-5, Occludin, ZO-1 and ZO-2 which are necessary proteins maintained tight junction functions to form the paracellular barrier were expressed in bEND.3 cells (Figure II-15). In addition, the diffusion barrier to radiolabeled sucrose, paracellular permeability marker was also formed. However, the low TEER values of bEND.3 cells ($<100 \text{ ohm} \times \text{cm}^2$) was reported and correlated with other studies (87, 98). Therefore, co-culture of endothelial cells and astrocytes was established (100-102) to mimic the BBB in *in vivo* because the endothelial surface is covered by end feet of astrocytes which maintain the barrier functions of BBB. Moreover, the expression of LDL receptors is enhanced by co-culture of endothelial cells with astrocytes (103).

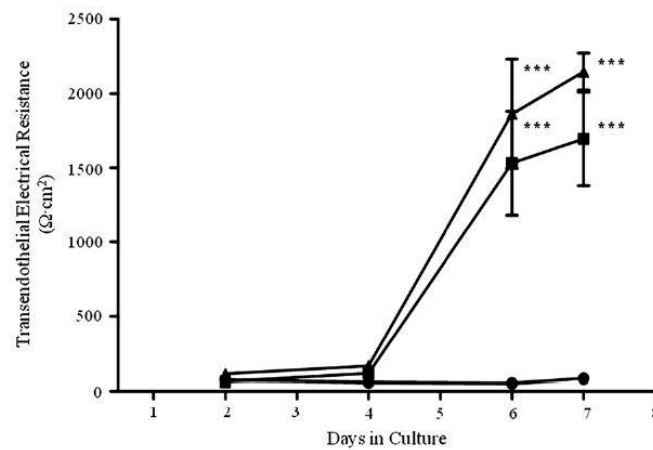


Figure II-16 Transendothelial electrical resistance (TEER) of primary porcine brain endothelial cell (PBEC) monoculture (●), PBEC co-cultured with primary rat astrocytes (■), PBEC co-cultured with rat astrocyte cell line, CTX TNA (▲) (104).

Primary porcine brain endothelial cells (PBEC) were co-cultured with either rat astrocyte cell line (CTX TNA2) or primary rat astrocytes isolated from 2-day old rat pups (104). The TEER values of both co-culture significant increase and higher than PBEC monolayer in day 6 after seeding ($p < 0.001$) (Figure II-16). This revealed that PBEC co-cultured with CTX TNA2 has a potential to be *in vitro* BBB model for brain transport study.

CHAPTER III

MATERIALS AND METHODS

Materials

All materials employed in this study were obtained from commercial sources and used as received.

- 1) Bromocriptine mesylate (Lot No. 72221000910, TEVA Czech Industries S.R.O., Czech Republic)
- 2) Castor oil (Lot No. 709308, Srichand United Dispensary Co. Ltd., Thailand)
- 3) Corn oil (Lot No. 040609, Thai Vegetable Oil Public Co. Ltd., Thailand)
- 4) Sunflower oil (Lot No.020311, Thai Vegetable Oil Public Co. Ltd., Thailand)
- 5) Olive oil (8346A6, SPIRE International L.L.C., United Arab Emirates)
- 6) Tween[®] 20 (Lot No. 709557, Srichand United Dispensary Co. Ltd., Thailand)
- 7) Tween[®] 80 (Lot No. 809861, Srichand United Dispensary Co. Ltd., Thailand)
- 8) Span[®] 80 (Lot No. 20910B, Srichand United Dispensary Co. Ltd., Thailand)
- 9) Cremophor[®] EL (Lot No. 81873116KO, BASF, Germany)
- 10) Polyethylene glycol400 (Lot No. 403351/1, Sigma-Aldrich, USA)
- 11) Propylene glycol (Lot No. 90511018GO, Srichand United Dispensary Co. Ltd., Thailand)
- 12) Glycerine (Lot No. 13/04, Srichand United Dispensary Co. Ltd., Thailand)
- 13) Ethyl alcohol (K37504083 729, MERCK, Germany)
- 14) Aerosil[®] 200 (Batch No. 4161061381, Nippon Aerosil Co. Ltd., Japan)
- 15) Aeroperl[®] 300 (Lot No. 3151011219, EVONIK Industries AG, Germany)
- 16) Neusilin US2[®] (Lot No. 010028, FUJI Chemical Industry Co. Ltd., Japan)
- 17) Hydrochloric acid (Lot No. K41831617, MERCK, Germany)
- 18) Ammonium carbonate (Lot No. 1002530, Agax Finechem Pty Ltd., Australia)

- 19) Acetonitrile (HPLC grade) (Lot No. 100197, Burdick & Jackson, Korea)
- 20) Methanol (HPLC grade) (Lot No. 10071753, Burdick & Jackson, Korea)
- 21) Potassium bromide (Lot No. SLBCO391V, Sigma-Aldrich, USA)
- 22) Fetal bovine serum (Lot No. 41Q1121K, Gibthai Co. Ltd., Thailand)
- 23) Dulbecco's Modified Eagle Medium (Lot No. 1552477, Gibthai Co. Ltd., Thailand)
- 24) 0.25% Trypsin-EDTA (Lot No. 1552477, Gibthai Co. Ltd., Thailand)
- 25) MEM Non-Essential amino acid solution (Lot No. 1516590, Gibthai Co. Ltd., Thailand)
- 26) Penicillin-Streptomycin (Lot No. 1235697, Gibthai Co. Ltd., Thailand)
- 27) Hank's Balanced Salt Solution (Lot No. 1213954, Gibthai Co. Ltd., Thailand)
- 28) 3-[4,5-Dimethylthiazol-2-yl]-2,5-diphenyltetra-zolium bromide (Lot No. MKBG1611V, Sigma-Aldrich, USA)

Equipment

- 1) 4-digit Analytical balance (A200S, Sartorius, Germany)
- 2) 5-digit Analytical balance (X205T, Mettler-Toledo, Switzerland)
- 3) Centrifuge (5810, Eppendorf, Germany)
- 4) Shaking Incubator (LSI-3016A, LabTech, Korea)
- 5) Differential scanning calorimeter (DSC822e, Mettler Toledo, USA)
- 6) Invert microscope (IX51, Olympus, Japan)
- 7) Zetasizer (Nano-ZS, Malvern, UK)
- 8) Powder rheometer (FT4 powder rheometer, Freeman Technology, UK)
- 9) Scanning Electron Microscope (JSM-6400, JEOL, Japan)
- 10) Transmission Electron Microscope (JEM-2100, JEOL, Japan)
- 11) Hydraulic tableting machine (4350.L, CARVER[®], USA)
- 12) Laminar air flow (Holten Laminar Air Model 1.2, Thermo Scientific, USA)
- 13) CO₂ Incubator (3111, Thermo Scientific, USA)
- 14) Ultracentrifuge (L-80, BECKMAN, USA)

- 15) Reverse-phase HPLC (SIL-20AHT, SHIMADZU[®], JAPAN)
- 16) Fluorescence-assisted cell sorter (BD-FACSAlibur, Becton Dickinson, USA.)
- 17) Microplate reader (VICTOR3, Perkin Elmer, USA).
- 18) TEER measurement (Millicell[®]-ERS meter, Millipore, USA)

Laboratory supplies

- 1) HPLC column (Hypersil[®]BDS C18 column, Thermo Scientific, USA)
- 2) Cell culture plates, 6-wells (Costar[®], USA)
- 3) 96-well Microplates (Costar[®], USA)
- 4) Transwell[®] Permeable supports, 6-wells (Costar[®], USA)
- 5) Apolipoprotein B (APOB) Human ELISA kit (GR161802-1, Abcam, UK)



Methods

1. Construction of pseudo-ternary phase diagrams (37, 49, 51)

Pseudo-ternary phase diagrams were used to prepare the ME formulations. The water titration technique was used to construct pseudo-ternary phase diagrams. Long chain triglyceride oils which possess high purity of long chain fatty acid including castor oil (87% ricinoleic acid), olive oil (80% oleic acid), sunflower oil (68% linoleic acid) and corn oil (60% linoleic acid) were selected as oil phase. The low toxic non-ionic surfactants with high HLB value, polyoxyethylene 20 sorbitan monooleate (Tween[®] 80, HLB=15), was used as the main surfactant. The other non-ionic surfactants including polyoxyl 35 castor oil (Cremophor[®] EL, HLB=14), sorbitan monolaurate (Span[®] 20, HLB=8.6), sorbitan monooleate (Span[®] 80, HLB=4.3) were selected to combine with Tween[®] 80 to investigate the effect of HLB and structure of surfactants on the ability of ME formation. Span[®] 80 (HLB=4.3) was combined with Tween[®] 80 (HLB=15) to adjust the HLB value of surfactants corresponding to the required HLB value of selected oils. The required HLB value to form o/w emulsion of sunflower oil, olive oil, corn oil and castor oil are 7, 7, 8 and 14, respectively. The combination ratio between Tween[®] 80 and Span[®] 80 to prepare a mixture of such specific HLB was calculated from following equations (65). Therefore, Tween[®] 80 and Span[®] 80 were mixed at ratio 1:1.89, 1:2.97, 1:2.97 and 1:0.103 in system containing corn oil, sunflower oil, olive oil and castor oil, respectively. In addition, ethanol (EtOH), propylene glycol (PG) and glycerin (Gly) were selected as cosurfactants.

$$\% \text{ of Tween}^{\circledR} 80 = \frac{100(\text{Desired HLB} - \text{HLB of Span}^{\circledR} 80)}{(\text{HLB of Tween}^{\circledR} 80 - \text{HLB of Span}^{\circledR} 80)} \quad \text{Equation III-1}$$

$$\% \text{ of Span}^{\circledR} 80 = 100 - \% \text{ of Tween}^{\circledR} 80 \quad \text{Equation III-2}$$

Surfactant and co-surfactant were mixed at fixed weight ratios of surfactant to cosurfactant (K_m) of 1:1, 2:1 and 3:1 giving surfactant mixtures. Oil and surfactant mixtures were then weighed in the screw-cap glass tubes and mixed at the weight ratios from 1:9 to 9:1. Thereafter, these mixtures were titrated dropwise with deionized (DI) water under moderate agitation using vortex mixture until the turbidity was shown. The weight percentage of oil, surfactant mixture and water which showed clear or transparent liquid were plotted as ME area on phase diagram. The maximum amount of water (%W_{max}) and oil (%O_{max}) solubilized and ratio of surfactant to water (S/W) obtained from ME region also calculated. All compositions contained in each system are shown in Table III-1.

Table III-1 The compositions contained in both single surfactant and surfactant mixture systems with/without cosurfactant.

Oils	Surfactants	Cosurfactants
1. Single surfactant systems		
Without cosurfactant		
Corn oil	Tween [®] 80	-
Sunflower oil	Tween [®] 80	-
Olive oil	Tween [®] 80	-
Castor oil	Tween [®] 80	-
With cosurfactant at K_m 1:1, 2:1 and 3:1		
Corn oil	Tween [®] 80	Propylene glycol Glycerin Ethanol
Sunflower oil	Tween [®] 80	Propylene glycol Glycerin

		Ethanol
Olive oil	Tween [®] 80	Propylene glycol Glycerin Ethanol
Castor oil	Tween [®] 80	Propylene glycol Glycerin Ethanol
2. Surfactant mixture systems		
2.1) Without cosurfactant		
Corn oil (required HLB = 8)	Tween [®] 80 : Span [®] 80 (1 : 1.89)	-
Sunflower oil (required HLB = 7)	Tween [®] 80 : Span [®] 80 (1 : 2.97)	-
Olive oil (required HLB = 7)	Tween [®] 80 : Span [®] 80 (1 : 2.97)	-
Castor oil (required HLB =14)	Tween [®] 80 : Span [®] 80 (1 : 0.103)	-
Corn oil	Tween [®] 80 : Cremophor [®] EL (1 : 1)	-
Sunflower oil	Tween [®] 80 : Cremophor [®] EL (1 : 1)	-
Olive oil	Tween [®] 80 : Cremophor [®] EL (1 : 1)	-
Castor oil	Tween [®] 80 : Cremophor [®] EL (1 : 1)	-
Corn oil	Tween [®] 80 : Span [®] 20 (1 : 1)	-

Sunflower oil	Tween [®] 80 : Span [®] 20 (1 : 1)	-
Olive oil	Tween [®] 80 : Span [®] 20 (1 : 1)	-
Castor oil	Tween [®] 80 : Span [®] 20 (1 : 1)	-
2.2) With cosurfactant at Km 1:1, 2:1 and 3:1		
Corn oil	Tween [®] 80 : Span [®] 80 (1 : 1.89)	Propylene glycol Glycerin Ethanol
Sunflower oil	Tween [®] 80 : Span [®] 80 (1 : 2.97)	Propylene glycol Glycerin Ethanol
Olive oil	Tween [®] 80 : Span [®] 80 (1 : 2.97)	Propylene glycol Glycerin Ethanol
Castor oil	Tween [®] 80 : Span [®] 80 (1 : 0.103)	Propylene glycol Glycerin Ethanol
Corn oil	Tween [®] 80 : Cremophor [®] EL (1 : 1)	Propylene glycol Glycerin Ethanol
Sunflower oil	Tween [®] 80 : Cremophor [®] EL (1 : 1)	Propylene glycol Glycerin Ethanol
Olive oil	Tween [®] 80 : Cremophor [®] EL (1 : 1)	Propylene glycol Glycerin

		Ethanol
Castor oil	Tween [®] 80 : Cremophor [®] EL (1 : 1)	Propylene glycol Glycerin Ethanol
Corn oil	Tween [®] 80 : Span [®] 20 (1 : 1)	Propylene glycol Glycerin Ethanol
Sunflower oil	Tween [®] 80 : Span [®] 20 (1 : 1)	Propylene glycol Glycerin Ethanol
Olive oil	Tween [®] 80 : Span [®] 20 (1 : 1)	Propylene glycol Glycerin Ethanol
Castor oil	Tween [®] 80 : Span [®] 20 (1 : 1)	Propylene glycol Glycerin Ethanol

2. Preparations of preconcentrate ME

The systems which showed clear or transparent liquid were accordingly prepared without water. All compositions of those systems were calculated as weight percentage and weighed in the screw-cap glass tubes. These mixtures were then mixed by vortex mixer and the drug was added into oil and surfactant mixture system. The prepared systems were equilibrated at room temperature for 24 hours. The stable formulations, no phase separation observed, were further characterized for SME properties.

3. SME characterizations (47, 49)

Before SME characterizations, the dilution of preconcentrate ME is required to simulate the fluid content in stomach. Two hundred and fifty milliliters of purified water were selected because a physiological volume of fluid available in the stomach in the fasted state is in the range of 250-300 ml and the standardized volume of coadministered fluid in *in vivo* studies is 250 ml (105).

One gram of preconcentrate ME was diluted with 250 ml of purified water under mild agitation using magnetic stirrer at 100 rpm for 30 minutes. The sample was then withdrawn to evaluate the SME properties.

3.1 Appearance

Samples were visually observed for their appearance in terms of clarity and transparency.

3.2 Droplets size and zeta potential determinations

Droplets size ($Z_{ave} \pm SD$), polydispersity index ($PdI \pm SD$) and zeta potential were determined by photon correlation spectroscopy (PCS) on Zetasizer Nano ZS (Malvern, UK) at a scattering angle of 90°. All measurements were performed in triplicate at a temperature of 20 ± 0.2 °C.

3.3 Morphology of droplets

The morphology of emulsion droplets was investigated by transmission electron microscope (TEM) (JEM-2100, JEOL, JAPAN). TEM was conducted with negative staining of phosphotungstic acid (PTA) solution (1% w/v) and dried in air at room temperature before loading in the microscope.

4. Solubility studies (20, 45, 49)

The saturated solubility of Bromocriptine mesylate (BM) in oils and surfactants and selected SME system were determined. An excess amount of BM was added to

each screw-capped test tube containing 2 ml of oil or surfactant or SME. The test tubes were shaken in an isothermal shaker (25 ± 0.1 °C) for 48 h. Each tube was centrifuged at 3000 rpm for 30 minutes to precipitate undissolved drug. The presented BM in the supernatant was dissolved with methanol, filtered through 0.45 μm of syringe filter and determined by high pressure liquid chromatography (SIL-20AHT, Shimadzu[®], Japan) equipped with UV detector (SPD-10 M20A, Shimadzu, Japan) and an automatic sampling system (SIL-20A, Shimadzu, Japan). The mixture of acetonitrile and 0.01M ammonium carbonate at 65:35 v/v was used as mobile phase. Separation was accomplished on a reversed phase Hypersil[®]BDS, C18 column (5 μm , 4.6 mm ID \times 25 cm) at flow rate of 1 ml/min. Effluents were monitored at 300 nm (16, 106).

5. Preparation of SME powders (86)

The SME or drug loaded SME liquid were prepared and transformed to SME powders by adsorption techniques. A constant aliquot of SME liquid was added in increment and blended with each solid carrier including Aerosil[®]200, Aeroperl[®]300 and Neusilin US2[®] in mortar at fixed SME liquid to solid carrier ratios by weight 0.5:1, 1:1, 1.5:1, 2:1, 2.5:1 and 3:1 yielding SME powders.

6. Characterization of solid carriers and SME powders

6.1 Determination of surface area of solid carriers

The Brunauer, Emmett and Teller (BET) technique was used for determining the surface area of porous solid carriers. Nitrogen gas, probe molecule, is exposed to a solid under investigation at liquid nitrogen conditions (Outgas Temp = 300°C, Outgas Time = 24.0 hours). The surface area of the solid carriers was evaluated from the measured monolayer capacity. The cross-sectional area of nitrogen was taken as 16.2 Å²/molecule.

6.2 Morphology studies

The shape and surface characteristics of SME powders were investigated by scanning electron microscope (SEM) (JSM-64800 LV, JEOL, JAPAN). Pure solid carriers served as a control for comparison with the SME powders.

6.3 Flowability studies

The SME powders were screened through Mesh No.18 before testing.

6.3.1) Compressibility index measurement (107)

Compressibility index of SME powders was determined by measuring the unsettled apparent volume (V_0) and the final tapped volume (V_f) of the powders introduced in cylinder after tapping the material until no further volume changes occur. The compressibility index is calculated as follows:

$$\text{Compressibility Index (\%)} = 100 \times [(V_0 - V_f) / V_0] \quad \text{Equation III-3}$$

6.3.2) Powder rheometer (108, 109)

FT4 powder rheometer (Freeman Technology, UK) was used to characterize the SME powder flow. Briefly, the split vessel was assembled and the blade was inserted into the FT4 powder rheometer. Solid carriers or SME powders were then loaded into the 25ml vessel with 25 mm diameter. Before measurement, the conditioning was processed to loosen and slightly aerate the powder in order to construct a homogeneously packed powders bed by traversing the blade downward and upward. The blade will move through the powders from the top of the vessel to the bottom (Figure III-1). The flow energy which represents the resistance to flow was measured for 8 times at 100mm/s of blade speed and another 3 times at 70, 40 and 10 of blade speed. The basic flow energy, BFE, is a single flow energy value recording the energy used at test number 7 was measured and plotted. The obtained

stability index (SI, energy test No.7 divided by energy test No.1) values were also evaluated.

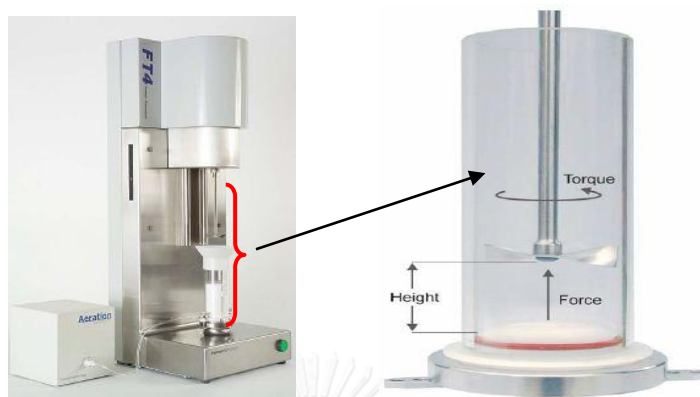


Figure III-1 Flowability measurement using FT4 Powder Rheometer.

6.4 Differential scanning calorimetry (DSC) analysis

The DSC chromatograms were obtained from DSC 822^e / TGA / STDA 851^e (Mettler Toledo, USA). About 1 to 3 mg of powder samples were weighed and sealed in the 40 μ l standard aluminum pan and analyzed by DSC in the range of 0-250 $^{\circ}$ C with a heating rate at 20 $^{\circ}$ C/min and a nitrogen flow of 60 ml/min.

7. Preparation of SME tablet

The SME powders prepared by Aerosil[®] 200 was used as a representative to study the effect of binder, disintegrant and lubricant on the physical properties of tablet such as hardness, friability and disintegration time which were independent variables by using orthogonal central composite design. The code levels for 3 independent variables ($k = 3$) were designated as -1.216, -1, 0, 1 and 1.216, respectively (Table III-2). The total experimental units were calculated as following equation.

$$N = 2^{k-F} + 2k + C \quad \text{Equation III-4}$$

Where; N = total experimental units
 k = number of independent variable (k = 3)
 F = fraction of full factorial (F = 0)
 C = number of center point (C = 1)

The SME liquid was adsorbed by Aerosil[®] 200 at suitable ratio, yielding SME powders, and mixed with binder (Polyvinylpyrrolidone K90), disintegrant (Kollidon[®] CL) and lubricant (magnesium stearate). The 2-5% w/w of Polyvinylpyrrolidone K90, 0.5-5% w/w of Kollidon[®] CL and 0.25-1% w/w of magnesium stearate were considered as the minimum and maximum weight percentage of these diluents to fill into the tablet (86) which were coded as -1 and 1 of factor level, respectively (Table III-2). The total experimental units required were 15 formulations are shown in Table III-3.

All diluents and SME powders were screened through mesh No.18 while magnesium stearate was screened through mesh No.80 before mixing. Drug loaded SME powders were mixed with the diluents except magnesium stearate for 10 minutes in planetary mixer. The magnesium stearate was then added and continued mixed for 2 minutes. After that, the mixing powders were compressed into the tablet using hydraulic tableting machine (4350.L, CARVER[®], USA). Each tablet contained 2.87 mg bromocriptine mesylate (equivalent to 2.5 mg bromocriptine) which is the same as pharmacological dose of marketed tablet. One milligram of maleic acid and edetate disodium were also added into the tablet to protect the degradation of drug.

Table III-2 Independent variables and there factor levels.

Independent variables	Symbol	Code factor levels				
		-1.216	-1	0	1	1.216
PVP K90	X1	1.676	2	3.5	5	5.324
Kollidon [®] CL	X2	0.014	0.5	2.75	5	5.486
Mg stearate	X3	0.169	0.25	0.625	1	1.081

Table III-3 Optimization method parameters for central composite design and response results.

Experimental No.	Code level of variables			Actual level of variables		
	X1	X2	X3	X1 (%)	X2 (%)	X3 (%)
1	-1	-1	-1	2	0.5	0.25
2	-1	-1	1	2	0.5	1
3	-1	1	-1	2	5	0.25
4	-1	1	1	2	5	1
5	1	-1	-1	5	0.5	0.25
6	1	-1	1	5	0.5	1
7	1	1	-1	5	5	0.25
8	1	1	1	5	5	1
9	-1.216	0	0	1.676	2.75	0.625
10	1.216	0	0	5.324	2.75	0.625
11	0	-1.216	0	3.5	0.014	0.625
12	0	1.216	0	3.5	5.486	0.625
13	0	0	-1.216	3.5	2.75	0.169
14	0	0	1.216	3.5	2.75	1.081
15	0	0	0	3.5	2.75	0.625

8. Reconstitution of SME tablet

The dilution of SME tablet was done to evaluate the self-microemulsion properties. As previous mentioned, the same volume (250 ml) of purified water was used as dilution medium. Moreover, 0.1 N HCL was also used to simulate the gastric fluid in stomach where the emulsification takes place and evaluate the change of droplet size under dissolution medium (0.1 N HCL).

The SME tablet was diluted with 250 ml of purified water and 0.1N HCL in beaker which was stirred at 100 rpm for 30 minutes. The mixtures were filtered through 0.45 μm of syringe filter to separate the solid suspension such as Kollidon[®] CL and magnesium stearate. The clear filtrate was then evaluated for size ($Z_{\text{ave}} \pm \text{SD}$) and size distribution ($\text{Pdl} \pm \text{SD}$) by photon correlation spectroscopy (PCS) on Zetasizer ZS (Malvern, UK). The samples were replicated and tested for 3 times in each formulation.

9. Evaluation of SME tablets

9.1 Diameter, thickness and hardness

Twenty sampling tablets were evaluated the diameter and thickness by Micrometer caliper (TECLOCK[®]) while THERMONIK[®] tablet tester was used for hardness evaluation.

9.2 Friability

The ERWEKA[®] friabilator was used to evaluate friability. Twenty sampling tablets were weighed and recorded as initial weight (W_0). Then, those tablets were taken into friabilator with setting speed at 25 rpm for 4 minutes. Total weight was recorded again as W_t and the friability was then calculated following equation below.

$$\% \text{ friability} = [(W_0 - W_t) / W_0] \times 100 \quad \text{Equation III-5}$$

9.3 Disintegration time

The disintegration time of six tablets was tested and recorded by MANESTY[®] tablet disintegration. One tablet was placed in each of the six tubes of the basket. Purified water was used as immersion fluid which was maintained at $37 \pm 2^\circ \text{C}$. The complete disintegration which no any fractions of tablet found on all basket-rack assembly within 15 minutes was accepted. The additional twelve tablets were repeated the test if 1 or 2 tablets fail to disintegrate completely. The disintegrated tablets should not fewer than 16 of the total of 18 tested tablets.

9.4 Assay

Twenty tablets were weighed and finely powdered. The powders, equivalent to 10 mg bromocriptine, were weighed and transferred accurately to beaker. Forty milliliters of methanol were added and stirred for 20 minutes. These mixtures were quantitatively filtered through a glass funnel into a 50 ml volumetric flask and rinsed the filter with methanol. The final volume was adjusted with methanol and then analyzed following the assay topic of bromocriptine mesylate tablet specified in USP34-NF29 (106) by HPLC method.

9.5 Dissolution test

Dissolution test of SME tablets were performed by paddle method with speed of 50 rpm in 500 ml of 0.1N hydrochloric acid at 37°C . Samples were withdrawn at 5, 10, 20 and 30 minutes through filters and the equal volume of fresh medium was replaced to keep constant volume. The concentration of bromocriptine mesylate was determined by reverse-phase HPLC (SIL-20AHT, SHIMADZU[®], JAPAN). The dissolution profiles of SME tablets were plotted and also compared to marketed tablet using difference factor (f1) and similarity factor (f2) which were calculated following below equations.

$$f1 = \left\{ \frac{\sum_{t=1}^n |R_t - T_t|}{\sum_{t=1}^n R_t} \right\} \times 100 \quad \text{Equation III-6}$$

$$f2 = 50 \times \log \left\{ \left[1 + \frac{1}{n} \sum_{t=1}^n (R_t - T_t)^2 \right]^{-0.5} \right\} \times 100 \quad \text{Equation III-7}$$

where; n = number of time points

R_t = cumulative percentage dissolved of reference product at time t

T_t = cumulative percentage dissolved of test product at time t

t = time point

10. Content uniformity of selected SME tablet

The suitable SME tablet was selected and then evaluated the uniformity of content. Not fewer than 30 tablets were randomized. The content of bromocriptine was quantified in each tablet following the uniformity of dosage units of bromocriptine mesylate tablet specified in USP34-NF29 (106). The acceptance value was calculated following Equation III-7.

$$\text{Acceptance value} = |M - \text{Average}| + kS \quad \text{Equation III-8}$$

when, $M = 98.5\%$ (In case of target content per dosage unit (T) = 100% and Average < 98.5%)

$k = 2.4$ (In case of sample size (n) = 10)

S = Sample standard deviation

11. Stability studies

Thirty SME tablets were kept in aluminium foil packed in amber glass, protect from light. The samples were stored at $5^\circ\text{C} \pm 3^\circ\text{C}$, $25 \pm 2^\circ\text{C}/60 \pm 5\% \text{RH}$ and $40 \pm 2^\circ\text{C}/75 \pm 5\% \text{RH}$ according to ICH guidelines (110). The drug content was analyzed at time 0 and 3 months.

12. High Pressure Liquid Chromatography (HPLC) analysis

12.1 HPLC conditions

HPLC:	HPLC (SIL-20AHT, Shimadzu [®] , Japan equipped with UV detector (SPD-10 M20A, Shimadzu, Japan) and an automatic sampling system (SIL-20A, Shimadzu, Japan)
Column:	Hypersil [®] BDS C18 column (5 µm, 4.6 mm ID × 25 cm) set at ambient temperature.
Injection volume:	20 µl
Flow rate:	1 ml/min
Mobile phase:	Acetonitrile and 0.01M ammonium carbonate at 65:35 v/v.

Mobile phase was filtered through membrane filter with a pore size of 0.45 µm and degassed for 30 minutes prior to use. The sample was also filtered through syringe membrane filter with a pore size of 0.45 µm before injection.

12.2 Validation of HPLC method

12.2.1) Specificity

Placebo SME tablet which contained all ingredients except bromocriptine mesylate, drug spiked placebo SME tablet and degradation products of bromocriptine mesylate which was subjected to 0.1N NaOH, 0.1N HCL, 30% H₂O₂, water, heat (60°C) and intense UV light were prepared. The peak of inactive ingredients, degradation products and bromocriptine mesylate should not overlapped.

12.2.2) Accuracy

The drug was spiked into the placebo SME tablet at 50%, 100% and 150% concentrations of actual drug loaded in the SME tablet yielding low, medium and high concentrations of quality control (QC) sample. Each concentration was analyzed in triplicate and calculated as recovery percentage.

12.2.3) Precision

1) Repeatability

The drug was spiked into the mobile phase at low, medium and high concentrations of QC sample. Each concentration was analyzed in triplicate within 1 day and calculated as %RSD.

2) Intermediate precision

The drug was spiked into the mobile phase at low, medium and high concentrations of QC sample. Each concentration was analyzed in triplicate for 3 days and calculated as %RSD.

12.2.4) Linearity

Six standard concentrations which covered the range of actual drug concentration were prepared. Each concentration was analyzed in triplicate. The equation of linear relation were plotted and calculated as r^2 (coefficient of determination).

12.2.5) Lower limit of detection (LOD) and quantitation (LOQ)

LOD and LOQ were estimated based on standard deviation of the response and the slope. The LOD and LOQ were calculated following equation No.6 and No.7, respectively.

$$\text{LOD} = 3.3s/S \quad \text{Equation III-9}$$

$$\text{LOQ} = 10s/S \quad \text{Equation III-10}$$

where, s = standard deviation of y-intercepts (s_a) or standard deviation of regression line ($s_{y,x}$)
 S = slope of calibration curve

13. Cell culture studies

Three formulations were prepared as test samples for cell culture studies including drug loaded SME tablet, drug spiked placebo SME tablet and marketed tablet. All tablet formulations were diluted with 250 ml of simulated intestinal fluid and stirred at 100 rpm for 30 minutes. Thereafter, the obtained suspensions were filtered through syringe filter. The clear filtrate was then taken to test in cell culture.

13.1 Caco-2 cells

Caco-2 cells (ATCC[®] HTB-37, passage No. 25-65) receiving from human's carcinoma colon were cultured in the 25 ml culture flasks. The complete medium contained Dulbecco's Modified Eagle Medium (DMEM; pH7.4) supplemented with 10% fetal bovine serum (FBS), 1% Penicilin/Streptomycin and 1% non-essential amino acid (NEAA). The cells were incubated at 37°C and 5% CO₂ conditions. They were sub-cultured when 70-80% growing reached.

13.1.1) Toxicity studies

The cell viability was tested by MTT assay. Caco-2 cells were trypsinized by 0.25% trypsin-EDTA and suspended in the complete medium. Then, 100 µl of cell suspensions, about 1×10^5 cells/ml, were added into each well of 96 wells plate. They were incubated at 37°C and 5% CO₂ conditions for 3 days until monolayer was formed. After that, 100 µl of test samples were added. After 24 hours incubation, the test samples were removed and washed with phosphate buffered saline (PBS) for 3 times. The 50 µl of 3-[4,5-Dimethylthiazol-2-yl]-2,5-diphenyltetra-zolium bromide (MTT substrate, 1 mg/ml in PBS) was added. After 3 hours incubation, MTT substrate was removed and 100 µl of dimethyl sulfoxide (DMSO) was added into each well. The plate was then agitated at 150 REVS/min for 20 minutes. The UV absorbance was performed at 570 ± 20 nm using microplate reader (VICTOR³, Perkin Elmer, USA). The viability of cells treated with test samples was compared to complete medium as a control which represented as 100% cell viability. The drug concentration that gave more than 80% viability was prepared for further studies.

13.1.2) Drug uptake and permeation studies

The Caco-2 cells, 1×10^6 cells/ml, were plated onto polyester filters with pore size $0.4 \mu\text{m}$ of 6-wells Transwell[®] and incubated at 37°C and 5% CO_2 conditions for 21 days. The complete medium was changed in every other day. After 21 days incubation, complete medium was replaced with Hank's balanced salt solution (HBSS, pH 7.4). The 2.5 ml of HBSS and 1.5 ml of test samples diluted with HBSS were added into the basolateral and apical compartment, respectively. Basolateral medium was taken at time 0, 2, 4 and 6 hours after incubation and the equal volume of HBSS was replaced every time. The permeated drug was analyzed by HPLC and the apparent permeability coefficients (P_{app}) of drug were calculated according to the following equations.

$$P_{\text{app}} = dQ/dt (1/AC_0) \quad \text{Equation III-11}$$

where,

- P_{app} = apparent permeability coefficient (cm/s)
- dQ/dt = steady state flux
- C_0 = initial concentration in the apical compartment
- A = surface area of the membrane filter (4.67 cm^2)

For drug analysis in Caco-2 cells, the cells were washed 3 times with PBS, then they were scraped out from the filters using cell scraper and suspended in the PBS. The cells were precipitated by centrifugation. After supernatant removal, 0.1% V/V of Tween[®] 20 in PBS was added and mixed to lyse the cells. The cell debris was separated out by centrifugation. The supernatants were taken for analyze the drug content.

Trans-epithelial electrical resistance (TEER) measurement was recorded using Millicell[®]-ERS meter (Millipore, MA, USA) before and after experimental. The observed TEER values ($\text{ohm} \times \text{cm}^2$) were corrected with the blank filter resistance.

13.1.3) Fluorescein uptake studies

The lipophilic form of FITC, 5-Dodecanoylamino fluorescein (DAF, Molecular Probes, USA.) was loaded into formulations as fluorescein marker. The 20- μg DAF was dissolved in DMSO and added into oil, surfactant or SME liquid before they were adsorbed with selected solid carrier and then tableting. The fluorescein loaded tablets were diluted with 250 ml of purified water and filtered through syringe filter. The filtrate was taken to test in Caco-2 cells.

Caco-2 cells, 1×10^6 cells/ml, were seeded onto 6-wells plate and incubated at 37°C and 5% CO₂ conditions until monolayer was reached. The complete medium was changed in every other day. Samples were incubated for 6 hours in each well. At the end of 6 hours, Caco-2 cells were washed 3 times with PBS. Then, they were scraped and resuspended in medium. The fluorescein uptake was analyzed by FACS equipped with argon laser, and detected with a G1 detector for green fluorescence signal (excitation of 485 nm and emission of 525 nm). The number of fluorescent events correlating to the particles taken up in cells was counted and the data were calculated and showed as mean of particle fluorescent.

13.1.4) Lymphatic transport studies (100, 111)

Caco-2 cells, 1×10^6 cells/ml, were plated onto polyester filters with pore size 0.4 μm of 6-wells Transwell[®] and incubated at 37°C and 5% CO₂ conditions for 21 days. The complete medium was changed every other day. After 21 days incubation, complete medium was replaced with 1.5 ml of serum free medium in the apical compartment and incubated for 1 day. Thereafter, medium was removed and the test samples and fresh complete medium were added to apical and basolateral

compartments, respectively. Caco-2 cells were incubated with test samples for 24 hours.

Basolateral medium was taken at time 24 hours and separated into lipoproteins including chylomicron and very low density lipoprotein (VLDL) according to method described in 13.1.4.1. ApoB analysis in Caco-2 cells was also carried out. Caco-2 cells were scraped from polyester filters using cell scraper and suspended in PBS. Cell suspensions were precipitated out by centrifugation. The supernatant was then removed and the cells were re-suspended and mixed in lysis buffer (1% Tween[®] 20, 10 mM Tris, 130 mM NaCl in PBS). After that, the cell debris was separated by centrifugation and the supernatant was taken to determine ApoB content founded in Caco-2 cells.

13.1.4.1) Lipoprotein extraction by density gradient ultracentrifugation method (36, 111)

Basolateral medium was subjected to density gradient ultracentrifugation to extract chylomicron and VLDL.

1) Chylomicron fraction

Four milliliters of basolateral medium in the centrifuge tube were over-laid with 2 ml of 1.006 kg/l potassium bromide (KBr). They were centrifuged at 10,000 rpm, 4°C for 30 minutes. Two milliliters of supernatant at the top which was identified as chylomicron were collected.

2) VLDL fraction

Basolateral medium received after chylomicron extraction were over-laid again with 2 ml of 1.006 kg/l KBr. Then, the centrifugation was done at 40,000 rpm, 4°C for 24 hours. Two milliliters of supernatant at the top was identified as VLDL were collected.

13.1.4.2) Apolipoprotein B (ApoB) analysis (111-113)

Apo B content in chylomicron, VLDL and Caco-2 cells was determined by enzyme-linked immunoassay (ELISA) kit. Briefly, fifty microliters of samples were added into coated 96 wells plate and incubated for 2 hours. After that, the plates were washed 5 times with 200 μ l of washing buffer. The 50 μ l of biotinylated apoB antibody was added per well and incubated for 1 hour. The 50 μ l of SP-conjugated was added after 5 times washing. After 30 minutes incubation, the plates were washed and incubated with 50 μ l of chromogen substrate for 10 minutes or until the optimal blue color density developed. The color will change from blue to yellow after stop solution was added to each well. The plate was then taken to read the absorbance at a wavelength of 450 nm using microplate reader (VICTOR³, Perkin Elmer, USA).

13.1.5) Drug analysis in lipoprotein

Each lipoprotein fraction were also taken to analyzed the drug by HPLC method described previously (12.1).

13.2) Mouse brain endothelial cells (bEnd.3) cocultured with rat astrocyte cells (CTX TNA2)

The bEnd.3 (ATCC[®] CRL-2299[™], passage No. 26-53) and CTX TNA2 (ATCC[®] CRL-2006[™] passage No. 29-45) were separately grown in 25 ml culture flask. The complete medium contained Dulbecco's Modified Eagle Medium (DMEM; pH7.4) supplemented with 10% fetal bovine serum (FBS), 1% Pen/Strep and 1% non-essential amino acid (NEAA). They were incubated at 5% CO₂ 37 °C conditions until 70-80% confluence reached.

The effect of lipoproteins on drug uptake and permeation through endothelial cells was evaluated. Therefore, the basolateral medium obtained from lymphatic transport studies in Caco-2 cells (13.1.4) which lipoproteins were secreted was taken to test in bEnd.3, CTX TNA2 or co-culture of bEnd.3 with CTX TNA2.

13.2.1) Toxicity studies

The toxicity of test sample was investigated in both bEnd.3 and CTX TNA2 which they were separately seed into each well of 96 wells plate. The MTT assay was used to identify the cell viability as described in 13.1.1.

13.2.2) Drug uptake and permeate studies

Coculturing the bEnd.3 cells and CTX TNA2 was done followed by Li et al. (114). Briefly, polyester filters with pore size 0.4 μm of 6-wells Transwell[®] were coated with 30 $\mu\text{g}/\text{ml}$ fibronectin and incubated for 2 hours. Transwell filters were inverted and 2×10^4 cells/filter of CTX TNA2 cells were seeded on the abluminal side. Thereafter, the filters were inverted back and CTX TNA2 cells were incubated in complete medium at 37°C and 5% CO_2 conditions for 2 days. After 2 days incubation, 1×10^6 cells/filter of bEnd.3 cells were seeded on the luminal side and left for coculturing with CTX TNA2 cells for 3 days. The complete medium was changed every other day.

The 1.5 ml of basolateral medium received from Caco-2 cells of each sample was added into apical compartment of 6-wells Transwell[®] while the HBSS was added into basolateral compartment. Basolateral medium was taken to analyze permeated drug at time 0, 2, 4 and 6 hours after incubation and the equal volume of HBSS was replaced every time. At the end of 6 hours, the cells were washed 3 times with PBS, then they were scraped out from the filters using cell scraper and suspended in the PBS. The cells were precipitated by centrifugation. After supernatant removal, 0.1% V/V of Tween[®] 20 in PBS was added and mixed to lyse the cells. The cell debris was separated out by centrifugation. The supernatants were taken for analyze the drug content.

Trans-epithelial electrical resistance (TEER) measurement was recorded using Millicell[®]-ERS meter (Millipore, MA, USA) before and after experimental.

13. Statistics analysis

All data obtained were presented as mean \pm standard deviation (S.D.). Data were analyzed by one-way ANOVA and Turkey or Dunnett's T3 for multiple comparisons. A probability $p < 0.05$ was considered statistically significant.



CHAPTER IV

RESULTS AND DISCUSSION

Self-microemulsion (SME) systems are the isotropic mixtures of oil, surfactant and/or cosurfactant. The difference between self-microemulsions and microemulsions (ME) systems is the absence of water in SME. Both systems closely relate because ME are spontaneously formed when SME are diluted with aqueous medium or biological media on mild agitation or under digestive motility (21). The SME would be expected to form o/w ME and behave in the same way as ME systems in vivo (41). In this study, the ME systems are firstly prepared using pseudo-ternary phase diagram. The optimal compositions except water obtained from phase diagram construction which showed the desirable characteristics of ME (clear or transparent liquid) were then mixed and diluted with 250 ml of purified water for further identify as SME.

1. Phase diagram behavior study

The pseudo-ternary phase diagrams were constructed to determine what suitable compositions including oil, surfactant, cosurfactant and water can produce ME. Those compositions without water, called pre-concentrate ME, were then diluted with 250 ml of purified water to investigate the dilution ability which represent the capability of SME formation. Each systems containing various type and ratio of oil, surfactant and/or cosurfactant and their ability to form ME and SME are shown in Table IV-1.

1.1) Effect of Polyoxyethylene 20 sorbitan monooleate (Tween[®] 80) on ME formation

Tween[®] 80 was reported that it could provide the ME region on phase diagram at lower concentration than other Tween series such as Tween[®] 85, 60 and 20 for

system containing palm kernel oil ester as oil phase (56). In addition, no ME formed when Tween[®] 20 and 40 were used compared to Tween[®] 60 and 80 for canola oil system (115). Those were not correlated to the present results because there was no ME obtained by using Tween[®] 80 as single surfactant in all systems (Table IV-1). It was probable that Tween[®] 80 might not have the ability to solubilize the selected long chain triglyceride oils and reduce the interfacial tension between oil and water leading to no subsequent promoting the ME formation. This might be due to that all of oils investigated in this study are long chain triglyceride oils which contain more than 14 carbon chain length of fatty acid (Table III-3) while palm kernel oil mostly composes of lauric acid with 12 carbon atom. The shorter chain length of palm kernel oil might lead to a greater extent of oil solubilized by Tween[®] 80 than a longer chain length oils. (53). The higher amount of palm kernel oil solubilized would result in easier ME formation due to the lower surfactant concentration required.

Table IV-1 The compositions contained in both single surfactant and surfactant mixture systems with/without cosurfactant and the ME/SME formation ability.

Oils	Surfactants	Cosurfactants	ME formation	SME formation
			Ratios of surfactant to cosurfactant	Ratios of surfactant to cosurfactant
Single surfactant systems			1:0	1:0
Corn oil	Tw80	-	×	-
Sunflower oil	Tw80	-	×	-
Olive oil	Tw80	-	×	-
Castor oil	Tw80	-	×	-

			1:1	2:1	3:1	1:1	2:1	3:1
Corn oil	Tw80	PG	✗	✗	✗	-	-	-
		Gly	✗	✗	✗	-	-	-
		EtOH	✗	✗	✗	-	-	-
Sunflower oil	Tw80	PG	✗	✗	✓	-	-	✗
		Gly	✗	✗	✗	-	-	-
		EtOH	✗	✗	✓	-	-	✗
Olive oil	Tw80	PG	✗	✗	✗	-	-	-
		Gly	✗	✗	✗	-	-	-
		EtOH	✗	✗	✗	-	✗	-
Castor oil	Tw80	PG	✓	✓	✓	✗	✗	✓
		Gly	✗	✗	✗	-	-	-
		EtOH	✓	✓	✓	✗	✗	✓
Surfactant mixture systems			1:0			1:0		
Corn oil (required HLB = 8)	Tw80 : Sp80 (1:1.89)	-	✓			✗		
Sunflower oil (required HLB = 7)	Tw80 : Sp80 (1:2.97)	-	✓			✗		
Olive oil (required HLB = 7)	Tw80 : Sp80 (1:2.97)	-	✓			✗		
Castor oil (required HLB =14)	Tw80 : Sp80 (1:0.103)	-	✓			✗		

			1:1	2:1	3:1	1:1	2:1	3:1
Corn oil	Tw80 : Sp80 (1:1.89)	PG	✗	✗	✓	-	-	✗
		Gly	✗	✗	✗	-	-	-
		EtOH	✓	✓	✓	✗	✗	✗
Sunflower oil	Tw80 : Sp80 (1:2.97)	PG	✗	✗	✓	-	-	✗
		Gly	✗	✗	✗	-	-	-
		EtOH	✓	✓	✓	✗	✗	✗
Olive oil	Tw80 : Sp80 (1:2.97)	PG	✗	✗	✓	-	-	✗
		Gly	✗	✗	✗	-	-	-
		EtOH	✗	✓	✓	-	✗	✗
Castor oil	Tw80 : Sp80 (1:0.103)	PG	✓	✓	✓	✗	✗	✗
		Gly	✗	✗	✗	-	-	-
		EtOH	✓	✓	✓	✗	✗	✗
			1:0			1:0		
Corn oil	Tw80 : CreEL (1:1)	-	✗			-		
Sunflower oil	Tw80 : CreEL (1:1)	-	✗			-		
Olive oil	Tw80 : CreEL (1:1)	-	✓			✗		
Castor oil	Tw80 : CreEL (1:1)	-	✓			✓		
			1:1	2:1	3:1	1:1	2:1	3:1
Corn oil	Tw80 : CreEL (1:1)	PG	✗	✗	✗	-	-	-
		Gly	✗	✗	✗	-	-	-
		EtOH	✗	✗	✗	-	-	-

Sunflower oil	Tw80 : CreEL (1:1)	PG	x	x	x	-	-	-
		Gly	x	x	x	-	-	-
		EtOH	x	x	x	-	-	-
Olive oil	Tw80 : CreEL (1:1)	PG	x	x	x	-	-	-
		Gly	x	x	x	-	-	-
		EtOH	x	x	x	-	-	-
Castor oil	Tw80 : CreEL (1:1)	PG	x	x	✓	-	-	✓
		Gly	x	x	x	-	-	-
		EtOH	✓	✓	✓	x	✓	✓
			1:0			1:0		
Corn oil	Tw80 : Sp20 (1:1)	-	✓			x		
Sunflower oil	Tw80 : Sp20 (1:1)	-	✓			x		
Olive oil	Tw80 : Sp20 (1:1)	-	✓			x		
Castor oil	Tw80 : Sp20 (1:1)	-	✓			x		
			1:1	2:1	3:1	1:1	2:1	3:1
Corn oil	Tw80 : Sp20 (1:1)	PG	x	x	✓	-	-	x
		Gly	x	x	x	-	-	-
		EtOH	✓	✓	✓	x	x	x
Sunflower oil	Tw80 : Sp20 (1:1)	PG	x	x	✓	-	-	x
		Gly	x	x	x	-	-	-
		EtOH	✓	✓	✓	x	x	x

Olive oil	Tw80 : Sp20 (1:1)	PG	✗	✗	✓	-	-	✗
		Gly	✗	✗	✗	-	-	-
		EtOH	✗	✗	✓	-	-	✗
Castor oil	Tw80 : Sp20 (1:1)	PG	✗	✗	✓	-	-	✗
		Gly	✗	✗	✗	-	-	-
		EtOH	✓	✓	✓	✗	✗	✗

✓ ME or SME formation was obtained

✗ No ME or SME formation was observed

- Not tested

1.2) Effect of combined surfactants on phase diagram behavior

1.2.1) Influence of surfactant's HLB

Tween[®] 80 and Span[®] 80 were mixed at ratio 1:1.89, 1:2.97, 1:2.97 and 1:0.103 in system containing corn oil, sunflower oil, olive oil and castor oil, respectively. It was found that all oils could form ME when the HLB values of surfactant mixtures were adjusted correlating with the required HLB value of each oils. ME could be formed even no cosurfactant was included (Table IV-1). This might be due to that the surfactant mixture could enhance the flexibility of surfactant layer and increase the surfactant's ability to partition at higher levels into the oil-water interface, both of which stabilized o/w microemulsion (55).

These results was in substantial agreement with Wang et al. (67) who reported that the smallest droplet size of nanoemulsions was obtained when the HLB values of surfactants and oils were matched. Huibers and Shah (57) also found that the ME was formed when the HLB of surfactant mixtures was in the optimal HLB range. They explained that the partition of surfactants at the interface would be favorable at the optimum HLB. Moreover, the lower content of surfactants needed to form ME was obtained when the lowest and highest HLB values of surfactants

were combined (56). One possible explanation was that such two surfactants located at the different site of the o/w interface which the lower HLB surfactant was inside while the higher HLB surfactant was outside, resulting each hydrocarbon chains in tail group of surfactants close together, enhancing the partition of surfactants at the interface. (115).

As can be seen in Figure IV-1, the maximum oil solubilized (%O_{max}) found in sunflower and corn oils (79.37%) in Tween[®] 80/Span[®] 80 system. This might be explained that all oils mainly compose of 18 carbons, differing only in the number of unsaturated bonds and the replacement of functional group. Olive and castor oil mainly compose of oleic acid (C18:1) and ricinoleic acid (C18:1) with a single unsaturated bond while the linoleic acid (C18:2) rich in sunflower and corn oils have two unsaturated bonds. Due to the polarizable nature of double bonds, the decreasing in lipophilicity of sunflower and corn oils arising from increasing degree of double bonds was possible to increase the interaction between triglyceride and surfactant molecules, leading to more oil solubilized in the ME system (116).



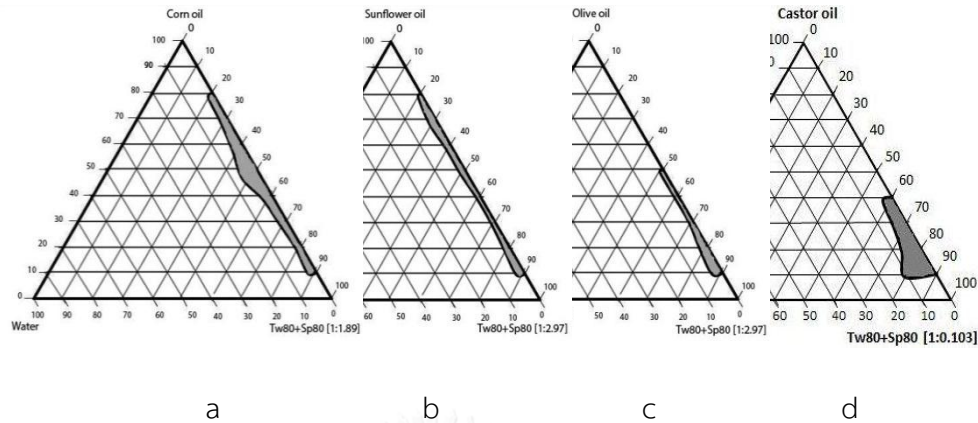


Figure IV-1 Phase diagram of a) corn oil/Tween[®] 80+Span[®] 80 at ratio 1:1.89, b) sunflower oil/Tween[®] 80+Span[®] 80 at ratio 1:2.97, c) olive oil/Tween[®] 80+Span[®] 80 at ratio 1:2.97 and d) castor oil/Tween[®] 80 +Span[®] 80 at ratio 1:0.103.

1.2.2) Influence of surfactant's structure

1.2.2.1) Tween[®] 80 and Span[®] 20 mixtures system

Beside the HLB concept, the structure of surfactants is also the consideration factor to select the suitable surfactant for promoting ME formation. As previous study by Wang et al. (67), they reported that even if the HLB values of surfactant mixture and oil were matched, the particle size of nanoemulsions was still different when surfactants of the different structure were combined. The lowest droplet size was obtained when the least similarity of two surfactants were used. In addition, Gullapalli et al. (58) also indicated that containing at least one surfactant with an unsaturated bond in surfactant blend gave the maximum stability of emulsion. Therefore, the presence of double bond and the different in carbon chain length of two surfactants such as Tween[®] 80 (unsaturated C18 chain) and Span[®] 20 (saturated C12 chain) were studied.

The results showed that the ME regions were obtained from all systems (Figure IV-2). These results confirmed that an inequality in carbon chain length between the hydrophilic (Tween[®]80) and lipophilic (Span[®]20) surfactants and the presence of the double bond could promote the ME formation by affecting the arrangement of the surfactants at the interface. The surfactant film which contains two surfactants with different in carbon chain length and have double bond in the side chain would arrange less compact than those equal chain length with no double bond. The looser film of surfactants at the interface might cause them easier convert to the ME when the water was introduced into the formulation (67).



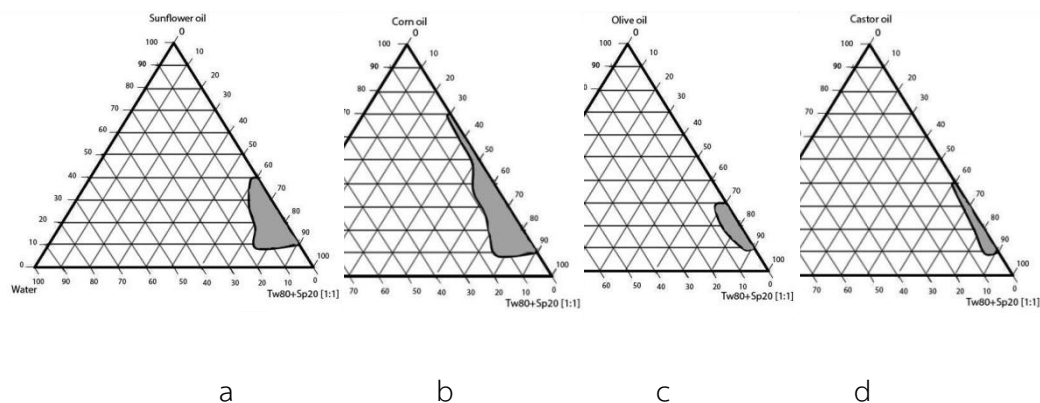


Figure IV-2 Phase diagram of long chain triglyceride oils including a) corn oil, b) sunflower, c) olive oil and d) castor oil in the Tween[®] 80 and Span[®] 20 mixtures system at ratio 1:1.

1.2.2.2) Tween[®] 80 and Cremophor[®] EL mixtures system

The compatibility between the lipophilic chain of surfactant and oil was also studied to investigate an efficiency of ME formation. Cremophor[®] EL is a glycerol polyethylene glycol ricinoleate which the hydroxyl group of castor oil triglyceride was ethoxylated with ethylene oxide. The similar structure of lipophilic tail group of Cremophor[®] EL (Triricinoleate) and castor oil (Triricinoleic acid) would lead castor oil well penetrate into the surfactant tail. The higher solubilization capacity which minimum content of surfactant was required to form ME system was observed when the structure of oil was similar to surfactant (56). Moreover, the efficiency of emulsion stabilization also depended on the degree of structural similarity between the hydrocarbon chain of oil and surfactant (58). The higher penetration of hydrocarbon chain of oil into the hydrophobic region of surfactant probably caused more flexible film structure at the interface leading to larger ME area (117).

In the castor oil/ Tween[®] 80 /Cremophor[®] EL/ water system, ME was formed (Figure IV-3) as expected due to the similarity structure between oil and surfactant. Olive oil could also produce ME but with the lower ME region than castor oil. No ME

areas were observed in corn oil and sunflower oil. One possible explanation was that increasing in degree of unsaturated in corn oil and sunflower oil caused more complicated (crooked) spatial arrangement of triglyceride hydrocarbon chain leading to decrease interaction energy between triglyceride molecules and surfactant when Cremophor[®] EL was used (116).

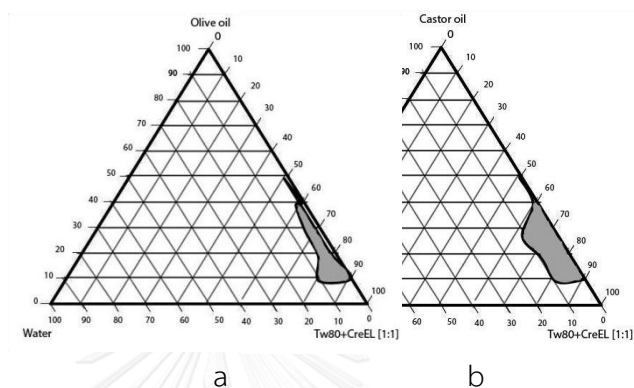


Figure IV-3 Phase diagram of long chain triglyceride oils including a) olive oil and b) castor oil in the Tween[®] 80 and Cremophor[®] EL mixture system at ratio 1:1.

1.3) Effect of cosurfactants on phase diagram behavior

The role of cosurfactants in the ME system is improving the dispersion capability of the system by facilitating water penetration into the formulation (38, 64). Their weak surface-active properties lead them more interfacial tension reduction than using surfactant alone. The rigid hydrocarbon region of the interfacial film was fluidized by cosurfactant leading to more flexible film and less condensed, promoting the ME formation (40).

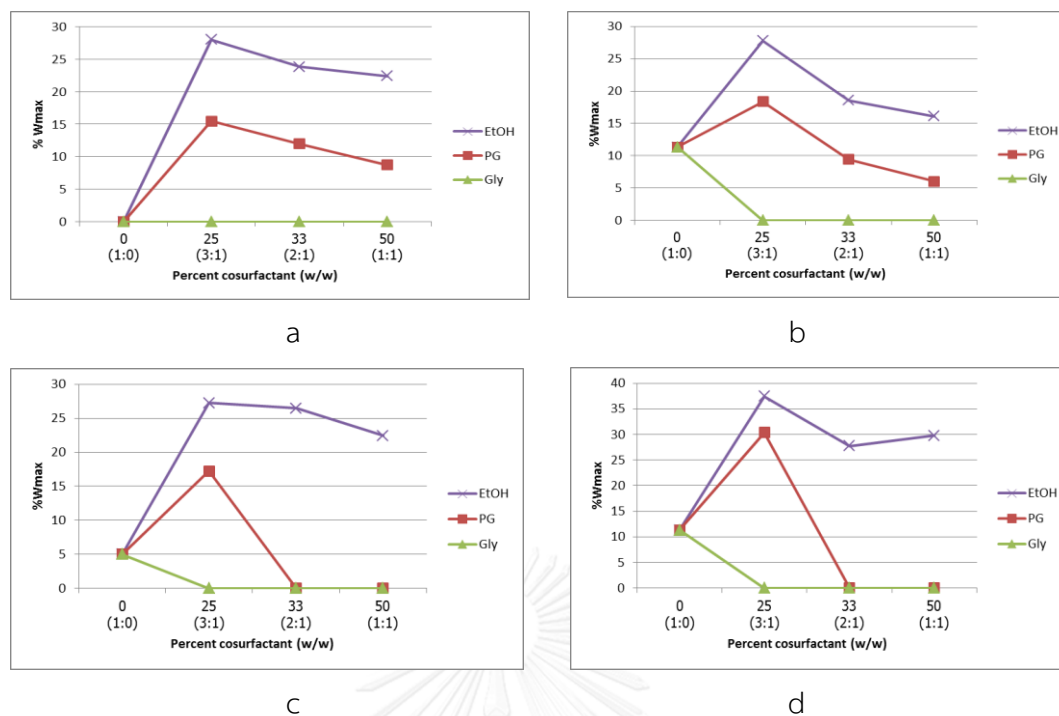


Figure IV-4 Effect of cosurfactant on %Wmax in a) Castor oil/Tw80/cosurfactant system, b) Castor oil/Tw80+Sp80/cosurfactant system, c) Castor oil/Tw80+Sp20/cosurfactant system, d) Castor oil/Tw80+CreEL/cosurfactant system.

The similar trend of %Wmax and %Omax values were obtained from each oils at various cosurfactants when the surfactant to cosurfactant ratios (84) were varied. Therefore, only the relationship between %Wmax or %Omax values and Km in various cosurfactant of castor oil which gave the greater number of ME formation are shown (Figure IV-4). It was found that all cosurfactants, except Gly, could increase %Wmax in both single surfactant and surfactant mixture systems. EtOH enhanced %Wmax at all Km, however, PG increased %Wmax at only Km 3:1 in surfactant mixture systems. The more hydrophilic of Gly (log P = -1.76) and PG (log P = -0.92) than EtOH (log P = -0.31) was probably lead Gly and PG migrated out from the surfactant film layer upon the water dilution to the external aqueous phase, disturbing the integrity of interfacial film, resulting in phase separation at lower amount of additional water. This was consistent with Bayrak and Iscan's (118) findings

that the too soluble alcohol substances in the aqueous phase was ineffective as cosurfactant.

As shown in Figure IV-5, %O_{max} in the EtOH systems increased when K_m were decreased from 3:1 to 2:1 and 1:1 (increasing in EtOH) while the opposite results were observed when PG was used as cosurfactant. At K_m 3:1 which contain the lowest PG content gave the highest %O_{max} compared to 2:1 and 1:1 ratios, however, it was not better than using surfactants alone in the surfactant mixture systems.



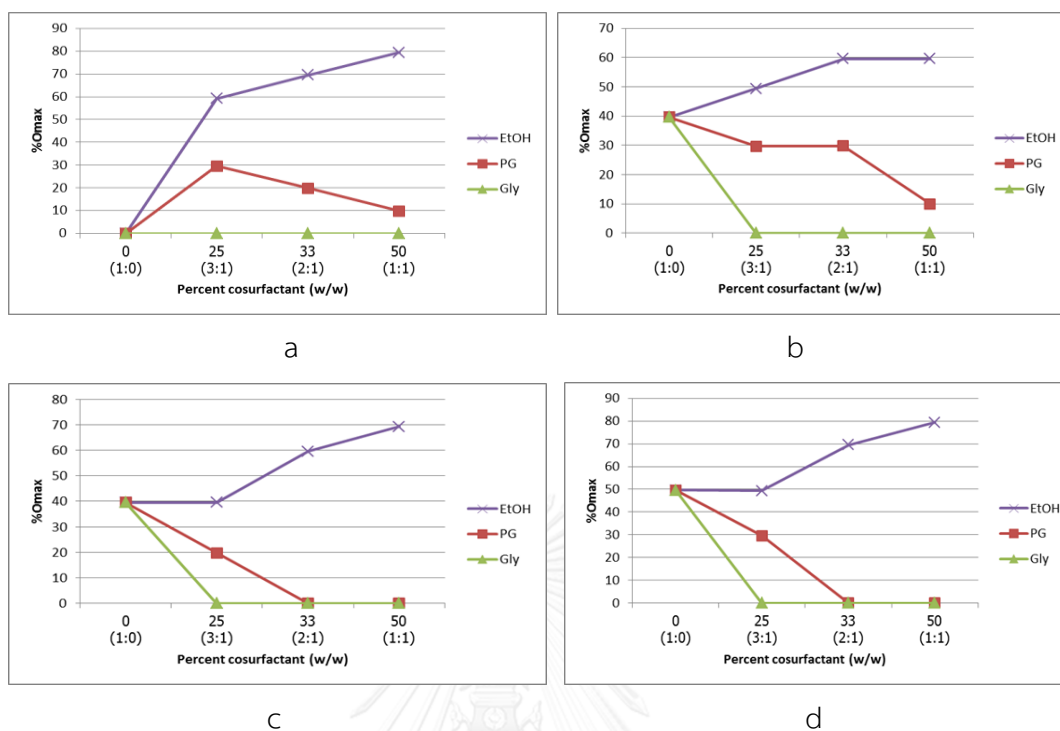


Figure IV-5 Effect of cosurfactant on %Omax in a) Castor oil/Tw80/cosurfactant system, b) Castor oil/Tw80+Sp80/cosurfactant system, c) Castor oil/Tw80+Sp20/cosurfactant system, d) Castor oil/Tw80+CreEL/cosurfactant system.

These results seemingly agreed with the above assumption that EtOH preferably located at the interfacial film but PG might partition out from the surfactant layer to aqueous phase. More addition of EtOH led to more flexible film which could still stabilize the o/w ME even at the high oil contents. On the contrary, the increment of PG could not enlarge the ME area when more oil contents were loaded because they could no longer promote the flexibility of surfactant film.

1.4) Dilution effect

SME or preconcentrate ME is the water-free system composing of oil, surfactant and/or cosurfactant. Such system can form fine o/w emulsion droplets (20) upon the dilution of water or biological media under mild agitation or gastric motion (21). Therefore, the surfactant should have ability to emulsify the oil and water into the single phase and the phase separation should no longer exist at a larger volume of water. The efficiency of surfactant to produce ME was represented as S/W value. The minimum S/W value denotes the maximum amount of additional water allowance to form ME along with lowest surfactant quantity contained in the system.

The minimum S/W values obtained from both single surfactant and surfactant mixture systems were compared (Figure IV-6). Those systems which possessed the lower minimum S/W values such as sunflower oil/Tw80+Sp20 (S/W = 4.69), Corn oil/Tw80+Sp20 (S/W = 5.36) and castor oil/Tw80+CreEL systems (S/W = 5.47) probably could produce ME when they were diluted with 250 ml of purified water. As seen in Table IV-1, it was found that only castor oil/Tw80+CreEL system could stabilize the ME upon dilution. At lower 8:2 of surfactant mixtures (Tw80+CreEL) to castor oil ratio, the diluted preconcentrate ME showed clear to transparent liquid.

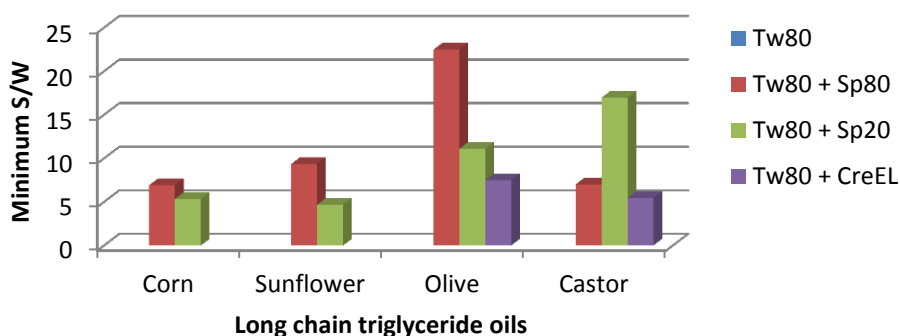


Figure IV-6 The minimum S/W values of both single surfactant and surfactant mixture system without cosurfactant.

These results suggested that only S/W values could not predict the dilutability of preconcentrate ME. Djekic et al. (119) reported that the interfacial film containing cosurfactant with larger hydrophilic and lipophilic group such as PEG40-hydrogenated castor oil was likely less sensitive on water dilution. This might be the reason that the ME structure of only castor oil/Tw80+CreEL system which contained PEG35-hydrogenated castor oil still existed at higher amount of water.

Addition of cosurfactant such as PG and EtOH into the castor oil/Tw80 and castor oil/Tw80+CreEL systems also produced the SME. However, the disadvantages of using cosurfactant were the destabilizing of ME droplets due to the partition of cosurfactant into the aqueous phase (41) and irritating to GI mucosa (21, 41). Therefore, castor oil/Tw80+CreEL system was selected to prepare the SME in this study.

2. SME characterizations

The preconcentrate ME containing castor oil/Tw80+CreEL (1:1) at ratios 5:5, 4.5:5.5, 4:6, 3.5:6.5, 3:7, 2.5:7.5, 2:8, 1.5:8.5, 1:9 of oil to surfactant mixture which showed ME area on phase diagram were prepared and further characterized for the SME properties.

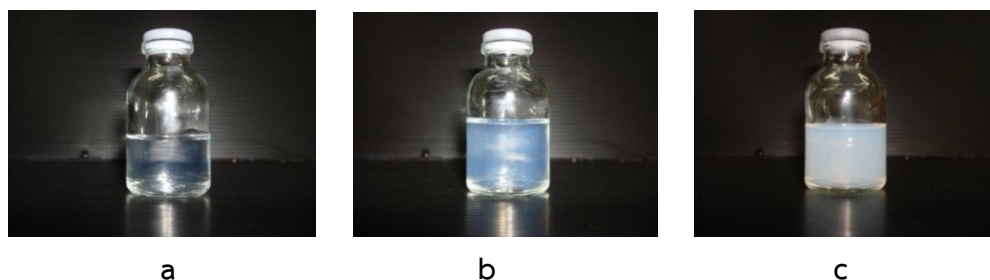


Figure IV-7 The appearance of liquid after dilution with 250 ml of purified water at the weight ratio a) 2:8, b) 2.5:7.5 and c) 3:7 of castor oil to Tw80+CreEL (1:1) mixtures.

The preparations were classified as SME when they appeared as a clear or transparent liquid and the droplets size was less than 100 nm after dilution with 250 ml of purified water. The result showed that the liquid tended to be turbid when the amount of castor oil was more than 20% w/w (Figure IV-7b) and their droplets size increased to more than 100 nm (Table IV-2). The narrow size distributions (Pdl = 0.1-0.3) were observed from all formulations and they were within an acceptable range (Pdl<0.7). The free fatty acid containing in castor oil might contribute slightly negative charge in ME. Therefore, the SME system composed of 20% castor oil, 40% Tween[®] 80 and 40% Cremophor[®] EL was selected for further study because this system contained the highest oil content that could still provide the ME with droplet size less than 100nm and the morphology of the ME droplets (Figure IV-8) were mostly spherical shape and correlated with size analysis.

Table IV-2 Particle size, size distribution and zeta potential of preconcentrate ME after being diluted with 250 ml of purified water.

Castor oil: Tween [®] 80: Cremophor [®] EL (% w/w)	Z-Ave (d.nm)	Pdl	Zeta (mV)
10 : 45 : 45	14.88	0.156	-9.24
	13.77	0.073	-3.38
	13.77	0.073	-2.85
	Average	14.14 ± 0.64	0.100 ± 0.048
15 : 42.5 : 42.5	16.10	0.087	0.944
	16.34	0.119	-2.230
	16.83	0.143	-0.736
	Average	16.42 ± 0.37	0.116 ± 0.028
20 : 40 : 40	56.27	0.333	-6.57
	73.06	0.307	-6.45
	61.47	0.354	-5.27
	Average	63.60 ± 8.60	0.331 ± 0.024
25 : 37.5 : 37.5	132.4	0.198	-7.84
	129.6	0.204	-7.67
	128.6	0.222	-8.74
	Average	130.2 ± 1.97	0.208 ± 0.012

3. Solubility studies

The solubility of BM in selected SME system composing of 20% castor oil, 40% Tween[®] 80 and 40% Cremophor[®] EL was evaluated and compared to those in individual oils and surfactants. As seen in Table IV-3, it was found the solubilities of drug in castor oil, Span[®] 20, Span[®] 80, Tween[®] 80, Cremophor[®] EL and SME system were higher than solubility of drug in water (0.8 mg/g) (16). The higher hydrophilicity of castor oil (HLB=14) than other oils (HLB=7-8) might lead to increase the solubility

of drug. In addition, the ability of drug loading capacity was highest in SME system. This result agreed with previous studies (49, 67) that self-micro/nanoemulsion systems enhanced drug solubilizing capacity.

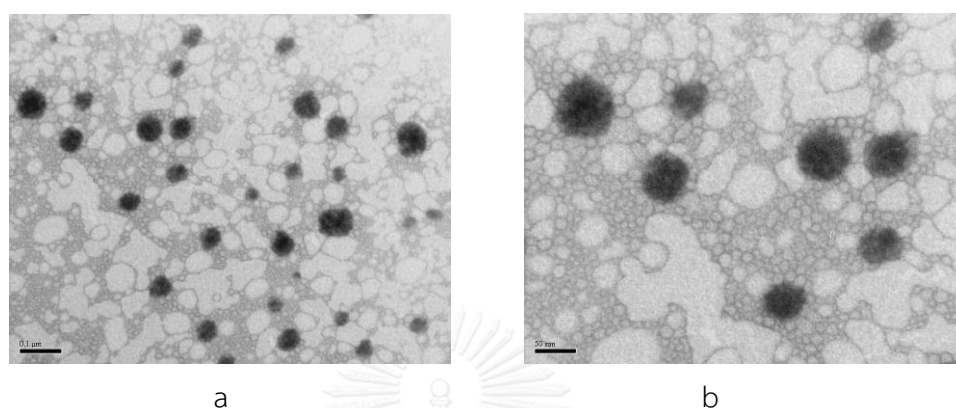


Figure IV-8 TEM micrograph of the ME droplets after dilution with 250 ml of purified water of castor oil/Tween[®] 80/Cremophor[®] EL (1:1) system at 20%w/w castor oil at magnitude a)×100,000 and b)×200,000.

Table IV-3 Drug solubility in long chain triglyceride oils, surfactants and selected SME system.

Solvents	Solubility (mg/g)
Castor oil	7.247 ± 0.024
Corn oil	0.115 ± 0.112
Olive oil	0.314 ± 0.005
Sunflower oil	0.082 ± 0.005
Span [®] 20	5.705 ± 0.034
Span [®] 80	7.946 ± 0.015
Tween [®] 80	18.023 ± 0.080
Cremophor [®] EL	19.362 ± 0.061
SME system	27.983 ± 0.085

4. Evaluation of drug loaded SME system

BM was loaded into the SME system at 80% of maximum solubility concentration (22.4 mg/g). One milliliter of SME system was then diluted with 250 ml of purified water and evaluated. It was found that droplet size of ME was no statistical difference between blank SME and drug loaded SME liquid (Table IV-4). The particle size and size distribution slightly increased but their size was still less than 100 nm and Pdl values were acceptable. However, the zeta potential changed from negative to positive charge. This was due to the positive charge of nitrogen molecules containing in peptide alkaloid compounds such as BM.

Table IV-4 Particle size, size distribution and zeta potential of drug loaded preconcentrate ME after being diluted with 250 ml of purified water.

Formulations	Z-Ave (d.nm)	Pdl	Zeta (mV)
Blank SME liquid	56.27	0.333	-6.57
	73.06	0.307	-6.45
	61.47	0.354	-5.27
Average	63.60 ± 8.60	0.331 ± 0.024	-6.10 ± 1.22
Drug loaded SME liquid	69.25	0.518	13.6
	70.64	0.402	11.9
	77.85	0.322	12.7
Average	72.58 ± 4.62	0.414 ± 0.099	12.73 ± 1.797

5. SME powders preparation

Free-flowing SME powders were required for further SME tablet preparation. Good flowability of powders will lead to no variation in tablet weight and good content uniformity. In this study, compressibility index measurement and powder rheometer were applied to study the powders flow.

Compressibility index was determined by measuring the bulk volume and tap volume of powders. The flow properties related to compressibility index were classified according to Carr (107) and shown in Table IV-5. Free flowing powders result in low percentage of compressibility index because their movement is less resistance between the particles. The flow characteristics obtained from solid carriers and SME powders are shown in Table IV-6.

Table IV-5 The relationship between the flow property and compressibility index (%) (107).

Flow property	Compressibility index (%)
Excellent	< 11
Good	11-15
Fair-aid not needed	16-20
Passable-may hang up	21-25
Poor-must agitate, vibrate	26-31
Very poor	32-37
Very. Very poor	> 37

It was found that the maximum ratio of SME liquid to solid carrier referring to the highest amount of SME liquid that could be loaded into the solid carrier and still gave an acceptable flow property were 2:1, 2:1 and 2.5:1 for Aerosil[®] 200, Aeroperl[®] 300 and Neusilin US2[®], respectively (Table IV-6). The highest specific surface area of Neusilin US2[®] (BET=409.51 m²/g) compared to Aeroperl[®] 300 (BET=264.20 m²/g) and Aerosil[®] 200 (BET=199.63 m²/g) probably result in higher liquid loading. The higher ratio than this maximum ratio caused wet mass powders which could not be evaluated. As seen in Figure IV-9, compressibility index decreased (better flowability) when the ratio of SME liquid to solid carrier increased for SME powders containing Aerosil[®] 200, however, different trend was observed when the Aeroperl[®] 300 and Neusilin US2[®] were used. The fuming characteristic of Aerosil[®] 200 (Figure IV-12a) which easily spread into the air and its own electrostatic charge probably caused them possessed a very poor flowability at initial. The adsorption of SME liquid on Aerosil[®] 200 might decrease this fume characteristic and hinder their electrostatic charge leading to better flowability. On contrarily, the spheroid granule of Aeroperl[®] 300 (Figure IV-12b) and Neusilin US2[®] (Figure IV-12c) led them gave a good flowing even no SME liquid was adsorbed. The poor flowing was found after adsorption, however, their compressibility index returned to low value at the maximum ratio of SME liquid to solid carrier. It was probably that the irregular shape of Aeroperl[®] 300 and Neusilin US2[®] occurred during the adsorption resulting in poorer flowability than initial substances. The spheroid shape might be formed again when all pores of carrier were completely filled by liquid at the highest liquid loading capacity (Figure IV-12e-f).

Table IV-6 Compressibility index and corresponding flow properties of solid SMEDDS.

SMEDDS : Solid carrier ratio	Solid carriers	Compressibility index (%)	Flow property
0.0 : 1	Aerosil [®] 200	33	Very poor
	Aeroperl [®] 300	18	Fair
	Neusilin US2 [®]	12	Good
0.5 : 1	Aerosil [®] 200	28	Poor
	Aeroperl [®] 300	26.53	Poor
	Neusilin US2 [®]	34	Very poor
1.0 : 1	Aerosil [®] 200	26	Poor
	Aeroperl [®] 300	30	Poor
	Neusilin US2 [®]	34	Very poor
1.5 : 1	Aerosil [®] 200	24	Passable
	Aeroperl [®] 300	26.67	Poor
	Neusilin US2 [®]	37	Very poor
2.0 : 1	Aerosil [®] 200	22	Passable
	Aeroperl [®] 300	22	Passable
	Neusilin US2 [®]	34	Very poor
2.5 : 1	Aerosil [®] 200	NA	NA
	Aeroperl [®] 300	NA	NA
	Neusilin US2 [®]	16	Fair

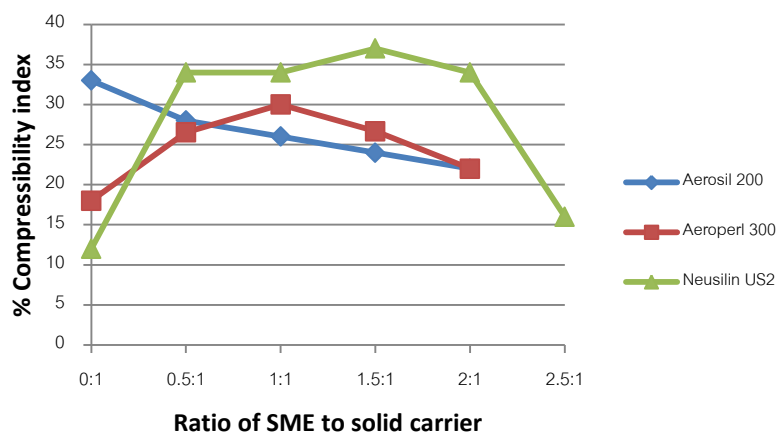


Figure IV-9 The compressibility index (%) results of SME powders containing Aerosil[®] 200, Aeroperl[®] 300 or Neusilin US2[®] at various weight ratios of SME liquid to solid carrier.

However, no single and simple test method can adequately characterize the flow properties of pharmaceutical powders because each method has various limitations including reproducibility, performances conditions and predictability (120). The combination of various methods was required to identify the powder flow.

The powder rheometer was recently used to investigate the flow properties of powders (108, 109). The basic flow energy (BFE) which is the energy required to establish a particular flow pattern. It is calculated from the work done for moving the blade through the powder from the top to the bottom of vessel and was recorded. Normally, the higher BFE value assumably represents poorer flowability. However, using BFE value to investigate the flow property may not be suitable for all powders, only stable powders which stability index is between 0.9 to 1.1 are favorable.

Figure IV-10 shows an obtained SI value from each carrier after adsorption with SME liquid at any ratios. The closets SI value to 1 means that those powders are robust and not affected by being made to flow produced from blade moving. Such

being made to flow might affect the powders causing de-aeration, agglomeration, segregation, moisture uptake and electrostatic charge if $SI > 1$ or attrition, de-agglomeration, over blending of an additive and coating of vessel and blade by additive if $SI < 1$.

The SI values of Aerosil[®] 200 were out of range in both before adsorption ($SI=0.51$) and after adsorption at 0.5:1 ratio of SME liquid to solid carrier ($SI=1.14$). An acceptable SI values were observed when the liquid was adsorbed more than 1:1 ratio of liquid to Aerosil[®] 200. This might be explained that coating the blade and vessel wall during the flow of Aerosil[®] 200 resulting from their fuming and electrostatic characteristics probably cause to reduce the friction leading to low energy used when pure Aerosil[®] 200 was measured. This was in agreement with the above assumption that addition of SME liquid into the pores of Aerosil[®] 200 likely diminished their fuming and electrostatic charge. On the contrary, the acceptable SI values were detected since pure Aeroperl[®] 300 and Neusilin US2[®] were measured. More smooth surface, spheroid shape and less bulky powders of both Aeroperl[®] 300 and Neusilin US2[®] compared to Aerosil[®] 200 resulted in free flowing even no SME liquid was loaded. The higher adsorption tended to increase SI values. Unacceptable SI values ($SI > 1.1$) were obtained when the liquid was loaded at ratios 0.5:1 and 1:1 for Aeroperl[®] 300 and 0.5:1, 1:1 and 1.5:1 for Neusilin US2[®]. At these low ratios, the amount of liquid might not be enough to adsorb into all pores. This possibly caused segregation between absorbed and non-adsorbed particles. The smaller size and less density of non-adsorbed particles might locate at the top whilst adsorbed particles sank to the bottom of vessel during flow measurement. This segregation likely led to increase in energy. The size and density of powders would not be different if all particles were equally adsorbed. This might be the reason that SI values decreased and returned to the acceptable range at ratios 1.5 and 2:1 for Aeroperl[®] 300 ($SI = 1.04$) and 2:1 and 2.5:1 for Neusilin US2[®] ($SI = 1.09$ and 1.10). It was probably that the amount of liquid at these ratios might be suitable to adsorb into all pores of those carriers which would not cause the segregation. Therefore, only ratios of SME liquid

to solid carrier (1:1, 1.5:1 and 2:1 of Aerosil[®] 200, 1.5 and 2:1 of Aeroperl[®] 300, 2:1 and 2.5:1 of Neusilin US2[®] which gave an acceptable SI value were further evaluated.

The BFE values increased when more SME was loaded (Figure IV-11). The lowest BFE values were found in Aerosil[®] 200 at 1.5:1 ratio followed by Neusilin US2[®] and Aeroperl[®] 300, respectively. However, the BFE value of Aerosil[®] 200 was higher than others when the amount of liquid increased to 2:1 ratio. In addition, at this ratio, the lowest BFE value was observed in Neusilin US2[®]. This might be explained that the lowest specific surface area of Aerosil[®] 200 probably caused them the poorest absorbing capacity. It might render being wet powder mass at 2:1 ratio leading to increase the flow resistance while Neusilin US2[®] and Aeroperl[®] 300 which possess higher porosity still remain empty pores for more adsorption.

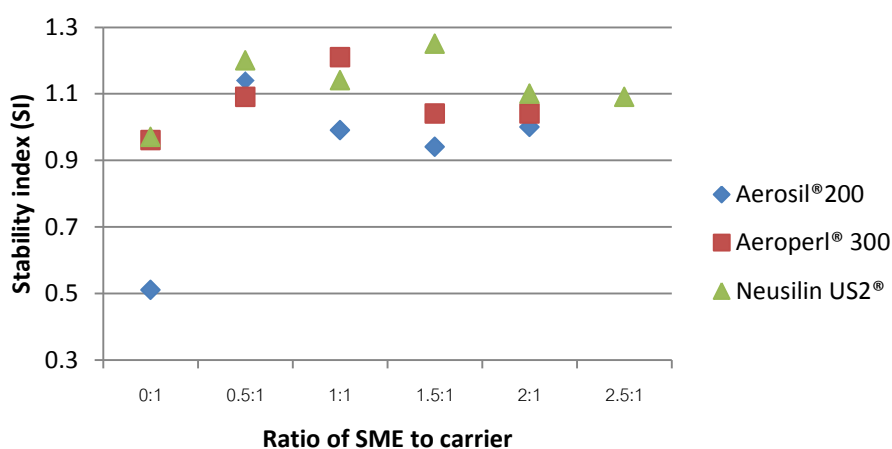


Figure IV-10 The stability index (SI) value of adsorbed Aerosil[®] 200, Aeroperl[®] 300 and Neusilin US2[®] at various ratios of SME to carrier.

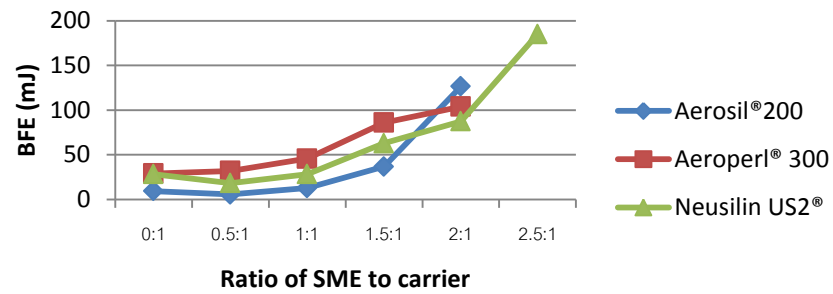


Figure IV-11 The BFE value of adsorbed Aerosil®200, Aeroperl® 300 and Neusilin US2® at various ratios of SME to carrier.

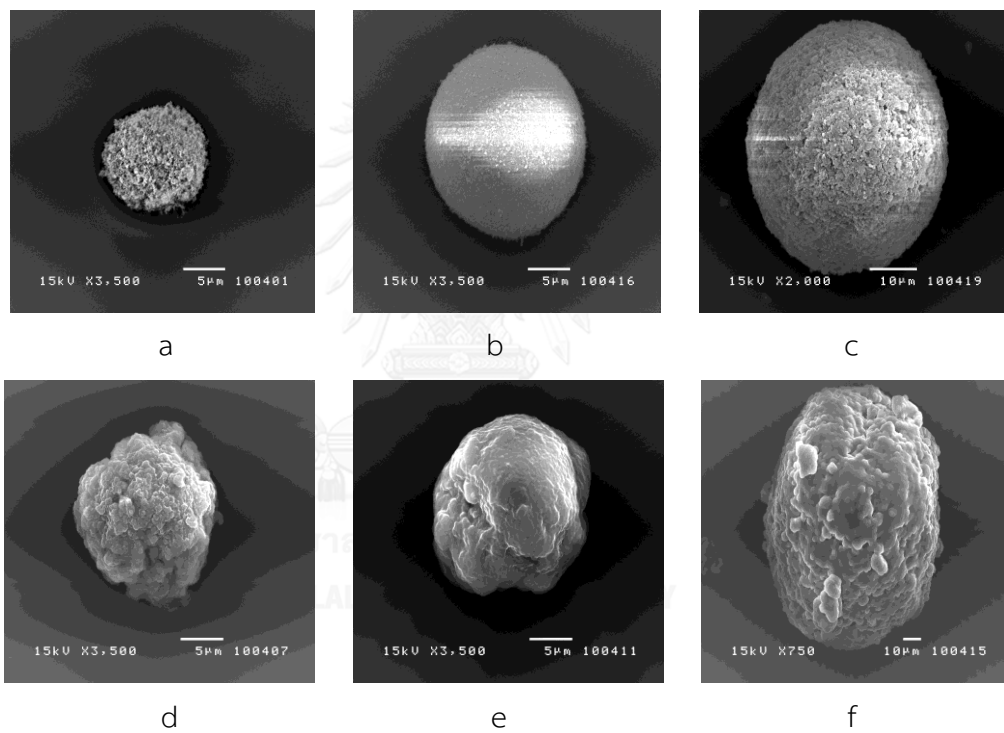


Figure IV-12 The morphology of a) Aerosil® 200, b) Aeroperl® 300, c) Neusilin US2®, d) SME powder at 1.5:1 ratio of SME liquid to Aerosil® 200, e) SME powder at 2:1 ratio of SME liquid to Aeroperl® 300, f) SME powder at 2.5:1 ratio of SME liquid to Neusilin US2®.

Therefore, the ratio of SME liquid to solid carrier at 1.5:1 of Aerosil[®] 200, 2:1 of Aeroperl[®] 300 and 2.5:1 of Neusilin US2[®] were selected for further SME tablet preparation because they showed the free flowing characteristic and no segregation observed when both compressibility index and powder rheometry were used to characterize. This might be due to that the amount of SME liquid at these ratios was appropriate to adsorb into all pores of those carriers. This was confirmed by the morphology of solid carriers before and after liquid loading (Figure IV-12). The surface of all solid carriers showed a lot of pores before SME adsorption (Figure IV-12a-c), however, they were completely replaced with SME liquid at the maximum ratio of liquid to solid carrier which was 1.5:1 of Aerosil[®] 200, 2:1 of Aeroperl[®] 300 and 2.5:1 of Neusilin US2[®] (Figure IV-12d-f). The SME liquid were embedded within the carrier and entrapped in the intraparticle pores. Moreover, the oblate spheroid of Aerosil[®] 200 and Aeroperl[®] 300 SME powders and prolate spheroid of Neusilin US2[®] SME powders were also observed.

The DSC chromatograms of pure drug, physical mixture of drug and solid carriers and drug loaded SME powders were also observed (Figure IV-13). Pure drug showed melting endotherm at 214°C indicating that the drug was in crystalline form. The endothermic peak was followed immediately by a strong exothermic degradation since bromocriptine mesylate decomposed under melting (16). The drug melting peak of 1:1 of drug:solid carrier physical mixture was shifted to the right but with similar pattern to pure drug. The solid carriers which were amorphous form might change the melting behavior of drug. The absence of drug peak in the drug loaded SME powder indicated that oil and surfactant used in self-microemulsion preparation might inhibit the crystallization of the drug. The drug might be in amorphous or disordered crystalline form which it was in molecularly dissolved state and no precipitation of drug while transforming into SME powder.

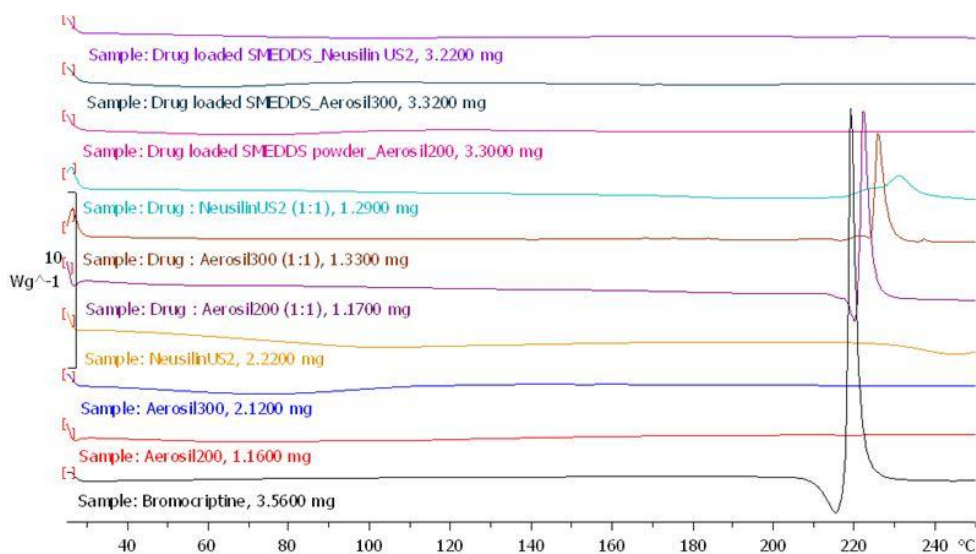


Figure IV-13 DSC chromatogram of bromocriptine mesylate, physical mixer of drug and solid carriers (1:1) and drug loaded SME powders.

6. Preparation of SME tablet

The SME powders prepared by Aerosil[®] 200 (SME liquid: Aerosil[®] 200 = 1.5:1) were formulated and mixed with polyvinylpyrrolidone K90, Kollidon[®] CL and magnesium stearate before tableting.

Table IV-7 Hardness, friability and disintegration time of optimized SME tablet.

No.	PVP K90 (%)	Kollidon® CL (%)	Mg stearate (%)	Hardness (kP)	Friability (%)	Disintegration time (min)
1	2	0.5	0.25	2.20	0.001	17.57
2	2	0.5	1	1.95	0.010	8.70
3	2	5	0.25	1.79	0.003	0.83
4	2	5	1	1.66	0.004	0.60
5	5	0.5	0.25	2.06	0.003	21.27
6	5	0.5	1	1.69	0.015	16.17
7	5	5	0.25	1.56	0.045	1.47
8	5	5	1	1.37	0.069	1.00
9	1.676	2.75	0.625	1.40	0.001	1.53
10	5.324	2.75	0.625	1.64	0.017	5.48
11	3.5	0.014	0.625	1.71	0.072	12.32
12	3.5	5.486	0.625	1.42	0.158	1.05
13	3.5	2.75	0.169	1.65	0.172	2.60
14	3.5	2.75	1.081	1.45	0.130	1.23
15	3.5	2.75	0.625	1.56	0.086	3.58

According to orthogonal composite design, the obtained response values for hardness (Y1), friability (Y2) and disintegration time (Y3) of SME tablet (Table IV-7) were analyzed and the mathematical models of each response were generated by using SPSS.

$$Y1 = 1.833 - 0.092X_2X_3 \quad ; R^2 = 0.634 \quad \text{Equation IV-1}$$

$$Y3 = 17.651 - 7.381X_2 + 0.800X_2^2 \quad ; R^2 = 0.897 \quad \text{Equation IV-2}$$

The Equation IV-1 and IV-2 represented multiple linear regression analysis for response hardness (Y1) and disintegration time (Y3) derived by the best fit method. There was no any fit model to predict the friability (Y3) from the independent factors, however, an acceptable friability values (<1%) according to USP34-NF29 were obtained from all experimental units.

Only Kollidon[®] CL and magnesium stearate interaction (X_2X_3) influenced the hardness (Y1) while Kollidon[®] CL (X_2) and its interaction (X_2X_2) influenced the disintegration time (Y3). The R^2 which indicated how well data fit a statistic model was only 0.634 for hardness prediction while it was 0.897 for disintegration time prediction. Therefore, the Equation IV-2 ($Y3 = 17.651 - 7.381X_2 + 0.800X_2^2$) was selected for further consideration.

According to Equation IV-2, the calculated Kollidon[®] CL content was above the maximum quantity required for tableting (5 %w/w) when the desirable disintegration time ($Y3 = 0.5$ mins) was set. Therefore, the suitable quantity of all excipients was considered from experimental units.

The disintegration time decreased with increasing amount of Kollidon[®] CL. The hardness of SME tablet was quite low (1.37 – 2.2 kP) but all provided a very low friability values (0.001% - 0.130%). The maximum quantity of Kollidon CL (5% w/w) in experimental units No.3 and 4 gave shorter disintegration time (< 1min), however, experiment unit No.3 showed better hardness profile. Therefore, the formulation composed of 2%PVP K90, 5% Kollidon CL and 0.25% magnesium stearate was further formulated using different solid carriers. The compositions of 350 mg SME tablet prepared by Aerosil[®] 200, Aeroperl[®] 300 and Neusilin US2[®] are presented in Table IV-8. Microcrystalline cellulose (MCC)102 was used as a diluent for direct compression while Edetate disodium and maleic acid were also added to protect the bromocriptine degradation.

Table IV-8 Composition of ingredients in SME tablet.

Ingredients	Mg/Tab		
	Aerosil [®] 200	Aeroperl [®] 300	Neusilin US2 [®]
Bromocriptine mesylate (equi to 2.5 mg bromocriptine)	2.87	2.87	2.87
SME powder including	213.545	192.185	179.375
Liquid SME (25.625 mg Castor oil, 51.25 mg Tween [®] 80, 51.25 mg Cremophor [®] EL)	(128.125)	(128.125)	(128.125)
Aerosil [®] 200 ; (SME:Aerosil [®] 200 = 1.5:1)	85.42	-	-
Aeroperl [®] 300 ; (SME:Aeroperl [®] 300 = 2:1)	-	64.06	-
Neusilin US2 [®] ; (SME:NeusilinUS2 [®] = 2.5:1)	-	-	51.25
Edetate disodium	1	1	1
Maleic acid	0.5	0.5	0.5
Maleic acid	0.5	0.5	0.5
PVP K90 (2% w/w)	7	7	7
Kollidon [®] CL (5% w/w)	17.5	17.5	17.5
Mg stearate (0.25% w/w)	0.875	0.875	0.875
MCC102 to	350	350	350

7. Reconstitution of SME tablet

As seen in Figure IV-14, the droplets size obtained from Aerosil[®] 200 tablet was similar to that of SME liquid, however, there was statistically different when Aeroperl[®] 300 and Neusilin US2[®] tablet were compared. This finding was similar to result from previous investigation by Oh et al. (121) who reported that no change in droplet size was observed when SME liquid was transformed to SME solid prepared by Aerosil[®] 200 but significant larger size was produced when SME solid was prepared by another hydrophilic carrier such as dextran. The incomplete desorption of SME liquid from solid carrier probably caused increasing in particle size due to lower surfactant to lipid ratio dispersed into dilution medium. Van et al. (111) revealed that some of hydrophilic non-ionic surfactant, Cremophor[®] EL, still attached into Neusilin US2[®] leading to decreasing Cremophor[®] EL content in aqueous phase after dispersion. However, all SME tablets could produce micro-sized droplets (<120 nm). Furthermore, the droplet size was not significantly changed when dilution medium, purified water, was replaced with 0.1N HCL (Table IV-9). This experiment was done to assure that the particle size of droplets in dissolution medium (0.1N HCL) still related to the size of ME dispersed in purified water.

8. Tablet evaluation

8.1) *Physical properties and drug content*

The measurement of diameter, thickness, hardness, friability and disintegration time are not specified in the USP monograph of bromocriptine mesylate tablet but they are usually assessed as in-house quality control to keep standardize for tableting. As can be seen in Table IV-10, the similar diameter and thickness of SME tablet were observed, however, hardness and disintegration time were highest in Neusilin US2[®] tablet followed by Aeroperl[®] 300 and Aerosil[®] 200 tablet.

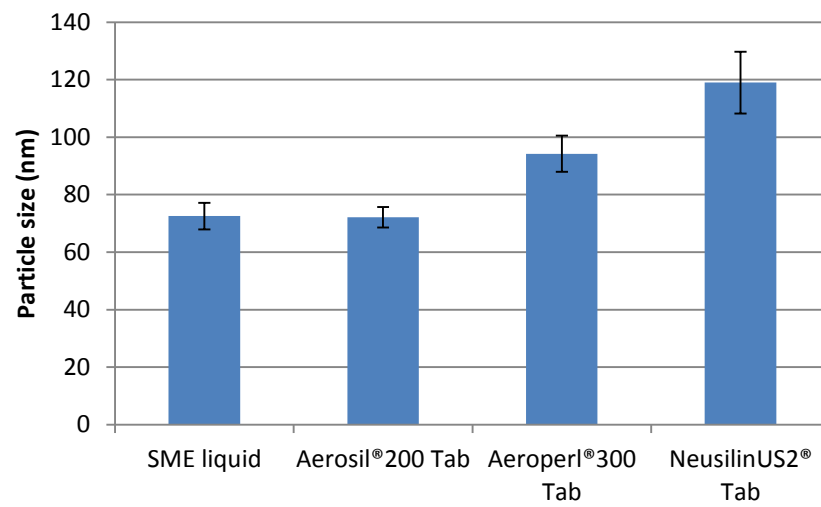


Figure IV-14 Particle size of droplets from SME tablet after dilution with 250 ml of purified water compared to SME liquid.



Table IV-9 Particle size and size distribution of SME tablet after dilution with 250 ml of purified water or 0.1N HCL.

SME Tablets	In purified water		In 0.1N HCL	
	Z-Ave (d.nm)	Pdl	Z-Ave (d.nm)	Pdl
Aerosil [®] 200_1	70.79	0.362	65.08	0.519
Aerosil [®] 200_2	69.44	0.461	79.65	0.392
Aerosil [®] 200_3	76.19	0.504	93.03	0.681
Average	72.14 ± 3.57	0.442±0.073	79.25 ± 13.98	0.531 ± 0.145
Aeroperl [®] 300_1	88.24	0.527	103.30	0.387
Aeroperl [®] 300_2	93.62	0.527	78.90	0.573
Aeroperl [®] 300_3	100.8	0.541	85.98	0.577
Average	94.22 ± 6.30	0.532±0.008	89.38 ± 12.55	0.513 ± 0.109
Neusilin US2 [®] _1	131.2	0.286	102.60	0.257
Neusilin US2 [®] _2	110.9	0.259	103.30	0.255
Neusilin US2 [®] _3	114.9	0.275	110.90	0.278
Average	119.0±10.75	0.273±0.014	105.60 ± 4.60	0.263 ± 0.013

This similar trend was also reported by Gumaste et al. (114) who explained that liquid was adsorbed inside the pores in case of Neusilin US2[®] while they preferred to distribute at the surface when silicon dioxide such as Aerosil[®] 200 was used as solid carrier. The adsorption of liquid at the surface hindered inter-particulate bonding leading to lower tensile strength. Although Neusilin US2[®] tablet gave better hardness, the much longer disintegration time was observed. Gumaste et al. (112) also found that complete disintegration and dispersion of Neusilin US2[®] tablet were achieved when the concentration of disintegrant had to increase to 10%.

Moreover, only Neusilin US2[®] tablet gave the lowest drug content (82.58% ± 1.26). On the contrary, more than 95% of drug founded in Aerosil[®] 200 and

Aeroperl[®] 300 tablet. The incomplete desorption of drug solubilized SME liquid from Neusilin US2[®] tablet after dispersion described above might be the reason that drug content found in Neusilin US2[®] tablet was lower than those found in Aerosil[®] 200 and Aeroperl[®] 300 tablet. An acceptable friability value (<1%) was obtained from all formulations assuming that they have handling ability during manufacturing, packaging and transportation.

Table IV-10 Physical characteristics and drug content of SME tablet.

SME tablets	Diameter (cm)	Thickness (mm)	Hardness (kP)	Friability (%)	Disintegration time (min)	%Label amount
Aerosil [®] 200 tab	0.99	4.03 ± 0.03	2.66 ± 0.18	0.33	1.07	96.72 ± 1.76
Aeroperl [®] 300 tab	0.99	4.17 ± 0.03	2.74 ± 0.14	0.19	1.55	95.54 ± 1.00
Neusilin US2 [®] tab	0.98	4.06 ± 0.03	3.04 ± 0.21	0.32	17.22	82.58 ± 1.26

8.2) Dissolution testing

As seen in Figure IV-15, the Aeroperl[®] 300 tablet showed the highest drug release. The dissolution at 30 minutes was more than 80% following the USP34-NF29 (106) specification for dissolution testing of bromocriptine mesylate tablet. In addition, Aeroperl[®] 300 tablet was the only one formulation showing the f1 and f2 within acceptable ranges (0-15 for f1, 50-100 for f2) (Table IV-11). On the contrary, the f1 and f2 of Aerosil[®] 200 and Neusilin US2[®] tablet were out of limit. It might be due to

the difference in solid carrier characteristics. Comparing between Aerosil[®] 200 and Aeroperl[®] 300, the higher in specific surface area, total pore volume and pore diameter of Aeroperl[®] 300 might promote the penetration of the dissolution medium into the adsorption sites and release more drug into the dissolution vessel. The lowest drug released obtained from Neusilin US2[®] tablet probably resulted from the longest disintegration time (> 15 minutes), although, it possesses the highest surface area and adsorption capacity. Moreover, larger particle size (80 μm) but the highest specific area (409.51 m^2/g) of Neusilin US2[®] compared to Aerosil[®] 200 (0.012 μm , 199.63 m^2/g) and Aeroperl[®] 300 (30 μm , 264.20 m^2/g) indicate that Neusilin US2[®] possesses a large number of long and narrow intra-particle pores. The entrapment of drug solubilized SME liquid in these tortuous pores might contribute to the slowest drug release from Neusilin US2[®] tablet. This result was consistent with previous study by Agar et al. (86) who reported that the smaller particle size of Neusilin UFL2[®] (5 μm) provided the higher drug release than Neusilin US2[®] (80 μm), even they have similar specific surface area. This was due to that the longer pores length of Neusilin US2[®] hindered the release of drug.

Therefore, Aeroperl[®] 300 tablet which complied with the specification of BM tablet under dissolution testing and showed an acceptable disintegration time and friability was selected for further evaluation.

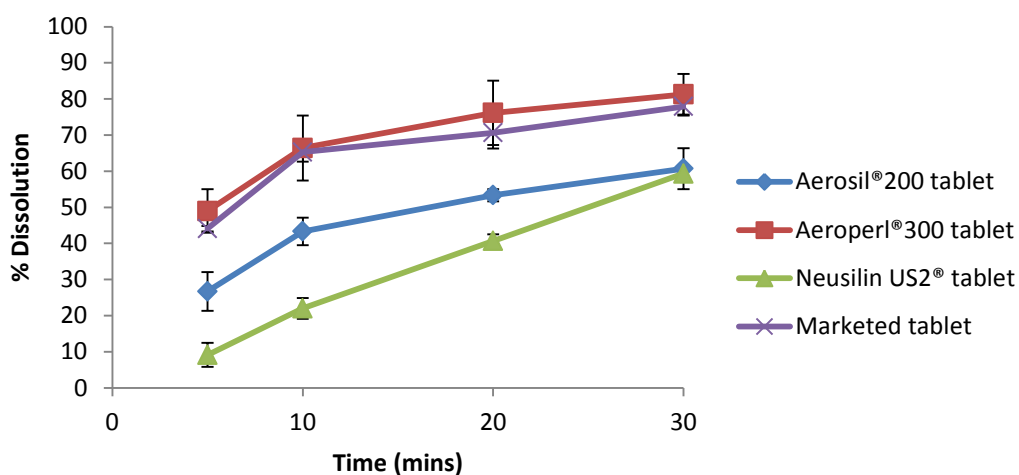


Figure IV-15 Dissolution profile of bromocriptine mesylate SME tablets prepared by Aerosil[®] 200, Aeroperl[®] 300 or Neusilin US2[®] tablets compared to marketed tablet.

Table IV-11 Similarity and difference factors of SME tablet compared to marketed tablet.

SME tablet	Similarity factor; f2	Difference factor; f1
Aerosil [®] 200 tablet	37	29
Aeroperl [®] 300 tablet	69	6
Neusilin US2 [®] tablet	24	49

9. Content uniformity

The %labeled amount of drug contained in Aeroperl[®] 300 SME tablets are shown in Table IV-12. According to the USP specification (106), the tablet will meet the criteria if the acceptance value of the first 10 tablets is less than or equal to 15.0. The calculated acceptance value was 9.81 which was lower than 15. Therefore, it was concluded that the content uniformity of SME tablet which composed of Aeroperl[®] 300 as solid carrier conformed to the USP specification.

Table IV-12 Drug content calculated as %Labeled amount of SME tablets.

Tablet No.	%Labeled amount
1	96.99
2	96.71
3	90.09
4	95.34
5	95.21
6	93.88
7	92.92
8	94.20
9	97.54
10	94.50
Average	94.45
S.D.	2.40
RSD	2.54

10. Stability studies

The stability of drug in SME tablets was studied in 3 storage conditions including $40\pm 2^{\circ}\text{C}/75\pm 5\%\text{RH}$, $25\pm 2^{\circ}\text{C}/60\pm 5\%\text{RH}$ and $5^{\circ}\text{C}\pm 3^{\circ}\text{C}$. According to Figure IV-16, the drug was stable ($91.88\%\pm 0.93$) when SME tablets were kept only at 5°C and the content changed less than 5% from its initial value ($95.05\%\pm 0.06$). The content of drug decreased to $82.28\%\pm 2.2$ and $74.66\%\pm 0.19$ when they were stored at $25^{\circ}\text{C}/60\%\text{RH}$ and $40^{\circ}\text{C}/75\%\text{RH}$, respectively. This revealed that the storage temperature extremely affected the degradation of BM. As reported by Komarova and Tolkache (36), the peptide ergot alkaloids like bromocriptine was susceptible to temperature, light, oxidizers, reducers and alkalis. The storage conditions including inert gas atmosphere, light resistant and tight package at lower 5°C were also recommended.

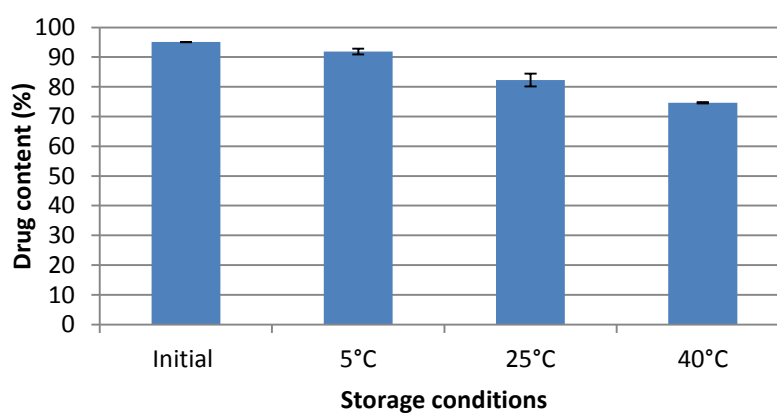


Figure IV-16 Percent drug content in SME tablet after storage at $40\pm 2^{\circ}\text{C}/75\pm 5\%\text{RH}$, $25\pm 2^{\circ}\text{C}/60\pm 5\%\text{RH}$ and $5^{\circ}\text{C}\pm 3^{\circ}\text{C}$ for 3 months ($n=3$).

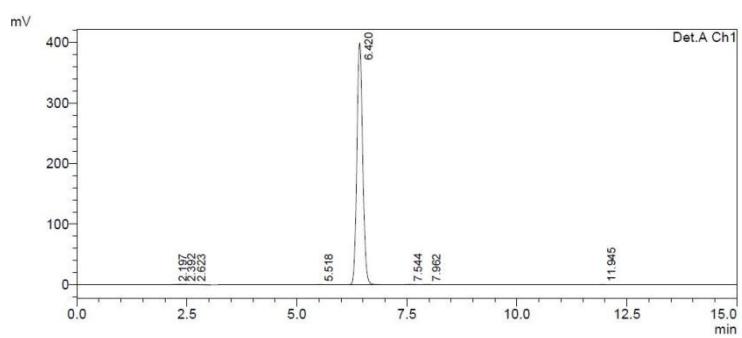
11. Validation of HPLC method

11.1) Specificity

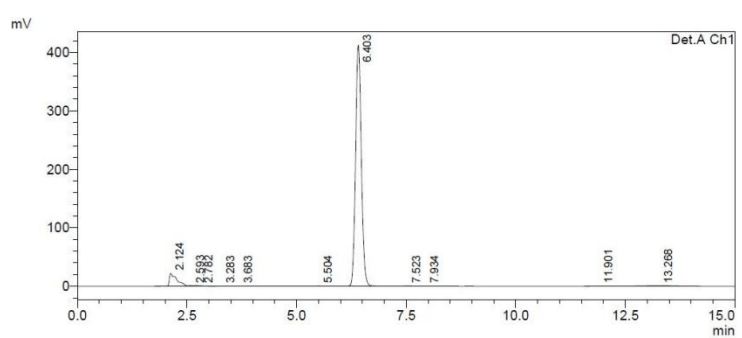
Specificity is the ability to assess unequivocally the drug in the presence of components including impurities or degradants which may be expected to be present. The results found that the peak of degradation products was observed when BM exposed to 0.1N NaOH, heat (60°C) and UV light and peak of tablet diluents was found in drug spiked placebo SME tablet (Figure IV-17). However, this analytical method could distinguish and quantify the response of drug from the response of other diluents and degradation products.

11.2) Accuracy

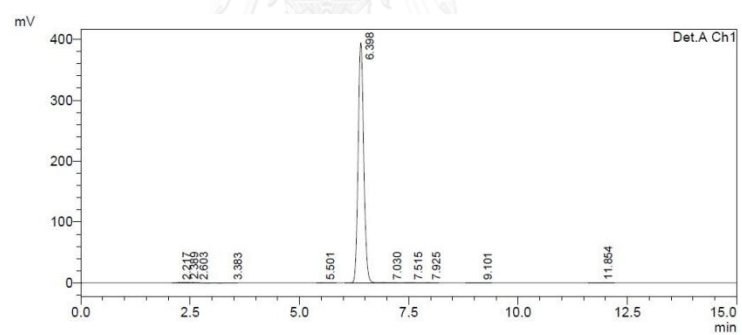
Accuracy is the closeness of agreement between the conventional true value and the value found. The content of drug in placebo SME tablet was analyzed and recorded as measured value. The recovery was then determined by comparing the measured value with the true value which was the actual content. The percent recovery was within 95-105% (Table IV-13).



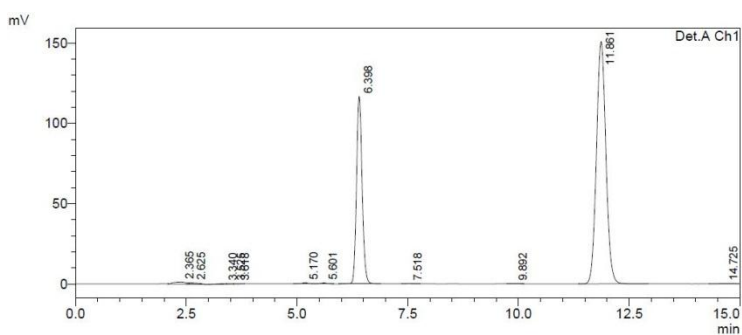
a



b



c



d

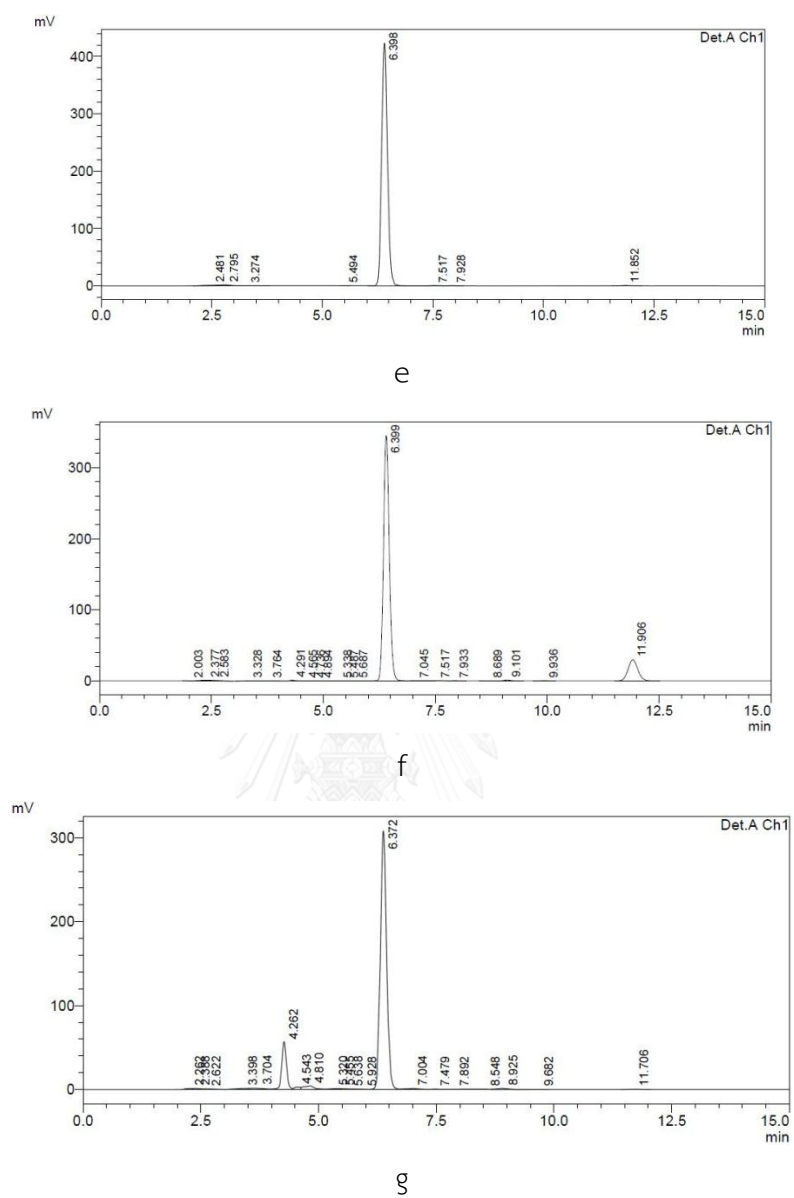


Figure IV-17 HPLC chromatogram of a) BM, b) BM spiked placebo SME tablet, c) BM exposed to 0.1N HCL, d) BM exposed to 0.1N NaOH, e) BM exposed to 30% H₂O₂, f) BM exposed to heat (60°C) and g) BM exposed to UV light.

Table IV-13 Percent recovery of drug found in SME tablet at 50%, 100% and 150% concentrations of actual drug loaded in the SME tablet.

Amount added	Amount found	Percent Recovery
1.49	1.56	104.97
1.43	1.49	103.95
1.50	1.57	104.57
2.90	3.02	104.27
2.91	3.04	104.45
2.88	2.96	102.81
4.38	4.59	104.86
4.52	4.73	104.73
4.42	4.57	103.34

11.3) Precision

Repeatability (intra-assay precision) which is the precision under the same operating conditions over a short interval of time and intermediate precision expressing different days variation within laboratory were tested. The results are shown in Table IV-14. The variation was expressed as %RSD which were not more than 2%. Therefore, this analytical method was accepted for precision testing.

Table IV-14 Percent drug content in mobile phase at 100% concentrations of actual drug loaded in the SME tablet.

Concentrations at 100% level	Day1	Day2	Day3
1	101.01	101.15	102.52
2	98.00	101.22	102.05
3	95.68	99.42	102.09
4	99.74	100.28	101.91
5	99.16	99.96	101.93
6	97.30	101.18	102.01
Mean	98.48	100.53	102.08
RSD (%)	1.92	0.76	0.22
Grand Mean	100.36		
Grand RSD (%)	0.97		

11.4) Linearity

Linearity is ability of an assay to elicit a direct and proportional response to changes in drug concentration within a given range. Six concentrations of drug were analyzed and the linear regression relation was generated. The correlation coefficient was 0.99995 (Figure IV-18).

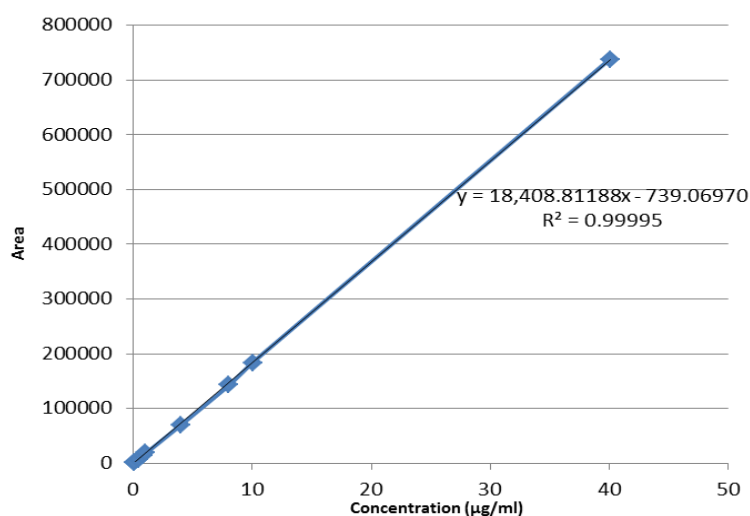


Figure IV-18 Relationship between peak area and concentrations of BM.

11.5) Detection Limit and Quantitation Limit (LOQ)

LOD is the lowest amount of drug in a sample which can be detected but not necessarily quantitated as an exact value while LOQ is the lowest amount of drug which can be quantitatively determined with suitable precision and accuracy. In this study, LOD and LOQ were calculated based on standard deviation of the response and the slope which was obtained from linear regression equation (Equation IV-3). The calculated LOD and LOQ were 0.322 µg/ml and 0.976 µg/ml, respectively.

$$Y_i = 18408.81188x - 739.06970$$

Equation IV-3

12. Cell culture studies

12.1) Caco-2 cells

12.1.1) Toxicity studies

After dispersion of SME tablet, the sample was filtered to separate the solid carrier and tablet's diluents. The supernatant was taken to incubate with Caco-2 cells. The results found that the cells were mostly dead at high drug concentration (11.48 µg/ml), however, the survival largely increased when the concentration of drug

decreased to 5.74 $\mu\text{g/ml}$ (Figure IV-19). Therefore, at 5.74 $\mu\text{g/ml}$ concentration of drug which gave more than 80% cell viability for all formulations was prepared to evaluate the uptake and permeation of drug in Caco-2 cells.

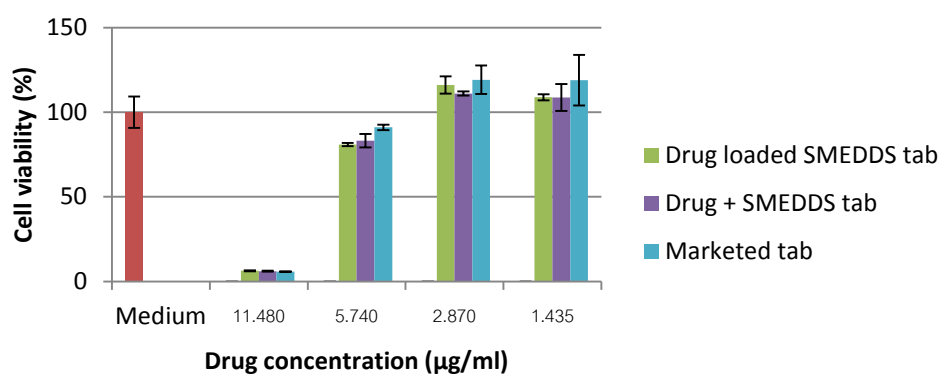


Figure IV-19 Percent cell viability of Caco-2 cells after treatment of test sample at various drug concentrations.

12.1.2) Drug uptake and permeate studies

The permeation and uptake studies were done by analyzing the drug content in basolateral medium and in Caco-2 cells, respectively. For permeation study, marketed formulation which is a plain tablet gave the highest drug permeated and significant higher than those obtained from drug loaded SME tablet and drug spiked placebo SME tablet at all time points analysis (Figure IV-20). The calculated apparent permeability coefficients (P_{app}) of both SME tablets were 0.88×10^{-6} cm/s and 0.86×10^{-6} cm/s, respectively while P_{app} of marketed tablet was 1.12×10^{-6} cm/s (Table IV-15). Therefore, SME tablet with P_{app} less than 1×10^{-6} cm/s are classified as low permeability but marketed tablet is classified as medium permeability. However, P_{app} values of all formulations were no significantly different.

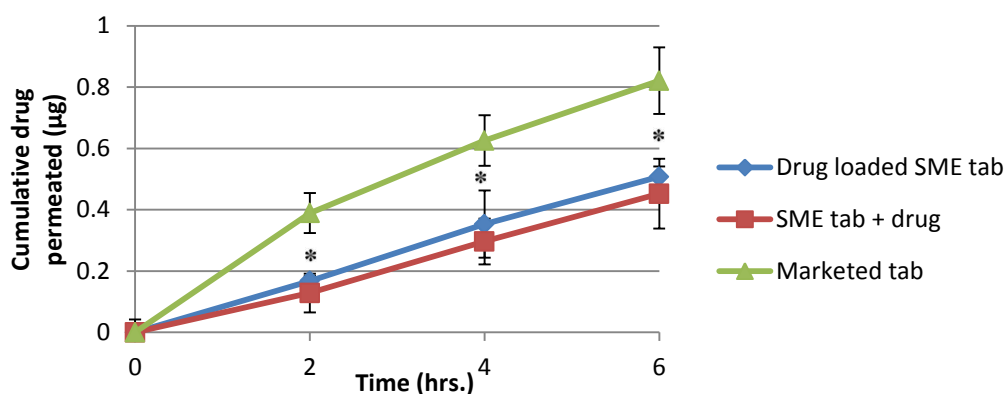


Figure IV-20 Permeation of drug through Caco-2 cells after treatment with test samples at 2, 4 and 6 hours, * $p < 0.05$ significantly different from marketed tablet.

On the contrary, the results of drug uptaked into Caco-2 cells were opposite. As seen in Figure IV-21, the higher drug content in Caco-2 cell was found when Caco-2 cells were treated with both drug-free or drug-loaded SME tablets compared to plain tablets.

TEER values of drug loaded SME tablet, drug spiked placebo SME tablet and marketed tablet were 381.38 ± 31.09 , 358.03 ± 23.04 and $350.25 \pm 16.84 \text{ ohm} \times \text{cm}^2$ at initial and 320.67 ± 31.09 , 303.55 ± 20.37 and $297.32 \pm 11.75 \text{ ohm} \times \text{cm}^2$ at the end of studies, respectively. The TEER values of Caco-2 cells incubated with all test samples after experimental finished were still above 80% cell viability compared to initial.

These results suggested that the microemulsion droplets of SME tablet was possibly adsorbed at the cell surface while the solution obtained from plain tablet could permeate immediately. Moreover, drug loaded microemulsions might undergo the process of lipoprotein synthesis for lymphatic transport. Such process including the synthesis and secretion of drug loaded lipoproteins from Caco-2 cells took a longer time (18-24 hours) (74, 122) than those in uptake and permeate evaluations (0-6 hours). These were likely to be the reason that the lower drug permeated found

in basolateral medium but higher drug content in Caco-2 cells were obtained from SME tablet compared to plain tablet.

Table IV-15 Apparent permeability coefficients (P_{app}) and percent TEER of Caco-2 cells at the end of studies.

Formulations	P_{app} ($\times 10^{-6}$ cm/s)	% TEER at the end of studies
Drug loaded SME tablet	0.88 ± 0.26	84.01 ± 1.37
Drug spiked placebo SME tablet	0.84 ± 0.12	84.78 ± 1.19
Marketed tablet	1.12 ± 0.10	84.92 ± 1.48

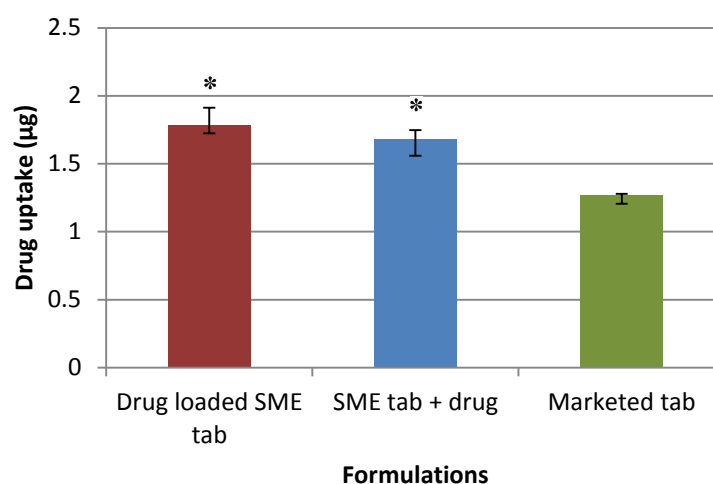
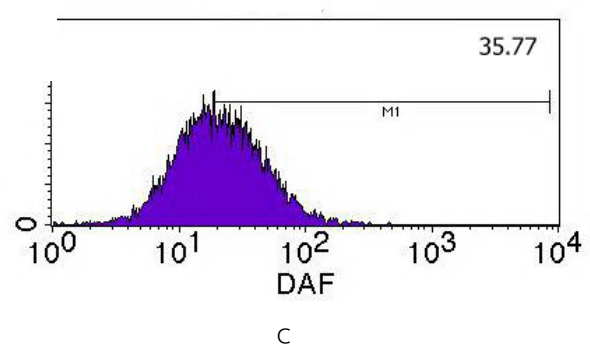
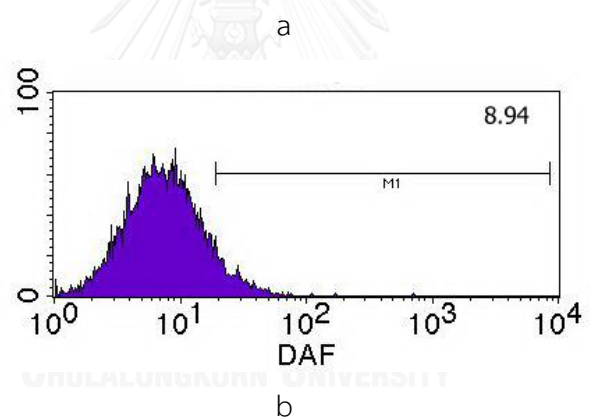
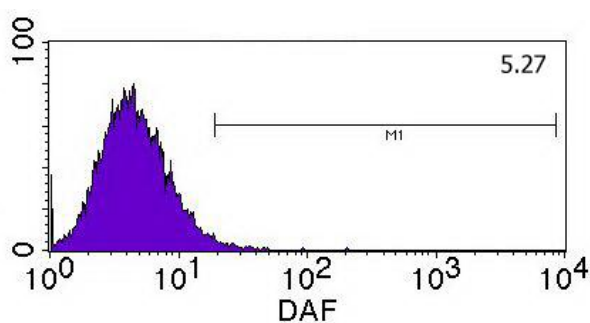


Figure IV-21 Drug content in Caco-2 cells after treatment with test samples for 6 hours, * $p < 0.05$ significantly different from marketed tablet.

12.1.3) Fluorescein uptake study

The effect of SME compositions on the increasing drug uptake in Caco-2 cells was also investigated. The DAF solution, lipophilic form of fluorescein-5-isothiocyanate or FITC, was loaded into oil or surfactants or SME liquid before adsorption with Aeroperl[®] 300 at 2:1 ratios and tableting. Each tablet was then

dispersed into purified water and filtered. The clear filtrate was taken to incubate with Caco-2 cells. After 6 hours incubation, the accumulation of fluorescein in Caco-2 cells was analyzed. The fluorescein loaded SME tablet showed the highest drug uptake (203.25) compared to fluorescein loaded medium (5.27), castor oil (8.94), Tween[®] 80 (35.77) and Cremophor[®] EL (69.44) (Figure IV-22). This finding indicated that the improving drug uptake of SME tablet likely resulted from microemulsions existing.



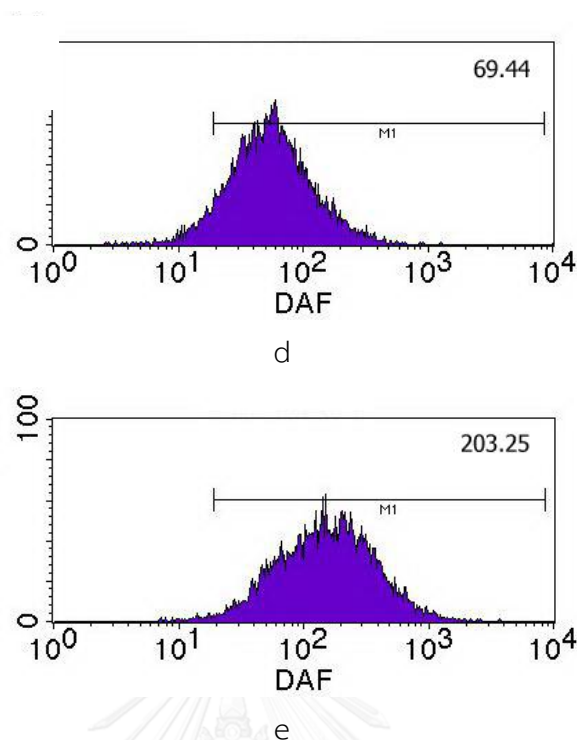


Figure IV-22 Fluorescein uptake of Caco-2 cells after 6 hours incubation with DAF loaded a) medium solution, b) castor oil tablet, c) Tween[®] 80 tablet, d) Cremophor[®] EL tablet and e) SME tablet.

12.1.4) Apolipoprotein B analysis

Chylomicron and VLDL, triglyceride-rich lipoproteins, are primary lipoprotein synthesized by the enterocyte cells after lipid absorption (23). These large particles (200-800 nm) cannot enter to blood capillaries but selectively taken up to lymphatic capillaries. These lipoproteins produced and secreted by Caco-2 cells were used as predictive tool to investigate the degree of lymphatic transport (24). The production and secretion of such lipoproteins between Caco-2 cells and animal models showed good in vitro/in vivo correlations (113).

Each lipoproteins can be separated depending on their differing density by density gradient ultracentrifugation method (71) into 2 fractions. The first fraction,

namely chylomicron fraction, is the fraction that chylomicron will be found while VLDL will be extracted into the second fraction, namely VLDL fraction.

Apolipoprotein B (apo B), a protein constituent, which is a part of secreted lipoproteins is an excellent marker for determine the lipoprotein synthesis (112, 123). An enzyme-linked immunoassay (ELISA) technique was used to quantify secreted apo B (112, 123, 124).

Table IV-16 Content of apolipoprotein B (apo B) detected in Caco-2 cells and secreted lipoprotein and percent TEER at the end of study.

Formulations	Amount of apo B (ng)			TEER (%)
	Total in cells	Distribution in secreted lipoproteins		
		Chylomicron fraction	VLDL fraction	
Drug loaded SME tablet	204.22 ± 15.55	35.82 ± 5.64*	12.18 ± 3.13	71.06 ± 2.49
Drug spiked SME tab	206.20 ± 14.07	11.29 ± 4.70*'	9.08 ± 3.98	70.38 ± 2.01
Marketed tablet	179.46 ± 8.97	3.12 ± 0.66	0.24 ± 1.01	76.26 ± 1.65

*p<0.05 significantly different from marketed tablet, **p<0.05 significantly different from drug loaded SME tablet

It was found that the apo B detected in Caco-2 cells was higher when SME formulations were given compared to plain tablet (Table IV-16). Moreover, apo B found in chylomicron and VLDL fractions obtained from basolateral medium of Caco-2 cells treated with SME formulations was higher than those treated with marketed tablet. These results revealed that long chain triglyceride oil in SME formulations

could promote apo B-containing chylomicron and VLDL synthesis and secretion while oil-free formulation such as marketed tablet could not stimulate chylomicron and VLDL synthesis. The lower stimulation of chylomicron and VLDL synthesis of marketed tablet led to less chylomicron and VLDL particles found in chylomicron and VLDL fractions. Therefore, the higher lipoprotein synthesis obtained from SME formulations could predict that such formulations were likely to improve the lymphatic transport.

For the determination of drug content in these two lipoprotein fractions, it was found that the content of drug in chylomicron fraction of drug loaded SME tablet ($0.0416 \pm 0.0022 \mu\text{g}$) and marketed tablet ($0.0491 \pm 0.0003 \mu\text{g}$) were comparable whilst the significantly lower content was found from drug spiked SME tab ($0.0240 \pm 0.0002 \mu\text{g}$) (Table IV-17). In addition, the content of drug in VLDL fraction was detected only from marketed tablet. This could be explained that the highest permeated drug through Caco-2 cells containing in basolateral medium from marketed tablet possible lead to higher drug content in chylomicron and VLDL fractions even less chylomicron and VLDL particles were be synthesized and secreted.

For the drug spiked placebo SME tablet formulation, the unincorporated drug into oil droplets for drug spiked placebo SME tablet could contribute to lower drug encapsulated into chylomicron leading to the lowest drug content found in lipoprotein fractions.

Table IV-17 Drug content in chylomicron and VLDL.

Formulations	Drug content in lipoprotein (μg)	
	Chylomicron fraction	VLDL fraction
Drug loaded SME tablet	0.0416 ± 0.0022	ND
Drug spiked SME tab	$0.0240 \pm 0.0002^{* \text{ ' } **}$	ND
Marketed tablet	0.0491 ± 0.0003	0.0219 ± 0.0058

* $p < 0.05$ significantly different from marketed tablet, ** $p < 0.05$ significantly different from drug loaded SME tablet, ND = Not detected

12.2 Mouse brain endothelial cells (bEnd.3) cocultured with rat astrocyte cells (CTX TNA2)

Due to the parkinson's treatment of bromocriptine mesylate, the permeated drug which was secreted by Caco-2 cells was further taken to evaluate the permeation and uptake in endothelial cells. Mouse brain endothelial cells (bEnd.3) and coculture of mouse brain endothelial cells (bEnd.3) and rat astrocyte cells (CTX TNA2) were cultured and the transendothelial electrical resistance (TEER) was measured after 5 days culturing. The TEER measurement represents paracellular barrier characteristics of BBB. The brain models which gave TEER value in the order of magnitude of hundred ($\text{ohm} \times \text{cm}^2$) are a good *in vitro* model of BBB (88). In this study, it was found that bEnd.3 monoculture had a TEER about 60-70 $\text{ohm} \times \text{cm}^2$ while bEnd.3 cocultured with CTX TNA2 had a TEER about 400-500 $\text{ohm} \times \text{cm}^2$ (Table IV-18). In line with previous research (100), this study found that coculturing between endothelial cell and astrocyte could increase TEER value. In addition the TEER value obtained from bEnd.3 monoculture was also comparable to other researches which showed that TEER was about 20 $\text{ohm} \times \text{cm}^2$ at day 3-5 and it could reach the maximum of 110 $\text{ohm} \times \text{cm}^2$ at day 8 (87, 125, 126). Therefore, bEnd.3 cocultured with CTX TNA2 cells was used as BBB model in this study.

Table IV-18 TEER values ($\text{ohm}\times\text{cm}^2$) of bEND3 cells monoculture and bEND3 cocultured with CTX TNA2 cells.

Formulations	bEND3 cells monoculture	bEND3 cocultured with CTX TNA2	
	Before treatment	Before treatment	After treatment
Drug loaded SME tablet	70.05 ± 9.34	599.32 ± 15.01	558.84 ± 16.40
SME tablet + drug	62.27 ± 11.75	583.75 ± 20.36	490.35 ± 4.67
Marketed tablet	65.38 ± 9.34	597.76 ± 12.36	571.30 ± 7.13

12.2.1) Toxicity study

The drug permeated through Caco-2 cells at 6 hours was taken from basolateral medium for further investigating the absorption in BBB model. The toxicity of sample to bEnd.3 and CTX TNA2 cells was firstly evaluated. Both bEnd.3 cells and CTX TNA2 cells survived more than 80% compared to medium as a control (Figure IV-23,24).

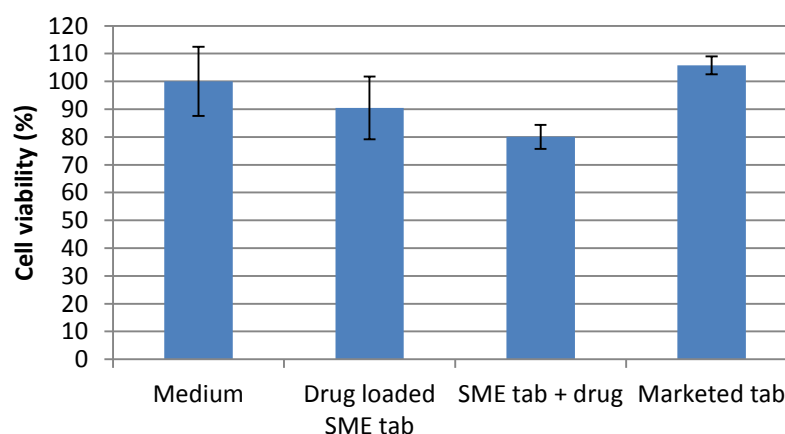


Figure IV-23 Percent cell viability of bEnd.3 after incubation with test sample for 6 hours.

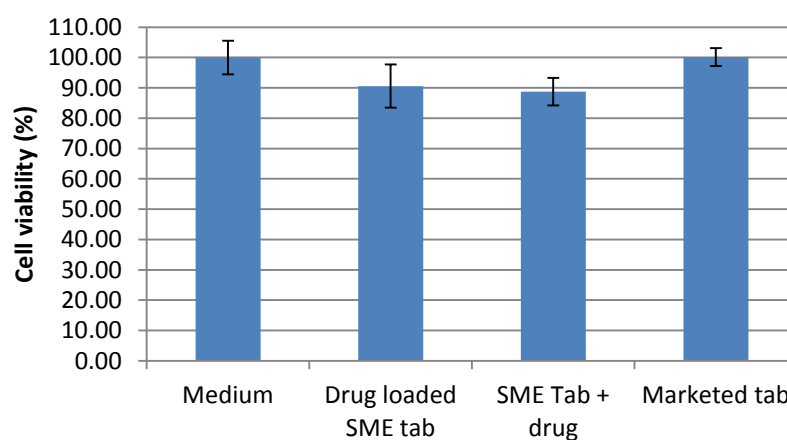


Figure IV-24 Percent cell viability of CTX TNA2 after incubation with test sample for 6 hours.

12.2.2) Drug uptake and permeation studies

For permeability study, the permeated drug was not found for all formulations. This is possible that the drug permeated into basolateral medium is below the detection limit of HPLC analysis due to low initial concentration in apical side. In addition, the BBB characteristics formed by bEnd.3 cells cocultured with astrocyte cells might be a barrier limiting drug transport through endothelial cells via paracellular pathway.

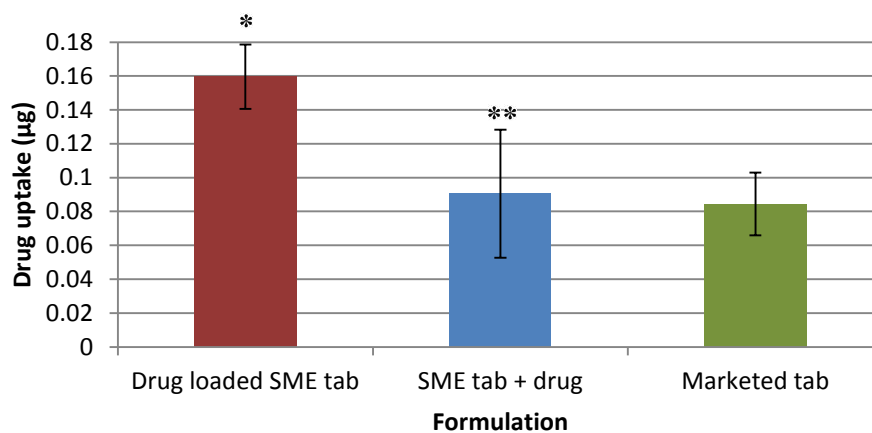
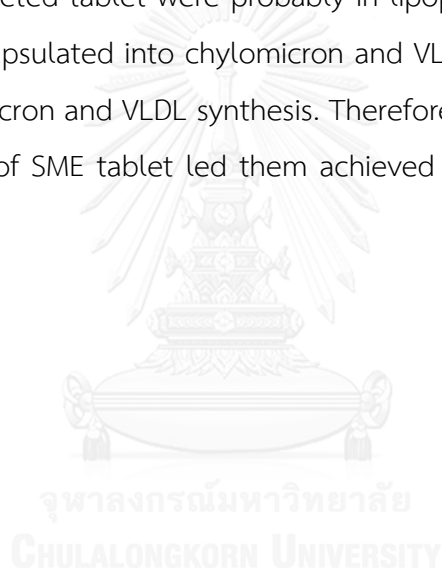


Figure IV-25 Content of drug in bEnd.3 cocultured with CTX TNA2 cells after incubation with test samples for 6 hours, * $p < 0.05$ significantly different from marketed tablet, ** $p < 0.05$ significantly different from drug loaded SME tablet.

On the contrary, the drug entrapped in the cells could be analyzed. As shown in Figure IV-25, drug uptake was the highest when the drug loaded SME tablet was given, however, there were no significant difference between drug spiked placebo SME tablet and marketed tablet ($p = 0.959$). This might be due to that apolipoprotein containing in lipoprotein stimulated drug uptake into the endothelial cells. Kreuter et al. (94) founded that coating hexapeptide dalargin loaded nanoparticles with apo B and apo E provided better antinociceptive effect after intravenous injection to mice than uncoated nanoparticles. They explained that the apolipoprotein overcoated nanoparticles would mimic lipoprotein particles. Such lipoprotein particles could bind and interact with lipoprotein-receptor endocytosis and then were taken up by the brain endothelial cells. The advantage of this transport pathway was applied for delivery nanoparticle coated with Tween[®] 80 into the brain by many researchers (94-97). They described that apolipoprotein in plasma was adsorbed on the surface of Tween[®] 80 after injection leading to binding with lipoprotein receptor on the surface of endothelial cells. Therefore, the significant higher drug found in chylomicron of drug loaded SME tablet ($0.0416 \pm 0.0022 \mu\text{g}$)

than those in drug spiked SME tablet ($0.0240 \pm 0.0002 \mu\text{g}$) possibly led to higher brain uptake (Table IV-17).

Comparing between drug loaded SME tab and marketed tablet, the drug content in chylomicron fraction of marketed tablet ($0.0491 \pm 0.0003 \mu\text{g}$) was higher than those in drug loaded SME tablet ($0.0416 \pm 0.0022 \mu\text{g}$), however, the lower uptake was found for marketed tablet. This might be due to that the very low chylomicron synthesis of marketed tablet ($3.12 \pm 0.66 \text{ ng}$) compared to drug loaded SME tablet ($35.82 \pm 5.64 \text{ ng}$) (Table IV-16) might lead to lower drug uptake. The drug molecules from marketed tablet were probably in lipoprotein fractions as free form, while they were encapsulated into chylomicron and VLDL in case of SME tablet due to the higher chylomicron and VLDL synthesis. Therefore, the higher secretion of drug loaded chylomicron of SME tablet led them achieved the brain uptake better than marketed tablet.



CHAPTER V

CONCLUSIONS

The SME tablet containing long chain triglyceride oil was developed to improve the solubility of BM, enhance the lymphatic transport by increasing lipoprotein synthesis, avoiding hepatic metabolism and promote the transport across endothelial cells.

Due to the spontaneous formation of SME, not all ingredients can produce ME. Therefore, the effect of nonionic surfactants regarding HLB and structure and cosurfactants on the SME formation ability when the long chain triglyceride oils which possess high purity of long chain fatty acid including castor oil (87% ricinoleic acid), olive oil (80% oleic acid), sunflower oil (68% linoleic acid) and corn oil (60% linoleic acid) were investigated.

Tween[®] 80 could not produce the ME indicating that single surfactant might not have the ability to reduce the interfacial tension between the selected long chain triglyceride oils and water. On the contrary, ME could form when the two non-ionic surfactant were mixed. The ME was obtained when the HLB values of surfactants and oils were matched by using the mixture of Tween[®] 80 and Span[®] 80. The difference in carbon chain length between the hydrophilic surfactant (Tween[®] 80) and lipophilic surfactant (Span[®] 80) also improved the ME formation because they probably affect the arrangement of the surfactant at the interface. The looser film of surfactants caused them easier conversion to ME when water was introduced. Castor oil showed larger ME area than others in Tween[®] 80 and Cremophor[®] EL mixture system. The similar structure of lipophilic tail group of Cremophor[®] EL and castor oil would lead castor oil well penetrated into the surfactant tail. The higher penetration of hydrocarbon chain of oil into the hydrophobic region of surfactant caused more flexible film structure at the interface leading to larger ME area.

In the system containing cosurfactant, more hydrophilic of glycerol and propylene glycol than ethanol probably led glycerol and propylene glycol located at the interface migrated out to the external aqueous phase, disturbing the integrity of interfacial film, resulting in phase separation at lower amount of additional water (shown as lower %W_{max} and %O_{max}). However, only castor oil/Tween[®] 80/Cremophor[®] EL system showed the self-ME properties when their preconcentrate ME were diluted with 250 ml of purified water. It revealed that the compatibility between the lipophilic chain of surfactant and hydrocarbon chain of selected long chain triglyceride oils would affect the flexibility of surfactant film at the interface sufficient for promoting the self-ME rather than the HLB or structural difference of surfactant mixtures. Therefore, castor oil/Tw80+CreEL system was selected to prepare the SME liquid.

SME liquid composed of 20% castor oil, 40% Tween[®] 80 and 40% Cremophor[®] EL contained the highest oil content that could still provide the ME with droplets size less than 100nm and the morphology of the ME droplets was mostly spherical shape. The solubility of BM was the highest in this SME system compared to surfactants and oils. The droplet size of ME were no statistical difference between blank SME and BM loaded SME liquid at 80% of saturated solubility ($p > 0.05$). The particle size and size distribution slightly increased but their size was still less than 100 nm and Pdl values were acceptable. However, the zeta potential changed from negative to positive charge due to the positive charge of nitrogen molecules containing in peptide alkaloid compounds such as BM.

For SME powders preparation, Aerosil[®] 200, Aeroperl[®] 300 and Neusilin US2[®] with different characteristics were selected as solid carrier. The suitable ratio of SME liquid to solid carrier was 1.5:1 for Aerosil[®] 200, 2:1 for Aeroperl[®] 300 and 2.5:1 for Neusilin US2[®]. These ratios gave the free flowing powders and no segregation when both compressibility index and powder rheometry were used to characterize. Their

pores were completely replaced with SME liquid and the oblate and prolate spheroid of SME powders was also observed under SEM. Following the DSC chromatograms, the absence of drug peak in the drug loaded SME powder indicated the drug might be in amorphous or disordered crystalline form which it was in molecularly dissolved state and no precipitation of drug while transforming into SME powder. After tableting, only Aeroperl[®] 300 tablet complied to the specification of bromocriptine mesylate tablet under dissolution testing. In addition, they also showed an acceptable disintegration time and friability. Therefore, Aeroperl[®] 300 tablet was selected and prepared for stability testing. The drug content changed less than 5% from its initial value ($95.05\% \pm 0.06$) when SME tablets were kept at 5°C for 3 months, however, they decreased to $82.28\% \pm 2.2$ and $74.66\% \pm 0.19$ at storage conditions of 25°C/60%RH and 40°C/75%RH, respectively.

As *in vitro* studies, three formulations were prepared as test samples for cell culture studies including drug loaded SME tablet, drug spiked placebo SME tablet and marketed tablet. The marketed tablet gave the highest drug permeated and significant higher than those obtained from drug loaded SME tablet and drug spiked placebo SME tablet at all time points analysis ($p < 0.05$) for permeation study in Caco-2 cells. The calculated apparent permeability coefficients (P_{app}) of both drug loaded SME tablet and drug spiked placebo SME tablet were 0.88×10^{-6} cm/s and 0.86×10^{-6} cm/s, respectively while P_{app} of marketed tablet was 1.12×10^{-6} cm/s. On the contrary, the results of drug uptake into Caco-2 cells were opposite. The higher drug content in Caco-2 cell was found when Caco-2 cells were treated with both drug loaded SME tablet and drug spiked placebo SME tablet compared to plain tablets ($p < 0.05$). It could be explained that the microemulsion droplets of SME tablet might adsorbed at the cell surface and drug loaded microemulsion might underwent the process of lipoprotein synthesis which the longer time was taken for lipoprotein synthesis and secretion.

The effect of SME compositions on the fluorescence uptake in Caco-2 cells was also investigated. It was found that the fluorescein loaded SME tablet showed the highest drug uptake than fluorescein loaded in oil or surfactant alone. This indicated that the improving drug uptake of SME tablet likely resulted from microemulsions existing.

The higher lipoprotein synthesis which is necessary for lymphatic transport was obtained from SME formulations because the apolipoprotein B detected in secreted chylomicron were significant higher when Caco-2 cells were treated with SME formulations compared to marketed tablet ($p < 0.05$). In addition, the drug uptake in brain was the highest when the co-culture of endothelial cells and astrocytes were incubated with drug loaded SME tablet ($p < 0.05$), however, there were no significant difference between those incubated with drug spiked placebo SME tablet and marketed tablet ($p = 0.959$). It was possible that apolipoprotein B-containing in lipoprotein obtained from drug loaded SME tablet might stimulated drug uptake into the endothelial cells. The significant higher drug found in chylomicron of drug loaded SME tablet than those in drug spiked SME tablet ($p < 0.05$) possible led to higher brain uptake.

The present study suggest that Aeroperl[®] 300 SME tablet has a potential to deliver the BM which possesses poorly-water soluble and extensively metabolized by the liver to the systemic circulation via lymphatic transport by increasing the lipoproteins (chylomicron and VLDL) synthesis and secretion. In addition, the increasing in lipoprotein secretion was correlated to enhancing the drug uptake into the brain in *in vitro* which is necessary for parkinson's treatment. However, the higher amount of antioxidant may be added to protect the degradation of drug and improve the stability of BM in SME tablet.

Additional studies that include the effect of intestinal enzymes, biliary lipids mucus layer on the SME absorption at enterocyte cells and biological events

involving transportation of secreted lipoprotein to blood-brain-barrier occurring *in vivo* are needed to investigate. Moreover, the receptor which is responsible for drug uptake in co-culture of bEnd.3 and CTX TNA2 is necessary to clearly determine that the improving brain uptake results from binding of lipoprotein to LDL receptor. Therefore, the LDL might be used as positive control compared to test samples.



REFERENCES

1. David P. Parkinson's disease. In: Kohlstadt I, editor. Food and Nutrients in Disease Management: CRC Press; 2009. p. 457-65.
2. Lebouvier T, Chaumette T, Paillusson S, Duyckaerts C, Bruley des Varannes S, Neunlist M, et al. The second brain and parkinson's disease. *European Journal of Neuroscience*. 2009;30(5):735-41.
3. Van Den Eeden SK, Tanner CM, Bernstein AL, Fross RD, Leimpeter A, Bloch DA, et al. Incidence of parkinson's disease: Variation by age, gender, and race/ethnicity. *American Journal of Epidemiology*. 2003;157(11):1015-22.
4. Tom F, Andrew WM, Roger AB. Parkinson's disease. In: Sewell RDE, editor. Protein Misfolding in Neurodegenerative Diseases: CRC Press; 2007. p. 382-402.
5. Wirdefeldt K, Adami H-O, Cole P, Trichopoulos D, Mandel J. Epidemiology and etiology of parkinson's disease: A review of the evidence. *European Journal of Epidemiology*. 2011;26(1):1-58.
6. Murrin LC. The Role of Dopamine in Parkinson's Disease. In: Ebadi M, Pfeiffer RF, editors. Parkinson's Disease: CRC Press; 2004. p.21-26.
7. Ajit Kumar, Zhigao Huang, Calne DB. Parkinson's Disease: Where Are We? In: Ronald F. Pfeiffer, Zbigniew K. Wszolek, Ebadi M, editors. Parkinson's Disease: CRC Press; 2004. p. 27-38.
8. Obeso JA, Olanow CW, Nutt JG. Levodopa motor complications in Parkinson's disease. *Trends in Neurosciences*. 2000;23:S2-7.
9. Kulkantrakorn K, Tiamkao S, Pongchaiyakul C, Pulkes T. Levodopa induced motor complications in Thai Parkinson's disease patients. *Journal of The Medical Association of Thailand*. 2006;89(5):632-7.
10. Stewart AF, Anthony JS. Levodopa. In: Pahwa R, Lyons KE, editors. Handbook of Parkinson's Disease, Fourth Edition: Informa Healthcare; 2003. p. 389-413.
11. Bhidayasiri R, Ling H. Treatment of Parkinson's disease in Thailand: review of the literature and practical recommendations. *Journal of The Medical Association of Thailand*. 2009;92(1):142-54.

12. Kapil DS, John CM. Treatment of early Parkinson's disease. In: Ronald F. Pfeiffer, Zbigniew K. Wszolek, Ebadi M, editors. *Parkinson's Disease*: CRC Press; 2004. p. 1029-38.
13. Mark AS. Dopamine agonists. In: Pahwa R, Lyons KE, editors. *Handbook of Parkinson's Disease, Fourth Edition. Neurological Disease and Therapy*: Informa Healthcare; 2003. p. 335-48.
14. Stowe RL, Ives NJ, Clarke C, van Hilten J, Ferreira J, Hawker RJ, et al. Dopamine agonist therapy in early Parkinson's disease. *The Cochrane Database of Systematic Reviews*. 2008(2):Cd006564.
15. Calandrella D, Antonini A. Pulsatile or continuous dopaminomimetic strategies in Parkinson's disease. *Parkinsonism and Related Disorders*. 2012;18:S120-2.
16. Giron-Forest DA, Schönleber WD. Bromocriptine Methanesulphonate. In: KlausFlorey F, editor. *Analytical Profiles of Drug Substances. Volume 8*: Academic Press; 1979. p. 47-81.
17. Degim IT, Acarturk F, Erdogan D, Demirez Lortlar N. Transdermal administration of bromocriptine. *Biological and Pharmaceutical Bulletin*. 2003;26(4):501-5.
18. Esposito E, Fantin M, Marti M, Drechsler M, Paccamiccio L, Mariani P, et al. Solid lipid nanoparticles as delivery systems for bromocriptine. *Pharmaceutical Research*. 2008;25(7):1521-30.
19. Esposito E, Mariani P, Ravani L, Contado C, Volta M, Bido S, et al. Nanoparticulate lipid dispersions for bromocriptine delivery: characterization and in vivo study. *European Journal of Pharmaceutics and Biopharmaceutics*. 2012;80(2):306-14.
20. Mandawgade SD, Sharma S, Pathak S, Patravale VB. Development of SMEDDS using natural lipophile: application to beta-Artemether delivery. *International Journal of Pharmaceutics*. 2008;362(1-2):179-83.
21. Ljiljana D, Marija P. Microemulsion Systems. In: Fanun M, editor. *Colloids in Drug Delivery*: CRC Press; 2010. p. 245-70.
22. Sun M, Zhai X, Xue K, Hu L, Yang X, Li G, et al. Intestinal absorption and intestinal lymphatic transport of sirolimus from self-microemulsifying drug delivery

systems assessed using the single-pass intestinal perfusion (SPIP) technique and a chylomicron flow blocking approach: Linear correlation with oral bioavailabilities in rats. *European Journal of Pharmaceutical Sciences*. 2011;43(3):132-40.

23. Porter CJH, Charman WN. Intestinal lymphatic drug transport: an update. *Advanced Drug Delivery Reviews*. 2001;50(1-2):61-80.

24. O'Driscoll CM. Lipid-based formulations for intestinal lymphatic delivery. *European Journal of Pharmaceutical Sciences*. 2002;15(5):405-15.

25. Trevaskis NL, Charman WN, Porter CJH. Lipid-based delivery systems and intestinal lymphatic drug transport: A mechanistic update. *Advanced Drug Delivery Reviews*. 2008;60(6):702-16.

26. Spencer BJ, Verma IM. Targeted delivery of proteins across the blood-brain barrier. *Proceedings of the National Academy of Sciences of the United States of America*. 2007;104(18):7594-9.

27. Tang B, Cheng G, Gu J-C, Xu C-H. Development of solid self-emulsifying drug delivery systems: preparation techniques and dosage forms. *Drug Discovery Today*. 2008;13(13-14):606-12.

28. De Lau LML, Breteler MMB. Epidemiology of Parkinson's disease. *The Lancet Neurology*. 2006;5(6):525-35.

29. Monica K, Caroline MT. Epidemiology of Parkinson's disease. In: Ebadi M, Pfeiffer RF, editors. *Parkinson's Disease*: CRC Press; 2004. p.31-48.

30. Ahlskog JE, John LG. Symptomatic treatment of Parkinson's disease. In: Ebadi M, Pfeiffer RF, editors. *Parkinson's Disease*: CRC Press; 2004. p.847-864.

31. Joseph J, Sandra K. Dopamine agonists in Parkinson's disease. In: Ebadi M, Pfeiffer RF, editors. *Parkinson's Disease*: CRC Press; 2004. p.865-880.

32. Kvernmo T, Hartter S, Burger E. A review of the receptor-binding and pharmacokinetic properties of dopamine agonists. *Clinical Therapeutics*. 2006;28(8):1065-78.

33. Bonuccelli U, Del Dotto P, Rascol O. Role of dopamine receptor agonists in the treatment of early Parkinson's disease. *Parkinsonism & Related Disorders*. 2009;15 Suppl 4:S44-53.

34. Van Hilten JJ, Ramaker CC, Stowe R, Ives NJ. Bromocriptine versus levodopa in early Parkinson's disease. *The Cochrane Database of Systematic Reviews*. 2007(4):Cd002258.
35. Takashima H, Tsujihata M, Kishikawa M, Freed WJ. Bromocriptine protects dopaminergic neurons from levodopa-induced toxicity by stimulating D(2)receptors. *Experimental Neurology*. 1999;159(1):98-104.
36. Komarova EL, Tolkachev ON. The Chemistry of Peptide Ergot Alkaloids. Part 1. Classification and Chemistry of Ergot Peptides. *Pharmaceutical Chemistry Journal*. 2001;35(9):504-13.
37. Ambikanandan M, Kiruba F, Manisha L, Tapan S. Microemulsions in biotechnology and pharmacy. In: Fanun M, editor. *Colloids in Biotechnology*: CRC Press; 2010. p. 381-415.
38. John BC, Michelle AL. Emulsions, Microemulsions, and Lipid-Based Drug Delivery Systems for Drug Solubilization and Delivery-Part II. In: Liu R, editor. *Water-Insoluble Drug Formulation, Second Edition*: CRC Press; 2008. p. 227-54.
39. Malmsten M. Microemulsions. In: Malmsten M, editor. *Surfactants and Polymers in Drug Delivery. Drugs and the Pharmaceutical Sciences*. New York: Marcel Dekker, Inc.; 2002.
40. Raid GA, Gamal MEM, Karen K-G, Anja G. Microemulsion systems and their potential as drug carriers. In: Fanun M, editor. *Microemulsions. Surfactant Science*: CRC Press; 2008. p. 248-82.
41. Lawrence MJ, Rees GD. Microemulsion-based media as novel drug delivery systems. *Advanced Drug Delivery Reviews*. 2000;45(1):89-121.
42. Pouton CW. Formulation of poorly water-soluble drugs for oral administration: Physicochemical and physiological issues and the lipid formulation classification system. *European Journal of Pharmaceutical Sciences*. 2006;29(3-4):278-87.
43. Kumar A, Sharma S, Kamble R. Self emulsifying drug delivery system (SEDDS): future aspects. *International Journal of Pharmacy & Pharmaceutical Sciences*. 2010;2:7-13.
44. Humberstone AJ, Charman WN. Lipid-based vehicles for the oral delivery of poorly water soluble drugs. *Advanced Drug Delivery Reviews*. 1997;25(1):103-28.

45. Kang BK, Lee JS, Chon SK, Jeong SY, Yuk SH, Khang G, et al. Development of self-microemulsifying drug delivery systems (SMEDDS) for oral bioavailability enhancement of simvastatin in beagle dogs. *International Journal of Pharmaceutics*. 2004;274(1-2):65-73.
46. Wu W, Wang Y, Que L. Enhanced bioavailability of silymarin by self-microemulsifying drug delivery system. *European Journal of Pharmaceutics and Biopharmaceutics*. 2006;63(3):288-94.
47. Grove M, Müllertz A, Nielsen JL, Pedersen GP. Bioavailability of seocalcitol: II: Development and characterisation of self-microemulsifying drug delivery systems (SMEDDS) for oral administration containing medium and long chain triglycerides. *European Journal of Pharmaceutical Sciences*. 2006;28(3):233-42.
48. Yao J, Lu Y, Zhou JP. Preparation of nobiletin in self-microemulsifying systems and its intestinal permeability in rats. *Journal of Pharmacy & Pharmaceutical Sciences*. 2008;11(3):22-9.
49. Cui J, Yu B, Zhao Y, Zhu W, Li H, Lou H, et al. Enhancement of oral absorption of curcumin by self-microemulsifying drug delivery systems. *International Journal of Pharmaceutics*. 2009;371(1-2):148-55.
50. Singh AK, Chaurasiya A, Awasthi A, Mishra G, Asati D, Khar RK, et al. Oral bioavailability enhancement of exemestane from self-microemulsifying drug delivery system (SMEDDS). *AAPS PharmSciTech*. 2009;10(3):906-16.
51. Cho YD, Park YJ. In vitro and in vivo evaluation of a self-microemulsifying drug delivery system for the poorly soluble drug fenofibrate. *Archives of Pharmacal Research*. 2014;37(2):193-203.
52. Mezghrani O, Ke X, Bourkaib N, Xu BH. Optimized self-microemulsifying drug delivery systems (SMEDDS) for enhanced oral bioavailability of astilbin. *An International Journal of Pharmaceutical Sciences*. 2011;66(10):754-60.
53. Warisnoicharoen W, Lansley AB, Lawrence MJ. Nonionic oil-in-water microemulsions: the effect of oil type on phase behaviour. *International Journal of Pharmaceutics*. 2000;198(1):7-27.

54. Djekic L, Primorac M. The influence of cosurfactants and oils on the formation of pharmaceutical microemulsions based on PEG-8 caprylic/capric glycerides. *International Journal of Pharmaceutics*. 2008;352(1-2):231-9.
55. Li P, Ghosh A, Wagner RF, Krill S, Joshi YM, Serajuddin AT. Effect of combined use of nonionic surfactant on formation of oil-in-water microemulsions. *International Journal of Pharmaceutics*. 2005;288(1):27-34.
56. Mahdi ES, Sakeena MH, Abdulkarim MF, Abdullah GZ, Sattar MA, Noor AM. Effect of surfactant and surfactant blends on pseudoternary phase diagram behavior of newly synthesized palm kernel oil esters. *Drug Design, Development and Therapy*. 2011;5:311-23.
57. Huibers PDT, Shah DO. Evidence for Synergism in Nonionic Surfactant Mixtures: Enhancement of Solubilization in Water-in-Oil Microemulsions. *Langmuir*. 1997;13(21):5762-5.
58. Gullapalli RP, Sheth BB. Influence of an optimized non-ionic emulsifier blend on properties of oil-in-water emulsions. *European Journal of Pharmaceutics and Biopharmaceutics*. 1999;48(3):233-8.
59. Alany RG, Rades T, Agatonovic-Kustrin S, Davies NM, Tucker IG. Effects of alcohols and diols on the phase behaviour of quaternary systems. *International Journal of Pharmaceutics*. 2000;196(2):141-5.
60. Bagwe RP, Kanicky JR, Palla BJ, Patanjali PK, Shah DO. Improved drug delivery using microemulsions: rationale, recent progress, and new horizons. *Critical Reviews In Therapeutic Drug Carrier Systems*. 2001;18(1):77-140.
61. Do L, Withayyapayanon A, Harwell J, Sabatini D. Environmentally Friendly Vegetable Oil Microemulsions Using Extended Surfactants and Linkers. *Journal of Surfactants and Detergents*. 2009;12(2):91-9.
62. Holm R, Müllertz A, Christensen E, Høy C-E, Kristensen HG. Comparison of total oral bioavailability and the lymphatic transport of halofantrine from three different unsaturated triglycerides in lymph-cannulated conscious rats. *European Journal of Pharmaceutical Sciences*. 2001;14(4):331-7.
63. Hauss DJ. Oral lipid-based formulations. *Advanced Drug Delivery Reviews*. 2007;59(7):667-76.

64. Pouton CW, Porter CJH. Formulation of lipid-based delivery systems for oral administration: Materials, methods and strategies. *Advanced Drug Delivery Reviews*. 2008;60(6):625-37.
65. Lowell G. Lipid based excipients for oral drug delivery. In: Hauss DJ, editor. *Oral Lipid-Based Formulations*: CRC Press; 2007. p.33-61.
66. Kohli K, Chopra S, Dhar D, Arora S, Khar RK. Self-emulsifying drug delivery systems: an approach to enhance oral bioavailability. *Drug Discovery Today*. 2010;15(21-22):958-65.
67. Wang L, Dong J, Chen J, Eastoe J, Li X. Design and optimization of a new self-nanoemulsifying drug delivery system. *Journal of Colloid and Interface Science*. 2009;330(2):443-8.
68. Porter CJH, Pouton CW, Cuine JF, Charman WN. Enhancing intestinal drug solubilisation using lipid-based delivery systems. *Advanced Drug Delivery Reviews*. 2008;60(6):673-91.
69. Gershkovich P, Hoffman A. Uptake of lipophilic drugs by plasma derived isolated chylomicrons: Linear correlation with intestinal lymphatic bioavailability. *European Journal of Pharmaceutical Sciences*. 2005;26(5):394-404.
70. Artursson P, Palm K, Luthman K. Caco-2 monolayers in experimental and theoretical predictions of drug transport. *Advanced Drug Delivery Reviews*. 2001;46(1-3):27-43.
71. Luchoomun J, Hussain MM. Assembly and secretion of chylomicrons by differentiated Caco-2 cells. Nascent triglycerides and preformed phospholipids are preferentially used for lipoprotein assembly. *Journal of Biological Chemistry*. 1999;274(28):19565-72.
72. During A, Hussain MM, Morel DW, Harrison EH. Carotenoid uptake and secretion by CaCo-2 cells: beta-carotene isomer selectivity and carotenoid interactions. *Journal of Lipid Research*. 2002;43(7):1086-95.
73. Van Greevenbroek MMJ, van Meer G, Erkelens DW, de Bruin TWA. Effects of saturated, mono-, and polyunsaturated fatty acids on the secretion of apo B containing lipoproteins by Caco-2 cells. *Atherosclerosis*. 1996;121(1):139-50.

74. Van Greevenbroek MM, Robertus-Teunissen MG, Erkelens DW, de Bruin TW. Lipoprotein secretion by intestinal Caco-2 cells is affected differently by trans and cis unsaturated fatty acids: effect of carbon chain length and position of the double bond. *American Journal of Clinical Nutrition*. 1998;68(3):561-7.
75. Yi T, Wan J, Xu H, Yang X. A new solid self-microemulsifying formulation prepared by spray-drying to improve the oral bioavailability of poorly water soluble drugs. *European Journal of Pharmaceutics and Biopharmaceutics*. 2008;70(2):439-44.
76. Oh DH, Kang JH, Kim DW, Lee BJ, Kim JO, Yong CS, et al. Comparison of solid self-microemulsifying drug delivery system (solid SMEDDS) prepared with hydrophilic and hydrophobic solid carrier. *International Journal of Pharmaceutics*. 2011;420(2):412-8.
77. Joshi M, Pathak S, Sharma S, Patravale V. Solid microemulsion concentrate (NanOsorb) of artemether for effective treatment of malaria. *International Journal of Pharmaceutics*. 2008;362(1-2):172-8.
78. Dixit RP, Nagarsenker MS. Optimized microemulsions and solid microemulsion systems of simvastatin: characterization and in vivo evaluation. *Journal of Pharmaceutical Sciences*. 2010;99(12):4892-902.
79. Nekkanti V, Karatgi P, Prabhu R, Pillai R. Solid self-microemulsifying formulation for candesartan cilexetil. *AAPS PharmSciTech*. 2010;11(1):9-17.
80. Li P, Hynes SR, Haefele TF, Pudipeddi M, Royce AE, Serajuddin AT. Development of clinical dosage forms for a poorly water-soluble drug II: formulation and characterization of a novel solid microemulsion concentrate system for oral delivery of a poorly water-soluble drug. *Journal of Pharmaceutical Sciences*. 2009;98(5):1750-64.
81. Sander C, Holm P. Porous magnesium aluminometasilicate tablets as carrier of a cyclosporine self-emulsifying formulation. *AAPS PharmSciTech*. 2009;10(4):1388-95.
82. Zvonar A, Berginc K, Kristl A, Gasperlin M. Microencapsulation of self-microemulsifying system: improving solubility and permeability of furosemide. *International Journal of Pharmaceutics*. 2010;388(1-2):151-8.

83. Setthacheewakul S, Mahattanadol S, Phadoongsombut N, Pichayakorn W, Wiwattanapatapee R. Development and evaluation of self-microemulsifying liquid and pellet formulations of curcumin, and absorption studies in rats. *European Journal of Pharmaceutics and Biopharmaceutics*. 2010;76(3):475-85.
84. Hentzschel CM, Sakmann A, Leopold CS. Suitability of various excipients as carrier and coating materials for liquisolid compacts. *Drug Development and Industrial Pharmacy*. 2011;37(10):1200-7.
85. Beg S, Swain S, Singh HP, Patra Ch N, Rao ME. Development, optimization, and characterization of solid self-nanoemulsifying drug delivery systems of valsartan using porous carriers. *AAPS PharmSciTech*. 2012;13(4):1416-27.
86. Agarwal V, Siddiqui A, Ali H, Nazzal S. Dissolution and powder flow characterization of solid self-emulsified drug delivery system (SEDDS). *International Journal of Pharmaceutics*. 2009;366(1-2):44-52.
87. Yuan W, Li G, Gil ES, Lowe TL, Fu BM. Effect of surface charge of immortalized mouse cerebral endothelial cell monolayer on transport of charged solutes. *Annals of Biomedical Engineering*. 2010;38(4):1463-72.
88. Imola Wilhelm, Csilla Fazakas, Krizbai IA. In vitro models of the blood-brain barrier. *Acta Neurobiologiae Experimentalis* 2011;71:113-28.
89. Scherrmann JM. Drug delivery to brain via the blood-brain barrier. *Vascular Pharmacology*. 2002;38(6):349-54.
90. Shinde RL, Jindal AB, Devarajan PV. Microemulsions and nanoemulsions for targeted drug delivery to the brain. *Current Nanoscience*. 2011;7:119-33.
91. Jones A, Shusta E. Blood-brain barrier transport of therapeutics via receptor-mediation. *Pharmaceutical Research*. 2007;24(9):1759-71.
92. Hussain MM, Strickland DK, Bakillah A. The mammalian low-density lipoprotein receptor family. *Annual Review of Nutrition*. 1999;19:141-72.
93. Wagner S, Zensi A, Wien SL, Tschickardt SE, Maier W, Vogel T, et al. Uptake mechanism of apoE-modified nanoparticles on brain capillary endothelial cells as a blood-brain barrier model. *PLoS ONE*. 2012;7(3):e32568.

94. Kreuter J, Shamenkov D, Petrov V, Ramge P, Cychutek K, Koch-Brandt C, et al. Apolipoprotein-mediated transport of nanoparticle-bound drugs across the blood-brain barrier. *Journal of Drug Targeting*. 2002;10(4):317-25.
95. Gulyaev AE, Gelperina SE, Skidan IN, Antropov AS, Kivman GY, Kreuter J. Significant transport of doxorubicin into the brain with polysorbate 80-coated nanoparticles. *Pharmaceutical Research*. 1999;16(10):1564-9.
96. Gao K, Jiang X. Influence of particle size on transport of methotrexate across blood brain barrier by polysorbate 80-coated polybutylcyanoacrylate nanoparticles. *International Journal of Pharmaceutics*. 2006;310(1-2):213-9.
97. Sun W, Xie C, Wang H, Hu Y. Specific role of polysorbate 80 coating on the targeting of nanoparticles to the brain. *Biomaterials*. 2004;25(15):3065-71.
98. Gumbleton M, Audus KL. Progress and limitations in the use of in vitro cell cultures to serve as a permeability screen for the blood-brain barrier. *Journal of Pharmaceutical Sciences*. 2001;90(11):1681-98.
99. Brown RC, Morris AP, O'Neil RG. Tight junction protein expression and barrier properties of immortalized mouse brain microvessel endothelial cells. *Brain Research*. 2008;1130(1):17-30.
100. Li G, Simon MJ, Cancel LM, Shi ZD, Ji X, Tarbell JM, et al. Permeability of endothelial and astrocyte cocultures: in vitro blood-brain barrier models for drug delivery studies. *Annals of Biomedical Engineering*. 2010;38(8):2499-511.
101. Radany EH, Brenner M, Besnard F, Bigornia V, Bishop JM, Deschepper CF. Directed establishment of rat brain cell lines with the phenotypic characteristics of type 1 astrocytes. *Proceedings of the National Academy of Sciences of the United States of America*. 1992;89(14):6467-71.
102. Abbott NJ, Dolman DE, Drndarski S, Fredriksson SM. An improved in vitro blood-brain barrier model: rat brain endothelial cells co-cultured with astrocytes. *Methods in Molecular Biology*. 2012;814:415-30.
103. Candela P, Gosselet F, Miller F, Buee-Scherrer V, Torpier G, Cecchelli R, et al. Physiological pathway for low-density lipoproteins across the blood-brain barrier: transcytosis through brain capillary endothelial cells *in vitro*. *Endothelium*. 2008;15(5-6):254-64.

104. Cantrill CA, Skinner RA, Rothwell NJ, Penny JI. An immortalised astrocyte cell line maintains the in vivo phenotype of a primary porcine in vitro blood-brain barrier model. *Brain Research*. 2012;1479:17-30.
105. Margareth R. C. Marques, Raimar Loebenberg, Almkainzi M. Simulated biological fluids with possible application in dissolution testing. *Dissolution Technologies*. 2011:15-28.
106. USP34-NF29. Bromocriptine mesylate. United States Pharmacopeia and National Formulary (USP 34-NF 29). 2. Rockville, MD: United book press, Inc.; 2011. p. 2076-79.
107. Carr RL. Evaluating flow properties of solids. *Chemical Engineering Journal*. 1965;72:163-8.
108. Freeman R. Measuring the flow properties of consolidated, conditioned and aerated powders — A comparative study using a powder rheometer and a rotational shear cell. *Powder Technology*. 2007;174(1-2):25-33.
109. Vasilenko A, Glasser BJ, Muzzio FJ. Shear and flow behavior of pharmaceutical blends — Method comparison study. *Powder Technology*. 2011;208(3):628-36.
110. Huynh-Ba K. Understanding ICH Guidelines Applicable to Stability Testing. In: Huynh-Ba K, Zahn M, editors. *Handbook of Stability Testing in Pharmaceutical Development*. New York: Springer Science+Business Media, LLC; 2009. p.22-40.
111. Van Speybroeck M, Williams HD, Nguyen TH, Anby MU, Porter CJ, Augustijns P. Incomplete desorption of liquid excipients reduces the in vitro and in vivo performance of self-emulsifying drug delivery systems solidified by adsorption onto an inorganic mesoporous carrier. *Molecular Pharmaceutics*. 2012;9(9):2750-60.
112. Gumaste SG, Pawlak SA, Dalrymple DM, Nider CJ, Trombetta LD, Serajuddin AT. Development of Solid SEDDS, IV: Effect of Adsorbed Lipid and Surfactant on Tableting Properties and Surface Structures of Different Silicates. *Pharm Research*. 2013;30(12):3170-85.
113. Seeballuck F, Lawless E, Ashford MB, O'Driscoll CM. Stimulation of triglyceride-rich lipoprotein secretion by polysorbate 80: in vitro and in vivo correlation using Caco-2 cells and a cannulated rat intestinal lymphatic model. *Pharm Research*. 2004;21(12):2320-6.

114. Gumaste SG, Dalrymple DM, Serajuddin AT. Development of Solid SEDDS, V: Compaction and Drug Release Properties of Tablets Prepared by Adsorbing Lipid-Based Formulations onto Neusilin(R) US2. *Pharm Research*. 2013;30(12):3186-99.
115. Cho YH, Kim S, Bae EK, Mok CK, Park J. Formulation of a cosurfactant-free O/W microemulsion using nonionic surfactant mixtures. *Journal of Food Science*. 2008;73(3):E115-21.
116. Phan T, Harwell J, Sabatini D. Effects of Triglyceride Molecular Structure on Optimum Formulation of Surfactant-Oil-Water Systems. *Journal of Surfactants and Detergents*. 2010;13(2):189-94.
117. Malcolmson C, Lawrence MJ. Three-component non-ionic oil-in-water microemulsions using polyoxyethylene ether surfactants. *Colloids and Surfaces B: Biointerfaces*. 1995;4(2):97-109.
118. Bayrak Y, Iscan M. Studies on the phase behavior of the system non-ionic surfactant/alcohol/alkane/H₂O. *Colloids and Surfaces A: Physicochemical and Engineering Aspects*. 2005;268(1-3):99-103.
119. Djekic L, Primorac M, Filipic S, Agbaba D. Investigation of surfactant/cosurfactant synergism impact on ibuprofen solubilization capacity and drug release characteristics of nonionic microemulsions. *International Journal of Pharmaceutics*. 2012;433(1-2):25-33.
120. Rakhi B. Shah, Mobin A. Tawakkul, Khan MA. Comparative evaluation of flow for pharmaceutical powders and granules. *AAPS PharmSciTech*. 2008;9(1):250-8.
121. Oh DH, Kang JH, Kim DW, Lee B-J, Kim JO, Yong CS, et al. Comparison of solid self-microemulsifying drug delivery system (solid SMEDDS) prepared with hydrophilic and hydrophobic solid carrier. *International Journal of Pharmaceutics*. 2011;420(2):412-8.
122. Van Greevenbroek MM, Voorhout WF, Erkelens DW, van Meer G, de Bruin TW. Palmitic acid and linoleic acid metabolism in Caco-2 cells: different triglyceride synthesis and lipoprotein secretion. *Journal of Lipid Research*. 1995;36(1):13-24.
123. Lorec AM, Juhel C, Pafumi Y, Portugal H, Pauli AM, Lairon D, et al. Determination of apolipoprotein B-48 in plasma by a competitive ELISA. *Clinical Chemistry*. 2000;46(10):1638-42.

124. Kinoshita M, Kojima M, Matsushima T, Teramoto T. Determination of apolipoprotein B-48 in serum by a sandwich ELISA. *Clinica Chimica Acta; International Journal of Clinical Chemistry*. 2005;351(1-2):115-20.
125. Fletcher NF, Brayden DJ, Brankin B, Worrall S, Callanan JJ. Growth and characterisation of a cell culture model of the feline blood–brain barrier. *Veterinary Immunology and Immunopathology*. 2006;109(3–4):233-44.
126. Koto T, Takubo K, Ishida S, Shinoda H, Inoue M, Tsubota K, et al. Hypoxia disrupts the barrier function of neural blood vessels through changes in the expression of claudin-5 in endothelial cells. *The American Journal of Pathology*. 2007;170(4):1389-97.



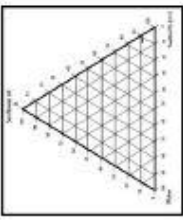
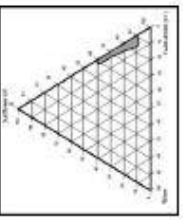


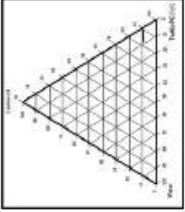
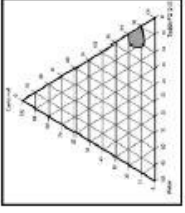
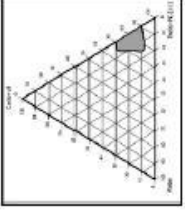
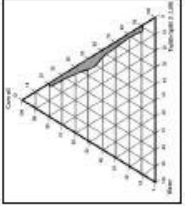
APPENDICES

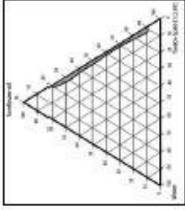
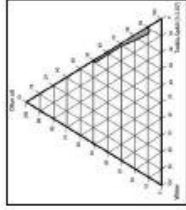
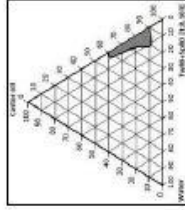
จุฬาลงกรณ์มหาวิทยาลัย
CHULALONGKORN UNIVERSITY

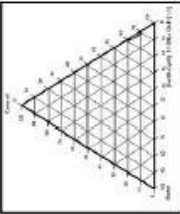
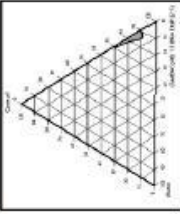
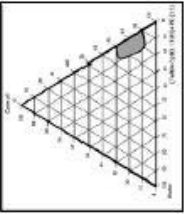
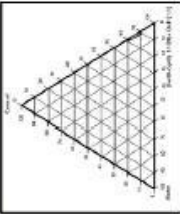
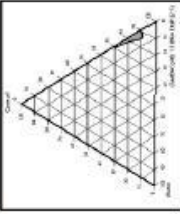
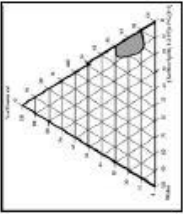
APPENDIX A
Self-microemulsion liquid

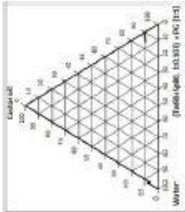
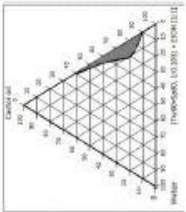
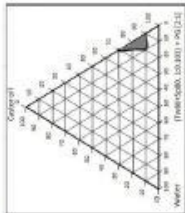
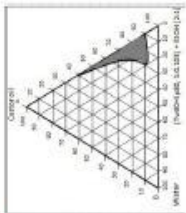
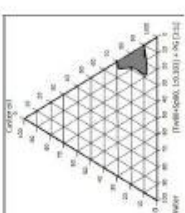
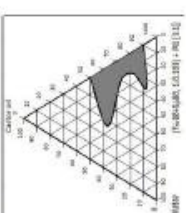
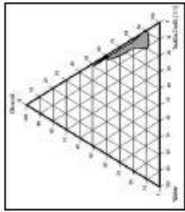
Table A-1 Pseudoternary phase diagram of ME systems

Oils	Surfactants	ME formation		
		Ratios of surfactant to cosurfactant		
		1:1	2:1	3:1
Sunflower oil	Tween 80			PG  EtOH 

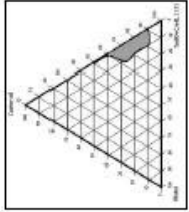
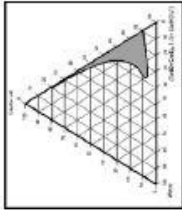
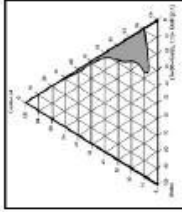
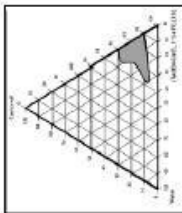
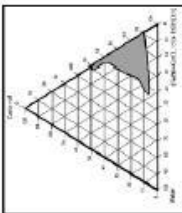
Castor oil	Tween 80			
		PG	PG	PG
		EtOH	EtOH	EtOH
Corn oil	Tween 80 : Sp80 (1:1.89)	1:0		
				

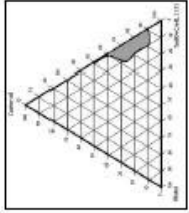
<p>Sunflower oil</p>	<p>Tw80 : Sp80 (1:2.97)</p>	
<p>Olive oil</p>	<p>Tw80 : Sp80 (1:2.97)</p>	
<p>Castor oil</p>	<p>Tw80 : Sp80 (1:0.103)</p>	

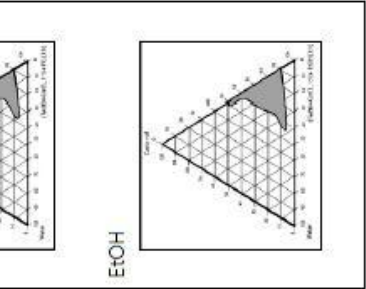
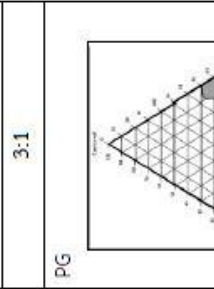
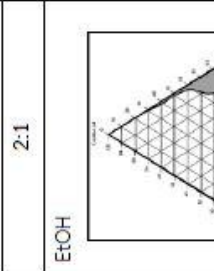
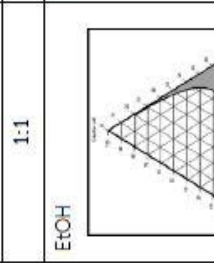
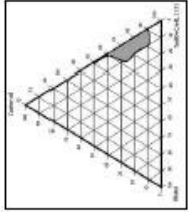
	1:1	2:1	3:1
<p>Corn oil</p> <p>Tw80 : Sp80 (1:1.89)</p>	<p>EtOH</p> 	<p>EtOH</p> 	<p>PG</p> 
<p>Sunflower oil</p> <p>Tw80 : Sp80 (1:2.97)</p>	<p>EtOH</p> 	<p>EtOH</p> 	<p>PG</p> 

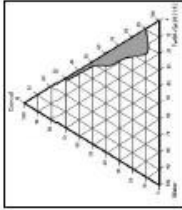
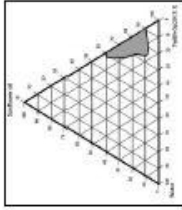
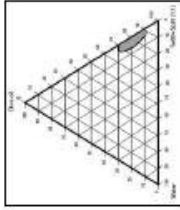
<p>Castor oil</p>	<p>Tw80 : Sp80 (1:0.103)</p>	<p>PG </p> <p>EtOH </p>	<p>PG </p> <p>EtOH </p>	<p>PG </p> <p>EtOH </p>
<p>Olive oil</p>	<p>Tw80 : CreEL (1:1)</p>	<p>1:0 </p>		

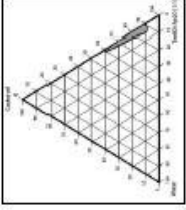
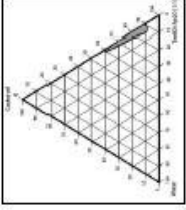
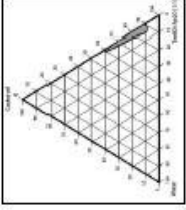
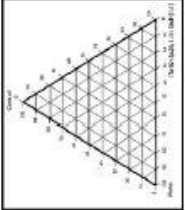
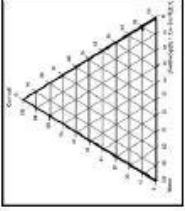
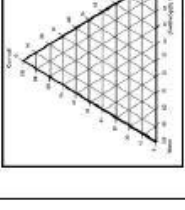
		EtOH	EtOH	EtOH
Olive oil	Tw80 : Sp80 (1:2.97)		EtOH	PG EtOH

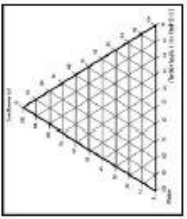
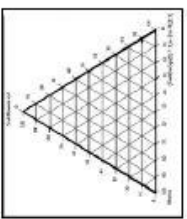
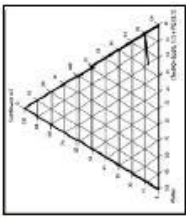
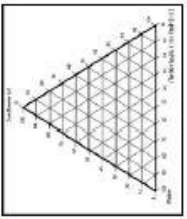
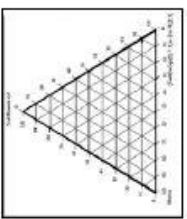
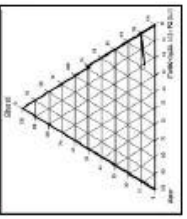
Castor oil	Tw60 : CreEL (1:1)	
Castor oil	Tw60 : CreEL (1:1)	<div style="display: flex; justify-content: space-around;"> <div style="text-align: center;"> <p>1:1</p>  <p>EtOH</p> </div> <div style="text-align: center;"> <p>2:1</p>  <p>EtOH</p> </div> <div style="text-align: center;"> <p>3:1</p> <div style="display: flex; flex-direction: column; align-items: center;">  <p>PG</p>  <p>EtOH</p> </div> </div> </div>

Castor oil					
Tw80 : CreEL (1:1)					
Castor oil					
Tw80 : CreEL (1:1)					
Castor oil					
Tw80 : CreEL (1:1)					



1:0		
Corn oil	Tw80 : Sp20 (1:1)	
Sunflower oil	Tw80 : Sp20 (1:1)	
Olive oil	Tw80 : Sp20 (1:1)	

Castor oil	Tw80 : Sp20 (1:1)		1:1		2:1		3:1
Corn oil	Tw80 : Sp20 (1:1)		1:1		2:1		3:1

Sunflower oil	Tw60 : Sp20 (1:1)	<p>EtOH</p> 	<p>EtOH</p> 	<p>PG</p> 
Olive oil	Tw60 : Sp20 (1:1)	<p>EtOH</p> 	<p>EtOH</p> 	<p>PG</p> 

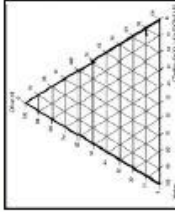
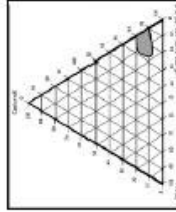
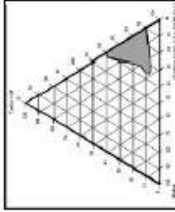
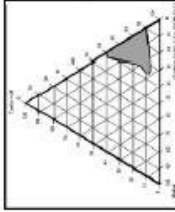
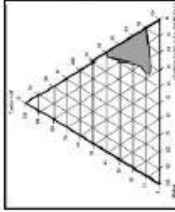
Castor oil				<p>EtOH</p> 
Castor oil Tw80 : Sp20 (1:1)			<p>PG</p> 	<p>EtOH</p> 
				<p>EtOH</p> 
				<p>EtOH</p> 

Table A-2 Statistical testing: Effect of amount of castor oil (10, 15, 20 and 25% w/w) on particle size.

Descriptives

	N	Mean	Std. Deviation	Std. Error	95% Confidence Interval for Mean		Minimum	Maximum
					Lower Bound	Upper Bound		
10%	6	13.9567	.47005	.19190	13.4634	14.4500	13.59	14.88
15%	6	16.6717	.61856	.25253	16.0225	17.3208	16.02	17.53
20%	6	77.7500	16.42754	6.70652	60.5104	94.9896	56.27	92.21
25%	6	141.7667	12.76788	5.21246	128.3676	155.1657	128.60	154.70
Total	24	62.5363	54.37477	11.09920	39.5758	85.4967	13.59	154.70

Test of Homogeneity of Variances

Levene Statistic	df1	df2	Sig.
39.244	3	20	.000

ANOVA

	Sum of Squares	df	Mean Square	F	Sig.
Between Groups	65834.718	3	21944.906	202.497	.000
Within Groups	2167.432	20	108.372		
Total	68002.150	23			

Multiple Comparisons

	(I) Oil	(J) Oil	Mean Difference (I-J)	Std. Error	Sig.	95% Confidence Interval	
						Lower Bound	Upper Bound
Dunnett T3	10%	15%	-2.71500(*)	.31717	.000	-3.7444	-1.6856
		20%	-63.79333(*)	6.70926	.001	-90.1262	-37.4605
		25%	-127.81000(*)	5.21599	.000	-148.2728	-107.3472
	15%	10%	2.71500(*)	.31717	.000	1.6856	3.7444
		20%	-61.07833(*)	6.71127	.001	-87.4059	-34.7508
		25%	-125.09500(*)	5.21858	.000	-145.5511	-104.6389
	20%	10%	63.79333(*)	6.70926	.001	37.4605	90.1262
		15%	61.07833(*)	6.71127	.001	34.7508	87.4059
		25%	-64.01667(*)	8.49395	.000	-91.5257	-36.5076
	25%	10%	127.81000(*)	5.21599	.000	107.3472	148.2728
		15%	125.09500(*)	5.21858	.000	104.6389	145.5511
		20%	64.01667(*)	8.49395	.000	36.5076	91.5257

* The mean difference is significant at the .05 level.



Table A-3 Solubility of drug (mg/ml) in various oils, surfactants and selected SME system at 25 ± 0.1 °C for 48 hours.

Solvents	Area	Dilution factor	Drug concentration (mg/ml)
Castor oil_001	278520	500	7.218816821
Castor oil_002	280077	500	7.259171904
Castor oil_003	280180	500	7.261841508
Corn oil_001	215612	10	0.111766734
Corn oil_002	237359	10	0.12303972
Corn oil_003	214304	10	0.111088706
Olive oil_001	601109	10	0.311596708
Olive oil_002	597403	10	0.30967563
Olive oil_003	616211	10	0.319425128
Sunflower oil_001	152744	10	0.079177866
Sunflower oil_002	168920	10	0.087563014
Sunflower oil_003	153507	10	0.079573382
Span [®] 20_001	109305	1000	5.666040303
Span [®] 20_002	110355	1000	5.720469125
Span [®] 20_003	110490	1000	5.727467116
Span [®] 80_001	152951	1000	7.928516815
Span [®] 80_002	153391	1000	7.951325083
Span [®] 80_003	153510	1000	7.957493682
Tween [®] 80_001	346198	1000	17.94585628
Tween [®] 80_002	349272	1000	18.10520314
Tween [®] 80_003	347565	1000	18.01671742
Cremophor [®] EL_001	374382	1000	19.40682952
Cremophor [®] EL_002	373985	1000	19.38625024
Cremophor [®] EL_003	372170	1000	19.29216614
SME system_001	538254	1000	27.90145791
SME system_001	539726	1000	27.97776194
SME system_001	541510	1000	28.0702391

Table A-4 Statistical testing: Effect of solvents on drug solubility.

Descriptives

	N	Mean	Std. Deviation	95% Confidence Interval for Mean		Minimum	Maximum
				Lower Bound	Upper Bound		
Castor	3	7.246600	.0241106	7.186706	7.306494	7.2188	7.2618
Corn	3	.115300	.0066776	.098712	.131888	.1111	.1230
Olive	3	.313567	.0051404	.300797	.326336	.3097	.3194
Sunflower	3	.082133	.0047385	.070362	.093904	.0792	.0876
Span20	3	5.704667	.0336687	5.621029	5.788304	5.6660	5.7275
Span80	3	7.945767	.0152713	7.907831	7.983703	7.9285	7.9575
Tween80	3	18.022600	.0798137	17.824332	18.220868	17.9459	18.1052
CremophorEL	3	19.361767	.0611122	19.209955	19.513578	19.2922	19.4068
SMEDDS	3	27.983167	.0844779	27.773312	28.193022	27.9015	28.0702
Total	27	9.641730	9.5740397	5.854366	13.429094	.0792	28.0702

Test of Homogeneity of Variances

Levene Statistic	df1	df2	Sig.
2.873	8	18	.030

ANOVA

	Sum of Squares	df	Mean Square	F	Sig.
Between Groups	2383.180	8	297.897	139038.088	.000
Within Groups	.039	18	.002		
Total	2383.218	26			

Multiple Comparisons

(I) Solvent	(J) Solvent	Mean Difference (I-J)	Std. Error	Sig.	95% Confidence Interval		
					Lower Bound	Upper Bound	
Dunn ett T3	Castor oil	Corn oil	7.1313000(*)	.0144443	.000	6.999481	7.263119
		Olive oil	6.9330333(*)	.0142331	.000	6.795189	7.070878
		Sunflower oil	7.1644667(*)	.0141865	.000	7.025134	7.303799
		Span20	1.5419333(*)	.0239089	.000	1.392237	1.691630
		Span80	-.6991667(*)	.0164776	.000	-.807269	-.591064
		Tween80	-10.7760000(*)	.0481371	.000	-11.204354	-10.347646
		CremophorEL	-12.1151667(*)	.0379299	.000	-12.421842	-11.808492
		SMEDDS	-20.7365667(*)	.0507209	.000	-21.195574	-20.277559
		Castor oil	-7.1313000(*)	.0144443	.000	-7.263119	-6.999481
		Olive oil	-.1982667(*)	.0048653	.000	-.228047	-.168486
		Sunflower oil	.0331667(*)	.0047273	.035	.003475	.062858
		Span20	-5.5893667(*)	.0198173	.000	-5.783714	-5.395019
		Span80	-7.8304667(*)	.0096229	.000	-7.904959	-7.755975
		Tween80	-17.9073000(*)	.0462415	.000	-18.394522	-17.420078
		CremophorEL	-19.2464667(*)	.0354932	.000	-19.616131	-18.876803
		SMEDDS	-27.8678667(*)	.0489255	.000	-28.384289	-27.351444
	Castor oil	-6.9330333(*)	.0142331	.000	-7.070878	-6.795189	
	Corn oil	.1982667(*)	.0048653	.000	.168486	.228047	
	Sunflower oil	.2314333(*)	.0040364	.000	.207571	.255295	
	Span20	-5.3911000(*)	.0196639	.000	-5.590686	-5.191514	
	Span80	-7.6322000(*)	.0093030	.000	-7.712091	-7.552309	
	Tween80	-17.7090333(*)	.0461759	.000	-18.198884	-17.219182	
	CremophorEL	-19.0482000(*)	.0354078	.000	-19.421206	-18.675194	
	SMEDDS	-27.6696000(*)	.0488636	.000	-28.188517	-27.150683	
	Castor oil	-7.1644667(*)	.0141865	.000	-7.303799	-7.025134	
	Corn oil	-.0331667(*)	.0047273	.035	-.062858	-.003475	
	Olive oil	-.2314333(*)	.0040364	.000	-.255295	-.207571	
	Span20	-5.6225333(*)	.0196302	.000	-5.823341	-5.421726	
	Span80	-7.8636333(*)	.0092316	.000	-7.945097	-7.782170	
	Tween80	-17.9404667(*)	.0461616	.000	-18.430899	-17.450034	
	CremophorEL	-19.2796333(*)	.0353891	.000	-19.653385	-18.905882	
	SMEDDS	-27.9010333(*)	.0488500	.000	-28.420501	-27.381566	
	Castor oil	-1.5419333(*)	.0239089	.000	-1.691630	-1.392237	
	Corn oil	5.5893667(*)	.0198173	.000	5.395019	5.783714	
	Olive oil	5.3911000(*)	.0196639	.000	5.191514	5.590686	

	Sunflower oil	5.6225333(*)	.0196302	.000	5.421726	5.823341
	Span80	-2.2411000(*)	.0213448	.000	-2.403684	-2.078516
	Tween80	-12.3179333(*)	.0500127	.000	-12.711144	-11.924722
	CremophorEL	-13.6571000(*)	.0402835	.000	-13.938000	-13.376200
	SMEDDS	-22.2785000(*)	.0525043	.000	-22.701256	-21.855744
Span80	Castor oil	.6991667(*)	.0164776	.000	.591064	.807269
	Corn oil	7.8304667(*)	.0096229	.000	7.755975	7.904959
	Olive oil	7.6322000(*)	.0093030	.000	7.552309	7.712091
	Sunflower oil	7.8636333(*)	.0092316	.000	7.782170	7.945097
	Span20	2.2411000(*)	.0213448	.000	2.078516	2.403684
	Tween80	-10.0768333(*)	.0469164	.000	-10.539566	-9.614101
	CremophorEL	-11.4160000(*)	.0363681	.000	-11.756704	-11.075296
	SMEDDS	-20.0374000(*)	.0495639	.000	-20.530326	-19.544474
Tween80	Castor oil	10.7760000(*)	.0481371	.000	10.347646	11.204354
	Corn oil	17.9073000(*)	.0462415	.000	17.420078	18.394522
	Olive oil	17.7090333(*)	.0461759	.000	17.219182	18.198884
	Sunflower oil	17.9404667(*)	.0461616	.000	17.450034	18.430899
	Span20	12.3179333(*)	.0500127	.000	11.924722	12.711144
	Span80	10.0768333(*)	.0469164	.000	9.614101	10.539566
	CremophorEL	-1.3391667(*)	.0580372	.000	-1.694956	-.983377
	SMEDDS	-9.9605667(*)	.0670988	.000	-10.356447	-9.564687
CremophorEL	Castor oil	12.1151667(*)	.0379299	.000	11.808492	12.421842
	Corn oil	19.2464667(*)	.0354932	.000	18.876803	19.616131
	Olive oil	19.0482000(*)	.0354078	.000	18.675194	19.421206
	Sunflower oil	19.2796333(*)	.0353891	.000	18.905882	19.653385
	Span20	13.6571000(*)	.0402835	.000	13.376200	13.938000
	Span80	11.4160000(*)	.0363681	.000	11.075296	11.756704
	Tween80	1.3391667(*)	.0580372	.000	.983377	1.694956
	SMEDDS	-8.6214000(*)	.0601975	.000	-8.997016	-8.245784
SMEDDS	Castor oil	20.7365667(*)	.0507209	.000	20.277559	21.195574
	Corn oil	27.8678667(*)	.0489255	.000	27.351444	28.384289
	Olive oil	27.6696000(*)	.0488636	.000	27.150683	28.188517
	Sunflower oil	27.9010333(*)	.0488500	.000	27.381566	28.420501
	Span20	22.2785000(*)	.0525043	.000	21.855744	22.701256
	Span80	20.0374000(*)	.0495639	.000	19.544474	20.530326
	Tween80	9.9605667(*)	.0670988	.000	9.564687	10.356447
	CremophorEL	8.6214000(*)	.0601975	.000	8.245784	8.997016

* The mean difference is significant at the .05 level.

a Dunnett t-tests treat one group as a control, and compare all other groups against it.

APPENDIX B
Self-microemulsion powder and tablet

Table B-1 Stability index of SME powders.

Ratio of SME liquid to solid carrier	Stability index		
	Aerosil [®] 200	Aeroperl [®] 300	Neusilin US2 [®]
0.0:1	0.63	0.92	0.94
	0.39	0.98	0.98
	0.53	0.96	1.00
0.5:1	1.13	1.10	1.24
	1.10	1.09	1.17
	1.18	1.10	1.19
1.0:1	1.02	1.17	1.16
	0.95	1.24	1.20
	1.01	1.22	1.07
1.5:1	0.92	1.02	1.17
	0.94	1.01	1.31
	0.98	1.07	1.26
2.0:1	0.96	0.98	1.04
	1.03	1.04	1.28
	1.02	1.12	0.98
2.5:1	NA	NA	1.07
	NA	NA	1.07
	NA	NA	1.12

Table B-2 Basic flow energy (BFE) of SME powders.

Ratio of SME liquid to solid carrier	BFE (mJ)		
	Aerosil [®] 200	Aeroperl [®] 300	Neusilin US2 [®]
0.0:1	10.57	30.84	28.68
	9.30	28.08	28.02
	8.20	28.15	28.08
0.5:1	5.09	33.59	18.43
	5.88	31.13	17.33
	5.66	31.10	18.86
1.0:1	12.40	42.56	28.66
	12.87	49.66	26.80
	12.84	44.60	29.50
1.5:1	37.02	86.45	57.55
	35.30	86.77	61.65
	37.69	84.82	69.34
2.0:1	138.21	115.02	90.65
	124.25	107.99	92.84
	116.90	88.91	78.63
2.5:1	NA	NA	207.49
	NA	NA	189.00
	NA	NA	158.22

Table B-3 Linear regression analysis: Effect of Polyvinylpyrrolidone K90, Kollidon[®] CL and Magnesium stearate on disintegration time.

Variables Entered/Removed^a

Model	Variables Entered	Variables Removed	Method
1	KollidonCL_X2		. Stepwise (Criteria: Probability-of-F-to-enter <= .050, Probability-of-F-to-remove >= .100).
2	X2X2		. Stepwise (Criteria: Probability-of-F-to-enter <= .050, Probability-of-F-to-remove >= .100).

a. Dependent Variable: DT



Model Summary^c

Model	R	R Square	Adjusted R Square	Std. Error of the Estimate	Change Statistics					Durbin-Watson
					R Square Change	F Change	df1	df2	Sig. F Change	
1	.838 ^a	.703	.680	4.00835	.703	30.698	1	13	.000	
2	.897 ^b	.805	.772	3.38166	.102	6.265	1	12	.028	2.162

a. Predictors: (Constant), KollidonCL_X2

b. Predictors: (Constant), KollidonCL_X2, X2X2

c. Dependent Variable: DT

ANOVA^c

Model		Sum of Squares	df	Mean Square	F	Sig.
1	Regression	493.219	1	493.219	30.698	.000 ^a
	Residual	208.869	13	16.067		
	Total	702.088	14			
2	Regression	564.860	2	282.430	24.697	.000 ^b
	Residual	137.228	12	11.436		
	Total	702.088	14			

a. Predictors: (Constant), KollidonCL_X2

b. Predictors: (Constant), KollidonCL_X2, X2X2

c. Dependent Variable: DT

Coefficients^a

Model		Unstandardized Coefficients		Standardized Coefficients	t	Sig.	95.0% Confidence Interval for B	
		B	Std. Error	Beta			Lower Bound	Upper Bound
1	(Constant)	14.560	1.806		8.062	.000	10.659	18.462
	KollidonCL_X2	-2.982	.538	-.838	-5.541	.000	-4.145	-1.819
2	(Constant)	17.651	1.961		9.000	.000	13.378	21.925
	KollidonCL_X2	-7.381	1.815	-2.075	-4.066	.002	-11.337	-3.426
	X2X2	.800	.320	1.277	2.503	.028	.104	1.496

a. Dependent Variable: DT

Table B-4 Linear regression analysis: Effect of Polyvinylpyrrolidone K90, Kollidon® CL and Magnesium stearate on hardness.

Variables Entered/Removed^a

Model	Variables Entered	Variables Removed	Method
1	X2X3	.	Stepwise (Criteria: Probability-of-F-to-enter \leq .050, Probability-of-F-to-remove \geq .100).

a. Dependent Variable: Hardness

Model Summary^b

Model	R	R Square	Adjusted R Square	Std. Error of the Estimate	Change Statistics					Durbin-Watson
					R Square Change	F Change	df1	df2	Sig. F Change	
1	.634 ^a	.402	.356	.19508	.402	8.731	1	13	.011	.784

a. Predictors: (Constant), X2X3

b. Dependent Variable: Hardness

ANOVA^b

Model		Sum of Squares	df	Mean Square	F	Sig.
1	Regression	.332	1	.332	8.731	.011 ^a
	Residual	.495	13	.038		
	Total	.827	14			

a. Predictors: (Constant), X2X3

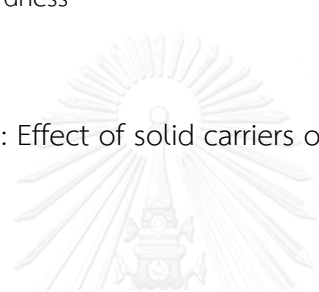
b. Dependent Variable: Hardness

Coefficients^a

Model		Unstandardized Coefficients		Standardized Coefficients	t	Sig.	95.0% Confidence Interval for B	
		B	Std. Error	Beta			Lower Bound	Upper Bound
1	(Constant)	1.833	.074		24.897	.000	1.674	1.992
	X2X3	-.092	.031	-.634	-2.955	.011	-.160	-.025

a. Dependent Variable: Hardness

Table B-5 Statistical testing: Effect of solid carriers on particle size of SME tablets after reconstitution.



Descriptives

	N	Mean	Std. Deviation	Std. Error	95% Confidence Interval for Mean		Minimum	Maximum
					Lower Bound	Upper Bound		
Liquid SME	3	72.5800	4.61657	2.66538	61.1118	84.0482	69.25	77.85
Aerosil200 Tab	3	72.1400	3.57176	2.06216	63.2672	81.0128	69.44	76.19
Aeroperl300 Tab	3	94.2200	6.30146	3.63815	78.5663	109.8737	88.24	100.80
NeusilinUS2 Tab	3	119.0000	10.75314	6.20833	92.2877	145.7123	110.90	131.20
Total	12	89.4850	20.93142	6.04238	76.1858	102.7842	69.25	131.20

Test of Homogeneity of Variances

Levene Statistic	df1	df2	Sig.
2.171	3	8	.169

ANOVA

	Sum of Squares	df	Mean Square	F	Sig.
Between Groups	4440.551	3	1480.184	31.259	.000
Within Groups	378.817	8	47.352		
Total	4819.368	11			

Multiple Comparisons

(I) Formulation	(J) Formulation	Mean Difference (I-J)	Std. Error	Sig.	95% Confidence Interval	
					Lower Bound	Upper Bound
Tukey HSD	Aerosil200 Tab	.44000	5.61855	1.000	-17.5526	18.4326
	Aeroperl300 Tab	-21.64000*	5.61855	.020	-39.6326	-3.6474
	NeusilinUS2 Tab	-46.42000*	5.61855	.000	-64.4126	-28.4274
Aerosil200 Tab	Liquid SME	-.44000	5.61855	1.000	-18.4326	17.5526
	Aeroperl300 Tab	-22.08000*	5.61855	.018	-40.0726	-4.0874
	NeusilinUS2 Tab	-46.86000*	5.61855	.000	-64.8526	-28.8674
Aeroperl300 Tab	Liquid SME	21.64000*	5.61855	.020	3.6474	39.6326
	Aerosil200 Tab	22.08000*	5.61855	.018	4.0874	40.0726
	NeusilinUS2 Tab	-24.78000*	5.61855	.010	-42.7726	-6.7874
NeusilinUS2 Tab	Liquid SME	46.42000*	5.61855	.000	28.4274	64.4126
	Aerosil200 Tab	46.86000*	5.61855	.000	28.8674	64.8526
	Aeroperl300 Tab	24.78000*	5.61855	.010	6.7874	42.7726

*. The mean difference is significant at the 0.05 level.

Table B-6 Statistical testing: Effect of dilution mediums (0.1N HCL and purified water) on particle size of Aerosil® 200 SME tablets after reconstitution.

Descriptives

	N	Mean	Std. Deviation	Std. Error	95% Confidence Interval for Mean		Minimum	Maximum
					Lower Bound	Upper Bound		
Water	3	72.1400	3.57176	2.06216	63.2672	81.0128	69.44	76.19
0.1N HCL	3	79.2533	13.97922	8.07091	44.5270	113.9796	65.08	93.03
Total	6	75.6967	9.92221	4.05073	65.2839	86.1094	65.08	93.03

Test of Homogeneity of Variances

Levene Statistic	df1	df2	Sig.
2.158	1	4	.216

ANOVA

	Sum of Squares	df	Mean Square	F	Sig.
Between Groups	75.899	1	75.899	.729	.441
Within Groups	416.352	4	104.088		
Total	492.252	5			

Table B-7 Statistical testing: Effect of dilution mediums (0.1N HCL and purified water) on particle size of Aeroperl[®] 300 SME tablets after reconstitution.

Descriptives

	N	Mean	Std. Deviation	Std. Error	95% Confidence Interval for Mean		Minimum	Maximum
					Lower Bound	Upper Bound		
Water	3	94.2200	6.30146	3.63815	78.5663	109.8737	88.24	100.80
0.1N HCL	3	89.3933	12.55301	7.24749	58.2099	120.5767	78.90	103.30
Total	6	91.8067	9.26842	3.78382	82.0801	101.5333	78.90	103.30

Test of Homogeneity of Variances

Levene Statistic	df1	df2	Sig.
1.812	1	4	.249

ANOVA

	Sum of Squares	df	Mean Square	F	Sig.
Between Groups	34.945	1	34.945	.354	.584
Within Groups	394.573	4	98.643		
Total	429.518	5			

Table B-8 Statistical testing: Effect of dilution mediums (0.1N HCL and purified water) on particle size of Neusilin US2[®] 300 SME tablets after reconstitution.

Descriptives

	N	Mean	Std. Deviation	Std. Error	95% Confidence Interval for Mean		Minimum	Maximum
					Lower Bound	Upper Bound		
Water	3	119.0000	10.75314	6.20833	92.2877	145.7123	110.90	131.20
0.1N HCL	3	105.6000	4.60326	2.65769	94.1649	117.0351	102.60	110.90
Total	6	112.3000	10.42094	4.25433	101.3639	123.2361	102.60	131.20

Test of Homogeneity of Variances

Levene Statistic	df1	df2	Sig.
3.365	1	4	.141

ANOVA

	Sum of Squares	df	Mean Square	F	Sig.
Between Groups	269.340	1	269.340	3.937	.118
Within Groups	273.640	4	68.410		
Total	542.980	5			

Table B-9 Diameter, thickness and hardness of SME tablets.

Tab No.	Diameter			Thickness			Hardness		
	Aerosil 200	Aeroperl 300	Neusilin US2	Aerosil 200	Aeroperl 300	Neusilin US2	Aerosil 200	Aeroperl 300	Neusilin US2
1	0.99	0.99	0.98	4	4.14	4.07	2.8	2.8	2.8
2	0.99	0.99	0.98	4.07	4.13	4.01	2.9	2.8	2.9
3	0.99	0.99	0.98	4.03	4.16	4.05	2.8	2.5	3.2
4	0.99	0.99	0.98	4.06	4.15	4.08	2.5	2.9	3.1
5	0.99	0.99	0.98	4	4.19	4.06	2.9	2.7	3.5
6	0.99	0.99	0.98	4.07	4.18	4.06	2.6	2.7	2.9
7	0.99	0.99	0.98	4.02	4.19	4.02	2.5	2.5	3
8	0.99	0.99	0.98	4.02	4.2	4.09	2.7	2.8	2.8
9	0.99	0.99	0.98	4.01	4.16	4.09	2.5	2.9	3.1
10	0.99	0.99	0.98	4.03	4.2	4.05	2.4	2.8	3.1



Table B-10 Percent drug dissolved from SME tablets at 5, 10, 20 and 30 minutes.

Formulations	Area	Conc. (mg/ml)	Drug amount in 10 ml (mg)	Drug amount in 500 ml (mg)	Drug amount in 490 ml (mg)	Drug dissolved (mg)	Cumulative amount (mg)	% Drug dissolved
5 mins								
Aerosil®200_1	59,427	0.00164	0.02	0.82	0.80	0.82	0.82	32.78
Aerosil®200_2	41,106	0.00113	0.01	0.57	0.56	0.57	0.57	22.60
Aerosil®200_3	44,719	0.00123	0.01	0.62	0.60	0.62	0.62	24.67
Aeroperl®300_1	99,702	0.00278	0.03	1.39	1.36	1.39	1.39	55.68
Aeroperl®300_2	78,845	0.00220	0.02	1.10	1.08	1.10	1.10	44.03
Aeroperl®300_3	84,602	0.00236	0.02	1.18	1.16	1.18	1.18	47.24
NeustlinUS2®_1	12,252	0.00034	0.00	0.17	0.17	0.17	0.17	6.84
NeustlinUS2®_2	23,134	0.00065	0.01	0.32	0.32	0.32	0.32	12.92
NeustlinUS2®_3	13,776	0.00030	0.00	0.19	0.19	0.19	0.19	7.69
10 mins								
Aerosil®200_1	74531	0.00206	0.02	1.03	1.01	0.22	1.04	41.77
Aerosil®200_2	72726	0.00201	0.02	1.00	0.90	0.45	1.01	40.57
Aerosil®200_3	85552	0.00236	0.02	1.18	1.16	0.50	1.19	47.69
Aeroperl®300_1	135,405	0.00378	0.04	1.89	1.85	0.53	1.92	76.73
Aeroperl®300_2	110,436	0.00300	0.03	1.54	1.51	0.46	1.56	62.55
Aeroperl®300_3	105,737	0.00295	0.03	1.48	1.45	0.32	1.50	59.99
NeustlinUS2®_1	33,498	0.00094	0.01	0.47	0.46	0.30	0.47	18.84
NeustlinUS2®_2	43,464	0.00121	0.01	0.61	0.59	0.29	0.61	24.53
NeustlinUS2®_3	40,365	0.00113	0.01	0.56	0.55	0.30	0.57	22.69

20 mins										
Aerosil® 200_1	93370	0.00250	0.03	1.29	1.26	0.20	1.32	52.99		
Aerosil® 200_2	91770	0.00253	0.03	1.27	1.24	0.20	1.30	51.00		
Aerosil® 200_3	97417	0.00269	0.03	1.34	1.32	0.19	1.30	55.10		
Aeroperl® 300_1	139,477	0.00415	0.04	2.00	2.04	0.22	2.14	35.71		
Aeroperl® 300_2	116,003	0.00330	0.03	1.65	1.62	0.14	1.70	60.05		
Aeroperl® 300_3	114,631	0.00320	0.04	1.01	1.70	0.37	1.07	74.69		
NeustlinUS2®_1	75,677	0.00211	0.02	1.06	1.04	0.60	1.07	42.77		
NeustlinUS2®_2	69,124	0.00193	0.02	0.97	0.95	0.37	0.90	39.34		
NeustlinUS2®_3	70,473	0.00197	0.02	0.90	0.96	0.43	1.00	39.96		
30 mins										
Aerosil® 200_1	105432	0.00291	0.03	1.45	1.42	0.19	1.52	60.67		
Aerosil® 200_2	95709	0.00264	0.03	1.32	1.29	0.00	1.30	55.07		
Aerosil® 200_3	115033	0.00320	0.03	1.60	1.57	0.20	1.66	66.41		
Aeroperl® 300_1	140,705	0.00415	0.04	2.00	2.04	0.04	2.10	37.37		
Aeroperl® 300_2	137,015	0.00305	0.04	1.92	1.09	0.31	2.01	30.39		
Aeroperl® 300_3	129,950	0.00363	0.04	1.01	1.70	0.04	1.90	76.14		
NeustlinUS2®_1	103,750	0.00290	0.03	1.45	1.42	0.41	1.40	59.29		
NeustlinUS2®_2	106,262	0.00297	0.03	1.00	1.45	0.54	1.52	60.05		
NeustlinUS2®_3	101,107	0.00203	0.03	1.41	1.30	0.45	1.45	57.90		

Table B-11 Stability of drug-loaded Aeroperl[®] 300 SME tablet after storage at 40±2°C/75±5%RH, 25±2°C/60±5%RH and 5°C±3°C for 3 months.

Storage conditions	Area	Conc. (mg/ml)	%LA amount
Initial			
Tab_001	4,340,053.00	9.5885	95.08
Tab_002	4,339,926.00	9.5882	95.08
Tab_003	4,335,623.00	9.5787	94.98
5°C±3°C			
Tab_001	3,936,883.00	9.1518	90.75
Tab_002	3,922,809.00	9.1191	90.43
Tab_003	3,998,295.00	9.2946	92.17
25±2°C/60±5%RH			
Tab_001	3,593,204.00	8.2669	83.24
Tab_002	3,473,352.00	7.9911	80.46
Tab_003	3,662,168.00	8.4255	84.84
40±2°C/75±5%RH			
Tab_001	3,443,994.00	7.4545	75.71
Tab_002	3,444,667.00	7.4559	75.73
Tab_003	3,459,479.00	7.4880	76.05

Method validation

1. Linearity

Table B-12 Drug concentrations and responding area obtained from HPLC chromatograms.

Concentration ($\mu\text{g/ml}$)	Area
0.08_001	1457
0.08_002	1432
0.08_003	1519
0.10_001	2221
0.10_002	2223
0.10_003	2229
0.40_001	7401
0.40_002	7559
0.40_003	7571
0.80_001	14652
0.80_002	14590
0.80_003	14752
1.00_001	19431
1.00_002	19071
1.00_003	18764
4.00_001	69400
4.00_002	70846
4.00_003	71487
8.00_001	142889
8.00_002	143789
8.00_003	143869
10.00_001	186900
10.00_002	184976
10.00_0.03	179979
40.00_001	734132
40.00_002	737065
40.00_0.03	742430

2. Accuracy

Table B-13 Percent recovery at 50%, 100% and 150% concentrations of actual drug loaded in the SME tablet.

Amount added (mg)	Actual conc. (mg/ml)	Area	Estimated conc. (mg/ml)	Amount founded (mg)	Percent recovery
1.490	0.00060	111351	0.006256421	1.564105196	104.9735031
1.430	0.00057	105829	0.005946159	1.48653976	103.9538294
1.500	0.00060	111671	0.0062744	1.568600115	104.573341
2.900	0.00116	215271	0.01209532	3.023829959	104.2699986
2.910	0.00116	216382	0.012157743	3.039435754	104.447964
2.880	0.00115	210787	0.01184338	2.960844914	102.8071151
4.380	0.00175	326958	0.018370619	4.59265482	104.8551329
4.520	0.00181	336996	0.018934619	4.733654792	104.7268759
4.420	0.00177	325162	0.018269708	4.56742709	103.3354545



3. Precision

Table B-14 Percent recovery at 100% concentrations of actual drug loaded in the SME tablet in different 3 days.

Day	Actual Conc. (mg/ml)	Area	Estimated Conc. (mg/ml)	% Recovery
1 st	0.0112	209566	0.0113	101.01
	0.0114	207743	0.0112	98.00
	0.0114	202951	0.0109	95.68
	0.0115	212770	0.0115	99.74
	0.0115	211576	0.0114	99.16
	0.0116	210520	0.0113	97.30
2 nd	0.0112	210572	0.0113	101.15
	0.0114	213643	0.0115	101.22
	0.0114	210663	0.0113	99.42
	0.0114	212433	0.0114	100.28
	0.0114	212513	0.0114	99.96
	0.0116	218686	0.0118	101.18
3 rd	0.0116	212384	0.0119	102.52
	0.0116	211413	0.0119	102.05
	0.0117	212946	0.0120	102.09
	0.0115	208941	0.0117	101.91
	0.0115	208996	0.0117	101.93
	0.0115	208432	0.0117	102.01

4. Detection Limit (LOD) and Quantitation Limit (LOQ)

Table B-15 Calculation of LOD and Quantitation Limit LOQ.

Conc (x)	Avg area (Y)	Yi	(Y-Yi)	(Y-Yi) ²
0.08016	1469.333333	736.5806603	732.752673	536926.4798
0.1002	2224.333333	1105.49325	1118.840083	1251803.131
0.4008	7510.333333	6639.182102	871.1512318	758904.4687
0.8016	14664.66667	14017.4339	647.2327637	418910.2504
1.002	19088.66667	17706.5598	1382.106863	1910219.38
4.008	70577.66667	73043.44832	-2465.781648	6080079.137
8.016	143515.6667	146825.9663	-3310.299663	10958083.86
10.02	183951.6667	183717.2253	234.4413291	54962.73677
40.08	737875.6667	737086.1105	789.5562163	623399.0186
Total				22593288.47
$(Y-Yi)^2/n-2$				3227612.638
S.D.				1796.555771
LOQ = 10S.D./slope				0.9759 µg/ml
LOD = 3.3S.D./slope				0.3221 µg/ml

APPENDIX C
***In vitro* cell culture studies**

Table C-1 Toxicity results in Caco-2 cells.

Formulations	UV absorbance at 570 ± 20 nm				Percent cell viability			
	11.480 µg/ml	5.740 µg/ml	2.870 µg/ml	1.435 µg/ml	11.480 µg/ml	5.740 µg/ml	2.870 µg/ml	1.435 µg/ml
Drug loaded	0.046	0.589	0.891	0.808	6.24	79.88	120.84	109.58
SME tab	0.048	0.598	0.817	0.812	6.51	81.10	110.80	110.13
	0.045	0.602	0.859	0.787	6.10	81.65	116.50	106.74
Drug + SME	0.046	0.582	0.820	0.817	6.24	78.93	111.21	110.80
tab	0.046	0.641	0.809	0.851	6.24	86.93	109.72	115.42
	0.042	0.616	0.827	0.736	5.70	83.54	112.16	99.82
Marketed Tab	0.044	0.664	0.911	0.831	5.97	90.05	123.55	112.70
	0.041	0.685	0.918	1.003	5.56	92.90	124.50	136.03
	0.042	0.665	0.807	0.797	5.70	90.19	109.45	108.09
Medium	0.774 0.658 0.780				100			

Table C-2 Permeation of drug through Caco-2 cells at 2, 4 and 6 hours.

Time	Formulations	Area	Drug conc. ($\mu\text{g}/\text{ml}$)	Drug amount in 2.5 ml (μg)	Drug amount in 1.5 ml (μg)	Drug permeated (μg)	Cumulative permeated (μg)
2 hrs	Drug loaded SIME tab	4911	0.059	0.147	0.080	0.147	0.147
		5405	0.064	0.161	0.096	0.161	0.161
		6707	0.070	0.195	0.117	0.195	0.195
	Drug + SIME tab	3326	0.042	0.105	0.063	0.105	0.105
		5441	0.065	0.162	0.097	0.162	0.162
		3031	0.047	0.119	0.071	0.119	0.119
	Marketed Tab	12253	0.137	0.343	0.206	0.343	0.343
		15301	0.171	0.427	0.256	0.427	0.427
		14277	0.159	0.397	0.230	0.397	0.397
4 hrs	Drug loaded SIME tab	9722	0.110	0.276	0.166	0.197	0.335
		10512	0.119	0.297	0.170	0.201	0.361
		10079	0.114	0.285	0.171	0.160	0.364
	Drug + SIME tab	7174	0.093	0.200	0.125	0.145	0.250
		10762	0.121	0.304	0.182	0.207	0.360
		7707	0.090	0.224	0.135	0.153	0.272
	Marketed Tab	14971	0.166	0.416	0.250	0.210	0.558
		10405	0.203	0.500	0.305	0.251	0.670
		17613	0.195	0.406	0.292	0.240	0.645

6 hrs	Drug loaded SIME tab	13039	0.146	0.364	0.219	0.199	0.584
		7021	0.091	0.204	0.122	0.026	0.307
		14730	0.164	0.410	0.246	0.230	0.602
	Drug + SIME tab	9661	0.110	0.274	0.165	0.150	0.399
		12550	0.141	0.352	0.211	0.169	0.588
		9970	0.113	0.282	0.169	0.148	0.420
	Marketed Tab	15382	0.170	0.426	0.255	0.176	0.729
		10630	0.206	0.515	0.309	0.210	0.809
		17788	0.196	0.491	0.295	0.199	0.845



Table C-3 Statistical testing: Effect of formulations on drug permeated through Caco-2 cells at 2 hours.

Descriptives

	N	Mean	Std. Deviation	Std. Error	95% Confidence Interval for Mean		Minimum	Maximum
					Lower Bound	Upper Bound		
					Drug loaded SME tab	3		
SME tab + drug	3	.1284	.02951	.01704	.0551	.2017	.11	.16
Marketed Tab	3	.3892	.04234	.02445	.2840	.4944	.34	.43
Total	9	.2285	.12508	.04169	.1323	.3246	.11	.43

ANOVA

	Sum of Squares	df	Mean Square	F	Sig.
Between Groups	.119	2	.059	54.261	.000
Within Groups	.007	6	.001		
Total	.125	8			

Test of Homogeneity of Variances

Levene Statistic	df1	df2	Sig.
.548	2	6	.604

Multiple Comparisons

(I) Formulation	(J) Formulation	Mean Difference (I-J)	Std. Error	Sig.	95% Confidence Interval		
					Lower Bound	Upper Bound	
Tukey HSD	Drug loaded SME tab	SME tab + drug	.03937	.02699	.373	-.0435	.1222
		Marketed Tab	-.22143 [*]	.02699	.000	-.3043	-.1386
	SME tab + drug	Drug loaded SME tab	-.03937	.02699	.373	-.1222	.0435
		Marketed Tab	-.26080 [*]	.02699	.000	-.3436	-.1780
	Marketed Tab	Drug loaded SME tab	.22143 [*]	.02699	.000	.1386	.3043
		SME tab + drug	.26080 [*]	.02699	.000	.1780	.3436

*. The mean difference is significant at the 0.05 level.

Table C-4 Statistical testing: Effect of formulations on drug permeated through Caco-2 cells at 4 hours.

Descriptives

	N	Mean	Std. Deviation	Std. Error	95% Confidence Interval for Mean		Minimum	Maximum
					Lower Bound	Upper Bound		
Drug loaded SME tab	3	.3532	.01595	.00921	.3136	.3928	.33	.36
SME tab + drug	3	.2966	.06298	.03636	.1401	.4530	.25	.37
Marketed Tab	3	.6257	.06485	.03744	.4646	.7868	.55	.68
Total	9	.4252	.15918	.05306	.3028	.5475	.25	.68

Test of Homogeneity of Variances

Levene Statistic	df1	df2	Sig.
2.995	2	6	.125

ANOVA

	Sum of Squares	df	Mean Square	F	Sig.
Between Groups	.186	2	.093	33.084	.001
Within Groups	.017	6	.003		
Total	.203	8			

Multiple Comparisons

	(I) Formulation	(J) Formulation	Mean Difference (I-J)	Std. Error	Sig.	95% Confidence Interval	
						Lower Bound	Upper Bound
Tukey HSD	Drug loaded SME tab	SME tab + drug	.05660	.04327	.441	-.0762	.1894
		Marketed Tab	-.27257 *	.04327	.002	-.4053	-.1398
	SME tab + drug	Drug loaded SME tab	-.05660	.04327	.441	-.1894	.0762
		Marketed Tab	-.32917 *	.04327	.001	-.4619	-.1964
	Marketed Tab	Drug loaded SME tab	.27257 *	.04327	.002	.1398	.4053
		SME tab + drug	.32917 *	.04327	.001	.1964	.4619

*. The mean difference is significant at the 0.05 level.

Table C-5 Statistical testing: Effect of formulations on drug permeated through Caco-2 cells at 6 hours.

Descriptives

	N	Mean	Std. Deviation	Std. Error	95% Confidence Interval for Mean		Minimum	Maximum
					Lower Bound	Upper Bound		
Drug loaded SME tab	3	.5074	.10988	.06344	.2345	.7804	.39	.60
SME tab + drug	3	.4522	.07465	.04310	.2668	.6376	.40	.54
Marketed Tab	3	.8210	.08231	.04752	.6165	1.0254	.73	.89
Total	9	.5935	.18914	.06305	.4481	.7389	.39	.89

Test of Homogeneity of Variances

Levene Statistic	df1	df2	Sig.
.332	2	6	.730

ANOVA

	Sum of Squares	df	Mean Square	F	Sig.
Between Groups	.237	2	.119	14.579	.005
Within Groups	.049	6	.008		
Total	.286	8			

Multiple Comparisons

(I) Formulation	(J) Formulation	Mean Difference (I-J)	Std. Error	Sig.	95% Confidence Interval		
					Lower Bound	Upper Bound	
Tukey HSD	Drug loaded SME tab	SME tab + drug	.05523	.07367	.745	-.1708	.2813
		Marketed Tab	-.31353 [*]	.07367	.013	-.5396	-.0875
	SME tab + drug	Drug loaded SME tab	-.05523	.07367	.745	-.2813	.1708
		Marketed Tab	-.36877 [*]	.07367	.006	-.5948	-.1427
	Marketed Tab	Drug loaded SME tab	.31353 [*]	.07367	.013	.0875	.5396
		SME tab + drug	.36877 [*]	.07367	.006	.1427	.5948

*. The mean difference is significant at the 0.05 level.

Table C-6 Statistical testing: Effect of formulations on P_{app} values.

Descriptives

	N	Mean	Std. Deviation	Std. Error	95% Confidence Interval for Mean		Minimum	Maximum
					Lower Bound	Upper Bound		
					Drug loaded SME tab	3		
SME tab + drug	3	.0000	.00000	.00000	.0000	.0000	.00	.00
Marketed tab	3	.0000	.00000	.00000	.0000	.0000	.00	.00
Total	9	.0000	.00000	.00000	.0000	.0000	.00	.00

Test of Homogeneity of Variances

Levene Statistic	df1	df2	Sig.
3.506	2	6	.098

ANOVA

	Sum of Squares	df	Mean Square	F	Sig.
Between Groups	.000	2	.000	2.274	.184
Within Groups	.000	6	.000		
Total	.000	8			

Table C-7 Drug uptake in Caco-2 cells at 6 hours.

Formulations	Drug uptake (μg)
Drug loaded SME tab_001	1.808
Drug loaded SME tab_002	1.901
Drug loaded SME tab_003	1.654
SME tab + drug_001	1.691
SME tab + drug_002	1.743
SME tab + drug_003	1.616
Marketed tab_001	1.263
Marketed tab_002	1.269
Marketed tab_003	1.278

Table C-8 Statistical testing: Effect of formulations on drug uptake in Caco-2 cells at 6 hours.

Descriptives

	N	Mean	Std. Deviation	Std. Error	95% Confidence Interval for Mean		Minimum	Maximum
					Lower Bound	Upper Bound		
					Drug loaded SME tab	3		
SME tab + drug	3	1.6835	.06404	.03697	1.5244	1.8426	1.62	1.74
Marketed Tab	3	1.2700	.00790	.00456	1.2503	1.2896	1.26	1.28
Total	9	1.5803	.24730	.08243	1.3902	1.7704	1.26	1.90

Test of Homogeneity of Variances

Levene Statistic	df1	df2	Sig.
3.317	2	6	.107

ANOVA

	Sum of Squares	df	Mean Square	F	Sig.
Between Groups	.450	2	.225	34.123	.001
Within Groups	.040	6	.007		
Total	.489	8			

Multiple Comparisons

	(I) Formulation	(J) Formulation	Mean Difference (I-J)	Std. Error	Sig.	95% Confidence Interval		
						Lower Bound	Upper Bound	
Tukey HSD	Drug loaded SME tab	SME tab + drug	.10409	.06628	.327	-.0993	.3075	
		Marketed Tab	.51760*	.06628	.001	.3142	.7210	
	SME tab + drug	Drug loaded SME tab	-.10409	.06628	.327	-.3075	.0993	
		Marketed Tab	.41350*	.06628	.002	.2101	.6169	
	Marketed Tab	Drug loaded SME tab	-.51760*	.06628	.001	-.7210	-.3142	
		SME tab + drug	-.41350*	.06628	.002	-.6169	-.2101	
	Dunnett t T3	Drug loaded SME tab	SME tab + drug	.10409	.08105	.567	-.2563	.4645
			Marketed Tab	.51760*	.07227	.039	.0634	.9718
SME tab + drug		Drug loaded SME tab	-.10409	.08105	.567	-.4645	.2563	
		Marketed Tab	.41350*	.03725	.015	.1849	.6421	
Marketed Tab		Drug loaded SME tab	-.51760*	.07227	.039	-.9718	-.0634	
		SME tab + drug	-.41350*	.03725	.015	-.6421	-.1849	

*. The mean difference is significant at the 0.05 level.

Table C-9 TEER values of Caco-2 cells before and after permeation and uptake studies.

Formulations	TEER values($\text{ohm}\times\text{cm}^2$)		%TEER at the end of experiments
	Before	After	
Drug loaded SME tab_001	396.95	336.24	84.71
Drug loaded SME tab_002	401.62	340.91	84.88
Drug loaded SME tab_003	345.58	284.87	82.43
SME tab + drug_001	373.60	312.89	83.75
SME tab + drug_002	368.93	317.56	86.08
SME tab + drug_003	331.57	280.2	84.51
Marketed tab_001	336.24	284.87	84.72
Marketed tab_002	368.93	308.22	83.54
Marketed tab_003	345.58	298.88	86.49

Table C-10 ApolipoproteinB content in Chylomicron (chy), VLDL and Caco-2 cells

Formulations	UV absorbance at 450 nm			Conc. ($\mu\text{g}/\text{ml}$)			Amount (ng)		
	Chy	VLDL	Caco-2 Cells	Chy	VLDL	Caco-2 Cells	Chy	VLDL	Caco-2 Cells
Drug loaded SME_1	0.227	0.188	0.446	0.0104	0.0039	0.0467	41.57	15.71	186.76
Drug loaded SME_2	0.210	0.181	0.480	0.0076	0.0028	0.0523	30.30	11.07	209.30
Drug loaded SME_3	0.218	0.179	0.491	0.0089	0.0024	0.0541	35.60	9.75	216.59
SME tab + drug_1	0.189	0.184	0.458	0.0041	0.0033	0.0487	16.38	13.06	194.71
SME tab + drug_2	0.180	0.178	0.499	0.0026	0.0023	0.0555	10.41	9.08	221.89
SME tab + drug_3	0.175	0.172	0.469	0.0018	0.0013	0.0505	7.09	5.10	202.01
Marketed tab_1	0.170	0.165	0.448	0.0009	0.0001	0.0470	3.78	0.46	188.08
Marketed tab_2	0.169	0.166	0.421	0.0008	0.0003	0.0425	3.12	1.13	170.18
Marketed tab_3	0.168	0.163	0.436	0.0006	0.0002	0.0450	2.45	-0.86	180.13

Table C-11 Statistical testing: Effect of formulations on apolipoprotein B content found in Caco-2 cells.

Descriptives

	N	Mean	Std. Deviation	Std. Error	95% Confidence Interval for Mean		Minimum	Maximum
					Lower Bound	Upper Bound		
					Drug loaded SME tablet	3		
SME tablet + drug	3	.0516	.00351	.00203	.0428	.0603	.05	.06
Marketed tablet	3	.0449	.00224	.00129	.0393	.0504	.04	.05
Total	9	.0492	.00430	.00143	.0458	.0525	.04	.06

Test of Homogeneity of Variances

Levene Statistic	df1	df2	Sig.
.777	2	6	.501

ANOVA

	Sum of Squares	df	Mean Square	F	Sig.
Between Groups	.000	2	.000	3.841	.084
Within Groups	.000	6	.000		
Total	.000	8			

Table C-12 Statistical testing: Effect of formulations on apolipoprotein B content found in Chylomicron.

Descriptives

	N	Mean	Std. Deviation	Std. Error	95% Confidence Interval for Mean		Minimum	Maximum
					Lower Bound	Upper Bound		
					Drug loaded SME tablet	3		
SME tablet + drug	3	.0028	.00118	.00068	-.0001	.0057	.00	.00
Marketed tablet	3	-.0003	.00105	.00061	-.0029	.0023	.00	.00
Total	9	.0038	.00420	.00140	.0006	.0071	.00	.01

Test of Homogeneity of Variances

Levene Statistic	df1	df2	Sig.
.052	2	6	.950

ANOVA

	Sum of Squares	df	Mean Square	F	Sig.
Between Groups	.000	2	.000	44.340	.000
Within Groups	.000	6	.000		
Total	.000	8			

Multiple Comparisons

(I) Formulations	(J) Formulations	Mean Difference (I-J)	Std. Error	Sig.	95% Confidence Interval		
					Lower Bound	Upper Bound	
Tukey HSD	Drug loaded SME tablet	.00613 [*]	.00100	.002	.0031	.0092	
	SME tablet + drug						
	Marketed tablet	.00923 [*]	.00100	.000	.0062	.0123	
	SME tablet + drug	Drug loaded SME tablet	-.00613 [*]	.00100	.002	-.0092	-.0031
		Marketed tablet	.00309 [*]	.00100	.048	.0000	.0062
Marketed tablet	Drug loaded SME tablet	-.00923 [*]	.00100	.000	-.0123	-.0062	
	SME tablet + drug						
	SME tablet	-.00309 [*]	.00100	.048	-.0062	.0000	

*. The mean difference is significant at the 0.05 level.

Table C-13 Statistical testing: Effect of formulations on apolipoprotein B content found in VLDL.

Descriptives

	N	Mean	Std. Deviation	Std. Error	95% Confidence Interval for Mean		Minimum	Maximum
					Lower Bound	Upper Bound		
					Drug loaded SME tablet	3		
SME tablet + drug	3	.0023	.00100	.00057	-.0002	.0047	.00	.00
Marketed tablet	3	-.0002	.00225	.00130	-.0058	.0054	.00	.00
Total	9	.0017	.00194	.00065	.0002	.0032	.00	.00

Test of Homogeneity of Variances

Levene Statistic	df1	df2	Sig.
3.725	2	6	.089

ANOVA

	Sum of Squares	df	Mean Square	F	Sig.
Between Groups	.000	2	.000	3.774	.087
Within Groups	.000	6	.000		
Total	.000	8			

Table C-14 TEER values of Caco-2 cells before and after ApolipoproteinB analysis.

Formulations	TEER values($\text{ohm}\times\text{cm}^2$)		%TEER at the end of experiments
	Before	After	
Drug loaded SME tab_001	448.32	326.90	72.92
Drug loaded SME tab_002	434.31	312.89	72.04
Drug loaded SME tab_003	396.95	270.86	68.24
SME tab + drug_001	392.28	284.87	72.62
SME tab + drug_002	448.32	308.22	68.75
SME tab + drug_003	401.62	280.20	69.77
Marketed tab_001	467.00	364.26	78.00
Marketed tab_002	448.32	340.91	76.04
Marketed tab_003	424.97	317.56	74.73

Table C-15 Statistical testing: Effect of formulations on drug content found in chylomicron.

Descriptives

	N	Mean	Std. Deviation	Std. Error	95% Confidence Interval for Mean		Minimum	Maximum
					Lower Bound	Upper Bound		
					Drug loaded SME tab	3		
SME tab + drug	3	.0240	.00020	.00011	.0235	.0244	.02	.02
Marketed tab	3	.0491	.00034	.00019	.0482	.0499	.05	.05
Total	9	.0382	.01122	.00374	.0296	.0468	.02	.05

Test of Homogeneity of Variances

Levene Statistic	df1	df2	Sig.
5.600	2	6	.042

ANOVA

	Sum of Squares	df	Mean Square	F	Sig.
Between Groups	.001	2	.000	296.668	.000
Within Groups	.000	6	.000		
Total	.001	8			

Multiple Comparisons

(I) Formulations	(J) Formulations	Mean Difference (I-J)	Std. Error	Sig.	95% Confidence Interval		
					Lower Bound	Upper Bound	
Dunnett t T3	Drug loaded SME tab	SME tab + drug	.01769*	.00128	.010	.0097	.0257
		Marketed tab	-.00740	.00129	.055	-.0152	.0004
	SME tab + drug	Drug loaded SME tab	-.01769*	.00128	.010	-.0257	-.0097
		Marketed tab	-.02510*	.00022	.000	-.0260	-.0242
	Marketed tab	Drug loaded SME tab	.00740	.00129	.055	-.0004	.0152
		SME tab + drug	.02510*	.00022	.000	.0242	.0260

*. The mean difference is significant at the 0.05 level.

Table C-16 Statistical testing: Effect of formulations on drug content found in VLDL.

Descriptives

	N	Mean	Std. Deviation	Std. Error	95% Confidence Interval for Mean		Minimum	Maximum
					Lower Bound	Upper Bound		
					Drug loaded SME tab	3		
SME tab + drug	3	.0000	.00000	.00000	.0000	.0000	.00	.00
Marketed tab	3	.0219	.00584	.00337	.0073	.0364	.02	.03
Total	9	.0073	.01131	.00377	-.0014	.0160	.00	.03

Test of Homogeneity of Variances

Levene Statistic	df1	df2	Sig.
12.079	2	6	.008

ANOVA

	Sum of Squares	df	Mean Square	F	Sig.
Between Groups	.001	2	.000	41.957	.000
Within Groups	.000	6	.000		
Total	.001	8			

Multiple Comparisons

(I) Formulations	(J) Formulations	Mean Difference (I-J)	Std. Error	Sig.	95% Confidence Interval		
					Lower Bound	Upper Bound	
Dunnett T3	Drug loaded SME tab	.00000	.00000	.	.0000	.0000	
	SME tab + drug	.00000	.00000	.	.0000	.0000	
	Marketed tab	-.02186*	.00337	.048	-.0433	-.0005	
	SME tab + drug	Drug loaded SME tab	.00000	.00000	.	.0000	.0000
		Marketed tab	-.02186*	.00337	.048	-.0433	-.0005
	Marketed tab	Drug loaded SME tab	.02186*	.00337	.048	.0005	.0433
	SME tab + drug	.02186*	.00337	.048	.0005	.0433	

*. The mean difference is significant at the 0.05 level.

Table C-17 TEER values ($\text{ohm}\times\text{cm}^2$) of bEND3 cells monoculture and bEND3 cocultured with CTX TNA2 cells.

Formulations	bEND3 cells monoculture	bEND3 cocultured with CTX TNA2	
	Before treatment	Before treatment	After treatment
Drug loaded SME tablet_1	70.05	588.42	541.72
Drug loaded SME tablet_2	79.39	593.09	560.4
Drug loaded SME tablet_3	60.71	616.44	574.41
SME tablet + drug_1	51.37	569.74	495.02
SME tablet + drug_2	74.72	607.1	490.35
SME tablet + drug_3	60.71	574.41	485.68
Marketed tablet_1	56.04	602.43	579.08
Marketed tablet_2	65.38	607.1	569.74
Marketed tablet_3	74.72	583.75	565.07

Table C-18 Toxicity results in bEND3 cells and CTX TNA2 cells.

Formulations	bEND3 cells		CTX TNA2 cells	
	UV absorbance at 570 ± 20 nm	Percent cell viability	UV absorbance at 570 ± 20 nm	Percent cell viability
Drug loaded SME tablet_1	0.254	102.14	0.448	82.75
Drug loaded SME tablet_2	0.223	89.67	0.500	92.36
Drug loaded SME tablet_3	0.198	79.62	0.523	96.61
SME tablet + drug_1	0.190	76.40	0.478	88.30
SME tablet + drug_2	0.211	84.85	0.457	84.42
SME tablet + drug_3	0.196	78.82	0.506	93.47
Marketed tablet_1	0.254	102.14	0.527	97.35
Marketed tablet_2	0.269	108.18	0.559	103.26
Marketed tablet_3	0.266	106.97	0.540	99.75
Medium_1	0.227		0.576	
Medium_2	0.235	100.00	0.526	100.00
Medium_3	0.284		0.522	

Table C-19 Drug uptake in bEND3 cocultured with CTX TNA2 cells.

Formulations	Drug uptake (μg)
Drug loaded SME tab_001	0.149271831
Drug loaded SME tab_001	0.181518808
Drug loaded SME tab_001	0.14791107
SME tab + drug_001	0.054184071
SME tab + drug_002	0.129590115
SME tab + drug_003	0.087482013
Marketed tab_001	0.088521398
Marketed tab_002	0.100562624
Marketed tab_003	0.064195747

Table C-20 Statistical testing: Effect of formulations on drug uptake in bEND3 cocultured with CTX TNA2 cell.

Descriptives

	N	Mean	Std. Deviation	Std. Error	95% Confidence Interval for Mean		Minimum	Maximum
					Lower Bound	Upper Bound		
					Drug loaded SME tablet	3		
SME tablet + drug	3	.0904	.03779	.02182	-.0035	.1843	.05	.13
Marketed Tablet	3	.0844	.01853	.01070	.0384	.1304	.06	.10
Total	9	.1115	.04291	.01430	.0785	.1445	.05	.18

Test of Homogeneity of Variances

Levene Statistic	df1	df2	Sig.
.850	2	6	.473

ANOVA

	Sum of Squares	df	Mean Square	F	Sig.
Between Groups	.010	2	.005	7.358	.024
Within Groups	.004	6	.001		
Total	.015	8			

Multiple Comparisons

(I) Formulations	(J) Formulations	Mean Difference (I-J)	Std. Error	Sig.	95% Confidence Interval	
					Lower Bound	Upper Bound
Tukey HSD	SME tablet + drug	.06915*	.02177	.044	.0023	.1360
	Marketed Tablet	.07514*	.02177	.031	.0083	.1419
SME tablet + drug	Drug loaded SME tablet	-.06915*	.02177	.044	-.1360	-.0023
	Marketed Tablet	.00599	.02177	.959	-.0608	.0728
Marketed Tablet	Drug loaded SME tablet	-.07514*	.02177	.031	-.1419	-.0083
	SME tablet + drug	-.00599	.02177	.959	-.0728	.0608

*. The mean difference is significant at the 0.05 level.

VITA

Miss Sirigul Thongrangsalit was born on 20th September 1984, in Suphanburi, Thailand. She graduated with the Bachelor of Science in Pharmacy (Second Class Honours) in 2007 from Faculty of Pharmacy, Silpakorn University, Nakhon Pathom, Thailand. Following graduation, she worked as a pharmacist at Charoen Bhaesaj Lab Limited for one year before attending the Doctoral of Philosophy Program in Pharmaceutics and Industrial Pharmacy since the first semester of the academic year 2010.

